Dipl.-Ing. Katharina Schmölzer

Mechanistic study of pro- and eukaryotic sialyltransferases

DISSERTATION

zur Erlangung des akademischen Grades

Doktorin der technischen Wissenschaften

eingereicht an der

Technischen Universität Graz

Betreuer

Univ.-Prof. Dipl.-Ing. Dr.techn. Bernd Nidetzky

Institut für Biotechnologie und Bioprozesstechnik, TU Graz

Graz, Juni 2014

EIDESSTATTLICHE ERKLÄRUNG

AFFIDAVIT

Ich erkläre an Eides statt, dass ich die vorliegende Arbeit selbstständig verfasst, andere als die angegebenen Quellen/Hilfsmittel nicht benutzt, und die den benutzten Quellen wörtlich und inhaltlich entnommenen Stellen als solche kenntlich gemacht habe. Das in TUGRAZonline hochgeladene Textdokument ist mit der vorliegenden Dissertation identisch.

I declare that I have authored this thesis independently, that I have not used other than the declared sources/resources, and that I have explicitly indicated all material which has been quoted either literally or by content from the sources used. The text document uploaded to TUGRAZonline is identical to the present doctoral dissertation.

Datum / Date

Unterschrift / Signature

Acknowledgement

First of all, I would like to express my appreciation to my supervisor Prof. Dr. Bernd Nidetzky for supporting me during these past three and a half years. Thanks for giving me the opportunity to be part of this research group. Special thanks go to Christiane, Doris and Tibor for their time, the great team work and the stimulating discussions. Many thanks to Katharina, Regina, Sarah and Susi for the support and the encouraging words that motivated me and kept me going even when times were tough. Also, thanks to all members of the Institute of Biotechnology and Biochemical Engineering for assistance wherever it was needed. Sincere thanks to my family, who unremittingly supported me and always believed in me.

"There is only one thing that makes a dream impossible to achieve: the fear of failure."
(Paulo Coelho, The Alchemist)

Abstract

Sialic acids are derivatives of neuraminic acid that have outstanding importance to human glycobiology in recognition and response processes. Sialyltransferases (STs) (EC 2.4.99) represent an important group of enzymes that catalyze transfer of a sialic acid residue from a CMP-activated donor substrate, typically CMP-*N*-acetylneuraminic acid (CMP-Neu5Ac) onto a carbohydrate acceptor by formation of either a α2,3-, α2,6- or α2,8-linkage. STs are widely distributed in animal tissues, but are also present in other organisms including yeasts and bacteria. A new multifunctional α2,3-ST (PdST) was identified from the *Pasteurella dagmatis* genome by sequence similarity with STs of glycosyltransferase family GT-80. An interesting and peculiar feature of PdST is a natural Ser-to-Thr interchange in the YDDGS-motif that is otherwise invariant in family GT-80 STs. Reversion of this natural residue substitution by site-directed mutagenesis revealed that Thr is necessitated for the fine-tuning of the catalytic properties of PdST, namely control of regioselectivity of sialyltransfer, control of the level of sialidase and trans-sialidase activity and balancing between substrate binding and catalytic turnover. Moreover, this natural mutation was shown to be beneficial for high-yielding synthesis of α2,3-sialosides. In contrast to mammalian STs and glycosyltransferases in general, bacterial STs often exhibit pronounced hydrolase activity toward CMP-activated sialyl donor substrates. It was demonstrated that hydrolysis of CMP-Neu5Ac by PdST occurs with axial-to-equatorial inversion at the anomeric center to release α-Neu5Ac product, presumably as result of a single displacement reaction, just like the canonical sialyltransfer to carbohydrate acceptors catalyzed by this enzyme. Stereochemical promiscuity indicated by formation of inversion and retention product simultaneously, as reported for *P. multocida* ST PmST1 from the same family GT-80, was ruled out rigorously for PdST. Mutational studies support stabilization of the CMP-leaving group in the PdST hydrolase mechanism through electrostatic interactions by a His residue. Furthermore, synthetic sialyloligosaccharides, consisting of Neu5Ac attached to galactose or *N*-acetylgalactosamine moieties through α2,3- or α2,6-linkage, are in great demand as functional food ingredients, nutraceutical medicine, and pathogen adsorbent materials. From the economical point of view, it would be highly advantageous to apply two variants of a single ST with α2,3- or α2,6-regioselectivty in sialoside synthesis, which have uniform synthesis conditions and substrate specificities. So far, synthesis of distinct regiospecific products necessitated different STs. Based on structure-guided active-site redesign of PdST complete switch from α2,3- to α2,6-regioselectivity was achieved while maintaining almost identical yields. Moreover, a N-terminally truncated variant of the human β-galactoside α2,6-ST I was successfully expressed in human

embryonic kidney (HEK) cells and has proved to be a suitable tool for the terminal modification of *N*-glycans due to its sialyltransferase and sialidase activity on a monoclonal antibody. Finally, we were able to successfully express a variant of the human α2,6-ST with a minimized catalytic domain in the methylotropic yeast *P. pastoris* in sufficient yields for a potential large scale application. This human α2,6-ST variant catalyzed sialic acid transfer to monoclonal antibody substrate with high specificity.

Zusammenfassung

Sialinsäuren, Derivate der Neuraminsäure, haben herausragende Bedeutung für die humane Glykobiologie in verschiedensten Zell-Zell-Interaktionsprozessen. Sialyltransferasen (STs) (EC 2.4.99) stellen eine wichtige Enzymgruppe dar, die den Transfer von Sialinsäureresten von CMP-aktivierten Donorsubstraten, typischerweise CMP-*N*-Acetylneuraminsäure (CMP-Neu5Ac), auf einen Kohlenhydratakzeptor unter Ausbildung einer α2,3-, α2,6- oder α2,8-Bindung katalysieren. STs sind weit verbreitet in Geweben tierischen Ursprungs, werden aber auch in anderen Organismen wie Hefen und Bakterien gefunden. Eine neue multifunktionale α2,3-ST (PdST) wurde im Genom von *Pasteurella dagmatis* durch Sequenzähnlichkeit mit STs der Glycosyltransferasefamilie GT-80 identifiziert. Eine interessante Besonderheit von PdST ist eine natürliche Ser-zu-Thr Mutation in einem ansonsten in Familie GT-80 hochkonservierten YDDGS Motiv. Umkehr dieses natürlichen Aminosäureaustausches durch zielgerichtete Mutagenese hat gezeigt, dass Thr in PdST für die Feinabstimmung der katalytischen Eigenschaften, nämlich Kontrolle der Regioselektivität des Sialyltransfers, Kontrolle von Sialidase- und Transsialidase-Aktivitätslevel und Abstimmung zwischen Substratbindung und katalytischem Umsatz, notwendig ist. Außerdem wurde gezeigt, dass sich diese natürliche Mutation äußerst vorteilhaft auf die Ausbeute bei der Synthese von α2,3-Sialosiden auswirkt. Im Gegensatz zu Säugetier-STs und Glycosyltransferasen im Allgemeinen zeigen bakterielle STs häufig eine ausgeprägte Hydrolyseaktivität gegenüber CMP-aktivierten Sialyldonorsubstraten. CMP-Neu5Ac Hydrolyse durch PdST erfolgt über eine axial-zu-äquatoriale Inversion am anomeren Zentrum und α-Neu5Ac wird als Produkt freigesetzt. Das verläuft höchstwahrscheinlich über einen „Single-Displacement" Mechanismus, ähnlich dem durch dieses Enzym katalysierten kanonischen Sialyltransfer auf einen Kohlenhydratakzeptor. Stereochemische Promiskuität, angezeigt durch die Bildung von Inversions- und Retentionsprodukt, wie für die aus derselben GT-80 Familie stammende *P. multocida* ST PmST1 berichtet, wurde rigoros ausgeschlossen. Mutationsstudien unterstützen eine Stabilisierung der CMP-Abgangsgruppe im PdST Hydrolysemechanismus mittels elektrostatischer Interaktionen mit einem His-Rest. Synthetische Sialyloligosaccharide, bestehend aus Neu5Ac verknüpft mit einer Galactose- oder *N*-Acetylgalactosamin-Gruppe über α2,3- oder α2,6-Bindungen, sind von großem Interesse als funktionelle Lebensmittel, Nahrungsergänzungsmittel und Pathogen adsorbierende Materialien. Aus ökonomischer Sicht wäre es aufgrund von einheitlichen Synthesebedingungen und Substratspezifitäten sehr vorteilhaft zwei Varianten einer einzigen ST mit α2,3- oder α2,6-Regioselektivität in der Sialosidsynthese anzuwenden. Bis jetzt erforderte die Synthese von unterschiedlichen regiospezifischen Produkten mehrere STs.

Komplette Änderung der PdST Regioselektivität von α2,3 zu α2,6, ohne Auswirkung auf die Ausbeute, wurde durch strukturbasierendes „Redesign“ des aktiven Zentrums erzielt. Außerdem konnte eine N-terminal verkürzte Variante der humanen β-Galactosid α2,6-ST I erfolgreich in HEK-Zellen exprimiert werden. Dieses Enzym hat sich aufgrund seiner Sialyltransferase- und Sialidase-Aktivität an einem monoklonalen Antikörper als geeignetes Tool für die N-terminale Modifizierung von *N*-Glykanen erwiesen. Darüber hinaus konnte eine Variante der humanen α2,6-ST mit minimierter katalytischer Domäne in der methylotrophen Hefe *P. pastoris* stabil und in ausreichender Menge für eine potenzielle Anwendung in größerem Maßstab exprimiert werden. Diese humane α2,6-ST Variante katalysierte den Sialinsäuretransfer auf monoklonale Antikörper mit hoher Spezifität.

Contents

- **Characterization of a multifunctional α2,3-sialyltransferase from *Pasteurella dagmatis*.** Schmölzer, K. et al. (2013) *Glycobiology* **23**, 1293-1304. 1

  Supporting information 13

- **Mechanistic study of CMP-Neu5Ac hydrolysis by α2,3-sialyltransferase from *Pasteurella dagmatis*.** Schmölzer, K., Luley-Goedl, C., Czabany, T., Ribitsch, D., Schwab, H., Weber, H. and Nidetzky, B. (2014) *accepted for publication in FEBS Letters* (FEBSLETTERS-D-14-00775R1) 30

  Supporting information 51

- **Complete switch from α2,3- to α2,6-regioselectivity in *Pasteurella dagmatis* β-D-galactoside sialyltransferase by active-site redesign.** Schmölzer, K., Czabany, T., Luley-Goedl, C., Ribitsch, D., Schwab, H. and Nidetzky B. (2014) *in preparation* 66

  Supporting information 72

- **Two variants of human β-galactoside α2,6-sialyltransferase I with distinct properties.** Luley-Goedl, C. et al. (2014) *in preparation* 85

- **High-quality production of human α2,6-sialyltransferase in *Pichia pastoris* requires control over N-terminal truncations by host-inherent protease activities.** Ribitsch, D. et al. (2014) *submitted to Microbial Cell Factories* (MS ID: 5860187381304371) 103

- **Appendix** 140
  pH dependency of multifunctional PdST 141
  Structures of wild-type PdST and mutants 142
  Characterization of PdST mutants 148
  References 163

- **List of publications** 164

Glycobiology vol. 23 no. 11 pp. 1293–1304, 2013
doi:10.1093/glycob/cwt066
Advance Access publication on August 22, 2013

Characterization of a multifunctional α2,3-sialyltransferase from *Pasteurella dagmatis*

Katharina Schmölzer[2], Doris Ribitsch[2], Tibor Czabany[3], Christiane Luley-Goedl[2], Deja Kokot[3], Andrzej Lyskowski[2], Sabine Zitzenbacher[2], Helmut Schwab[2,4], and Bernd Nidetzky[1,2,3]

[2]Austrian Centre of Industrial Biotechnology, Petersgasse 14, 8010 Graz, Austria; [3]Institute of Biotechnology and Biochemical Engineering, Graz University of Technology, Petersgasse 12/I, 8010 Graz, Austria; and [4]Institute of Molecular Biotechnology, Graz University of Technology, Petersgasse 14, 8010 Graz, Austria

Received on April 3, 2013; revised on August 1, 2013; accepted on August 16, 2013

A new multifunctional α2,3-sialyltransferase has been discovered in *Pasteurella dagmatis*. The enzyme, in short PdST, was identified from the *P. dagmatis* genome by sequence similarity with sialyltransferases of glycosyltransferase family GT-80. In addition to its regioselective sialyltransferase activity (5.9 U/mg; pH 8.0), purified PdST is alternatively active at low pH as α2,3-sialidase (0.5 U/mg; pH 4.5) and α2,3-trans-sialidase (1.0 U/mg; pH 4.5). It also shows cytidine-5′-monophosphate *N*-acetyl-neuraminic (CMP-Neu5Ac) hydrolase activity (3.7 U/mg; pH 8.0) when no sialyl acceptor substrate is present in the reaction. After sialyltransferase PmST1 from *P. multocida*, PdST is the second member of family GT-80 to display this remarkable catalytic promiscuity. A unique feature of PdST, however, is a naturally occurring Ser-to-Thr substitution within a highly conserved $Y^{112}DDGS^{116}$ sequence motif. In PmST1, the equivalent Ser^{143} is involved in binding of the CMP-Neu5Ac donor substrate. Reversion of the natural mutation in a T116S-PdST variant resulted in a marked increase in α2,3-trans-sialidase side activity (4.0 U/mg; pH 4.5), whereas the major sialyltransferase activity was lowered (3.8 U/mg; pH 8.0). The Michaelis–Menten constant for CMP-Neu5Ac was decreased 4-fold in T116S mutant when compared with wild-type PdST (K_M = 1.1 mM), indicating that residue 116 of PdST contributes to a delicate balance between substrate binding and catalytic activity. D-Galactose and various β-D-galactosides function as sialyl acceptors from CMP-Neu5Ac, whereas other hexoses (e.g. D-glucose) are inactive. Structure comparison was used to rationalize the particular acceptor substrate specificity of PdST in relation to other GT-80 sialyltransferases that show strict α2,3-regioselectivity, but are flexible in using α/β-galactosides for sialylation.

[1]To whom correspondence should be addressed: Tel: +43-316-873-8400; Fax: +43-316-873-8434; e-mail: bernd.nidetzky@tugraz.at

Keywords: bacterial sialyltransferase / glycosyltransferase family GT-80 / natural mutation / N-terminal elongation / structure–function relationships

Introduction

Sialic acids are derivatives of neuraminic acid that have outstanding importance to human glycobiology. *N*-Acetylneuraminic acid (Neu5Ac) is the most common form of sialic acid. Attached to glycoproteins and glycolipids, it is widespread among the different human tissues where a great variety of extracellular recognition processes depend on the adequate presentation of Neu5Ac molecules (Varki 2008; Schauer 2009). A number of human pathogenic microbes employ modification with Neu5Ac, a process often referred to as sialylation, to counteract defense mechanisms of the infected host. Interference with microbial sialylation pathways, therefore, presents a promising approach for the development of anti-infective therapies (Zhuo and Bellis 2011).

Sialyltransferases catalyze transfer of a sialic acid residue from a CMP-activated donor substrate, typically CMP-Neu5Ac, onto a carbohydrate acceptor. Chemically, the enzymatic reactions involve an axial-to-equatorial substitution at the anomeric center (C2) of sialic acid, thus yielding α-2-*O*-sialosides as their products. In hexose or hexoside acceptors (e.g. D-galactose, D-galactosamine, D-galactosides), the C3 or C6 are sites recognized for sialylation. Alternatively, the C8 of Neu5Ac or another sialic acid acceptor may become sialylated. A common functional classification of sialyltransferases, therefore, distinguishes between α2,3-, α2,6- and α2,8-regioselective enzymes. A number of sialyltransferases have previously been identified and characterized from human infective bacteria (Yamamoto et al. 2006; Kondadi et al. 2012; Li and Chen 2012). In a sequence-based classification of glycosyltransferases that currently comprises 94 families, bacterial sialyltransferases have been categorized into family GT-38, GT-42, GT-52 and GT-80. Among these families, family GT-80 involves the largest diversity of enzyme specificities and was the focus of this research. Based on biochemical data for 10 of its currently 18 entries, family GT-80 is further subdivided according to enzyme regioselectivity into α2,3-, α2,6- and mixed α2,3/α2,6-specific sialyltransferases.

Crystallographic structure data are available for sialyltransferases from each subgroup within family GT-80: α/β-galactoside α2,3-sialyltransferase from *Photobacterium phosphoreum* (Iwatani et al. 2009); β-galactoside α2,6-sialyltransferase from *Photobacterium* sp. JT-ISH-224 (Kakuta et al. 2008) and

α2,3/α2,6-sialyltransferase PmST1 from *Pasteurella multocida* (Ni et al. 2006, 2007). The three enzymes adopt a highly similar protein fold characteristic of glycosyltransferase fold family GT-B (Coutinho et al. 2003). Their fold comprises two Rossmann fold-like domains, with a deep cleft in between them that harbors the active site. Structures of PmST1 in the apo-form and in complex with different ligands show that ligand binding induces large conformational changes in and around the active site (Ni et al. 2006). Like a number of other glycosyltransferases that exploit substrate-binding energy to morph their catalytic centers into the reactive conformation (Qasba et al. 2005; Milac et al. 2007), PmST1 also seems to utilize induced fit for promoting catalysis. When discussing later the remarkable catalytic promiscuity of α2,3/α2,6-sialyltransferases, it will, therefore, be important to recall the possibility of active-site conformational flexibility. A family-wide structure-based sequence comparison revealed three highly conserved sequence motifs (Table I) that comprise key residues for substrate binding and catalysis (Yamamoto et al. 2008).

Aside from their different regioselectivities, family GT-80 sialyltransferases also differ in how well they accommodate variations in the structure of their preferred acceptor substrate. Activity of α2,6-sialyltransferases is strongly linked to a terminal β-galactoside acceptor group (Yamamoto et al. 1996, 2007; Tsukamoto et al. 2008). The α2,3/α2,6-sialyltransferase PmST1 is also specific for β-galactosides (Yu et al. 2005). The α2,3-sialyltransferases on the contrary are flexible concerning sialylation of α- and β-galactosides (Takakura et al. 2007; Tsukamoto et al. 2007, 2008). Among this group, the enzyme from *P. phosphoreum* shows a remarkably broad substrate scope that includes various galactosides, but also methyl-α/β-D-gluco-, D-manno- and even L-fucosides (Tsukamoto et al. 2007). Sialyltransferases are, therefore, promising biocatalysts for the synthesis of sialosides (Yu, Chokhawala, et al. 2006; Yu, Huang, et al. 2006; Lau et al. 2011; Oh et al. 2011). Their different acceptor specificities are, however, not fully rationalized from the currently available structural basis.

Another important distinction between sialyltransferases of family GT-80 emerges from consideration of alternative transformations catalyzed next to the main sialyltransferase reaction. These transformations involve hydrolysis of CMP-Neu5Ac, hydrolysis of sialosides ("sialidase") and sialyltransfer between sialosides ("trans-sialidase"). The β-galactoside α2,6-sialyltransferases are hardly active as sialidases (Mine et al. 2010). Their trans-sialidase activity appears to be also low and was noticed only recently in the enzyme from *P. damselae* (Cheng et al. 2010). The same applies for α2,3-sialyltransferases. They are hardly active as sialidases (Takakura et al. 2007; Tsukamoto et al. 2007) and there is no current evidence for trans-sialidase activity. The α2,3/α2,6-sialyltransferase PmST1 in contrast displays a large diversity of catalytic functions (Yu et al. 2005). The different reactions catalyzed are summarized in Scheme 1. Both α2,3- and α2,6-sialosides serve as substrates for hydrolysis or trans-sialylation. The stereochemical course of the trans-sialylation differs from that of the "normal" sialyltransfer in that it involves an equatorial-to-equatorial (α-retaining) substitution at the anomeric carbon. Little is currently known about the molecular basis for this remarkable mechanistic promiscuity of PmST1. The enzyme is best active as sialidase and trans-sialidase in a pH range well below the optimum pH for the canonical sialyltransferase reaction (Yu et al. 2005). Mutagenesis data are consistent with the notion that residues of PmST1 involved in sialidase activity are exploited differently than in sialyltransfer from CMP-Neu5Ac (Ni et al. 2007; Sugiarto et al. 2011). PmST1 is the only current member of family GT-80 representing a multifunctional α2,3/α2,6-sialyltransferase. We postulate that valuable complementary information might be gained from the characterization of another representative of this special type of sialyltransferase.

PdST from *P. dagmatis* is introduced in this work. The enzyme resembles PmST1 concerning the multiplicity of reactions catalyzed (Scheme 1). However, it shows distinct regioselectivity and acceptor substrate specificity. Another

Table I. Partial sequence alignment displaying conserved functional motifs from GT-80 glycosyltransferases

	Sialyltransferase	Accession number	YDDGS-motif	FKGHP-motif	SS-motif
P. multocida	a2,3/a2,6	AAY89061	LNLY[139]DDGS[143]MEY	IYF[308]KGHP[312]RGG	GGVAS[355]SLYFS
P. dagmatis	a2,3	AFY98851	LNLY[112]DDGT[116]MEY	IYF[281]KGHP[285]RGG	GGVAS[328]SLYFS
P. damselae	a2,6	BAA25316	ISLY[227]DDGS[231]SEY	LPF[398]KGHP[403]AGG	AGIAS[445]SLYFT
P. leiognathi	a2,6	BAF91416	INLY[227]DDGS[231]AEY	LPF[398]KGHP[403]RGG	GGIAS[445]SLYFS
P. phosphoreum	a2,3	BAF63530	LNFY[146]DDGS[150]AEY	LPF[314]KGHP[318]SAT	GGMGS[359]SVFFS
Vibrio sp.	a2,3	BAF91160	LHFY[140]DDGS[144]AEY	LPF[308]KGHP[312]SAT	GGMGS[353]SVFFS
H. ducreyi	a2,3	AAP95068	LQLY[123]DDGS[127]EGI	LLI[293]KGHA[297]NSP	GGFAS[340]TSMIN

P. multocida, *Pasteurella multocida* α2,3/α2,6-sialyltransferase (PmST1); *P. dagmatis*, *Pasteurella dagmatis* α2,3-sialyltransferase (PdST); *P. damselae*, *Photobacterium damselae* α2,6-sialyltransferase; *P. leiognathi*, *Photobacterium leiognathi* α2,6-sialyltransferase; *P. phosphoreum*, *Photobacterium phosphoreum* α/β-galactoside α2,3-sialyltransferase; *Vibrio* sp., *Vibrio* sp. α/β-galactoside α2,3-sialyltransferase; *H. ducreyi*, *Haemophilus ducreyi* α2,3-sialyltransferase. Sequence alignment was performed with ClustalW using a blosum scoring matrix and an open gap penalty of 10. Catalytically important aspartate and histidine are indicated by an arrow.

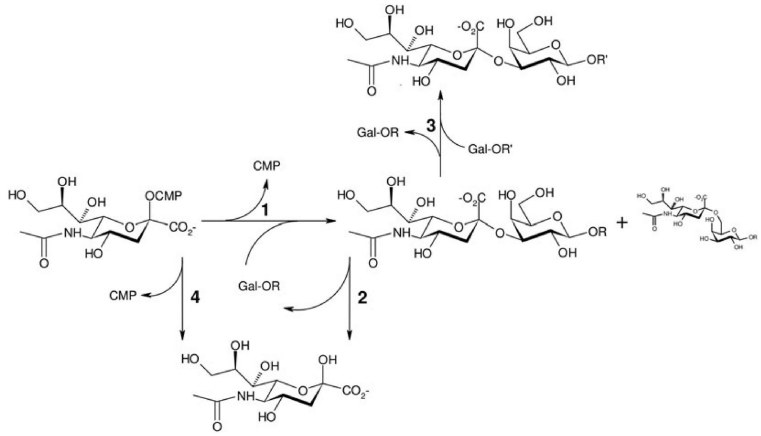

Scheme 1. Reactions catalyzed by multifunctional sialyltransferases, in particular ∇3PdST. **1**, α2,3/α2,6-Sialyltransferase activity; **2**, α2,3-Sialidase activity; **3**, α2,3-trans-sialidase activity; **4**, CMP-Neu5Ac hydrolysis. Gal-OR and Gal-OR' are acceptor substrates containing a terminal β-galactosyl moiety.

interesting and peculiar feature of PdST is the natural occurrence of a Ser-to-Thr substitution in the YDDGS-motif that is otherwise invariant in family GT-80 sialyltransferases (Table I). We have reversed the natural residue substitution and show through comparative characterization of wild-type enzyme and T116S mutant that fine-tuning of the catalytic properties of PdST requires residue 116 to be a threonine. These enzyme properties seem to involve control of regioselectivity of sialyltransfer, control of the level of sialidase and trans-sialidase activity and balancing between substrate binding and catalytic turnover.

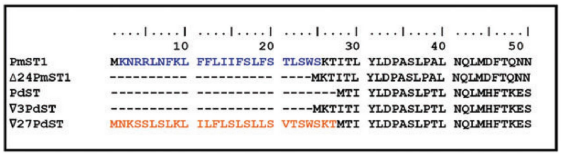

Fig. 1. Multiple alignment of N-terminal amino acid sequences in PdST and PmST1 variants and constructs (Pm, *Pasteurella multocida*; Pd, *P. dagmatis*). Blue, N terminus of PmST1; orange, elongated N terminus of ∇27PdST.

Results

Identification of PdST and analysis of its sequence

BLAST database search using PmST1 (Yu et al. 2005) as the search object revealed a hypothetical protein from the genome of *P. dagmatis* strain ATCC43325 as a prominent hit. The protein, which we named PdST, is 74% identical in amino acid sequence to PmST1. The PdST open reading frame (1158 bp) encodes a protein comprising 385 amino acids with a calculated mass of 45.3 kDa. PdST is, therefore, smaller than PmST1, which consists of 412 amino acids and has a mass of 48.1 kDa. Comparison of genome data for *P. dagmatis* and *P. multocida* indicates that size differences between PdST and PmST1 are most likely explained by alternative translation starts separated by 27 amino acids, as depicted in Figure 1.

Three highly conserved sequence motifs provide a characteristic signature for sialyltransferases of family GT-80 (Yamamoto et al. 2008). Table I shows a partial multiple sequence alignment that highlights the conserved motifs and the putative catalytic residues (Asp, His) present in them. Interestingly, PdST displays a previously unobserved Ser-to-Thr substitution within the YDDGS-motif. To eliminate the possibility of sequence error in the published genome data, we amplified the PdST gene from *P. dagmatis* genomic DNA and determined its sequence, thus confirming residue 116 to be a threonine. The analysis also substantiated the triplet codon for the presumed initiator methionine.

Elongation of the N-terminus of PdST enhances expression in Escherichia coli

Yu et al. (2005) reported that the expression of full-length PmST1 in *E. coli* resulted in recovery of a truncated protein in which 25 amino acids had been processed off the enzyme's authentic N-terminus. A deletion construct Δ24PmST1 having residues 2–25 removed had gained resistance to proteolysis and was expressed well in the bacterial host. Three PdST expression constructs were therefore designed, as shown in Figure 1. Each construct contained a C-terminal hexahistidine-tag that comprised 13 amino acids in total. The basal construct started from the putative initiator Met in the genomic sequence (amino acids 1–385). In accordance to Δ24PmST1, the correspondingly N-terminally elongated variant of PdST by 3 amino acids was prepared and is identified as ∇3PdST. Finally, the region further upstream in the *P. dagmatis* genome encodes a putative N-terminal extension of 27 amino acids that is highly similar to the one found in full-length PmST1. This N-terminal extension was appended to PdST, thus generating ∇27PdST. Note that ∇3PdST and ∇27PdST are therefore counterpart constructs of Δ24PmST1 and full-length PmST1, respectively. The different PdST gene constructs were cloned into a pET23(a) expression

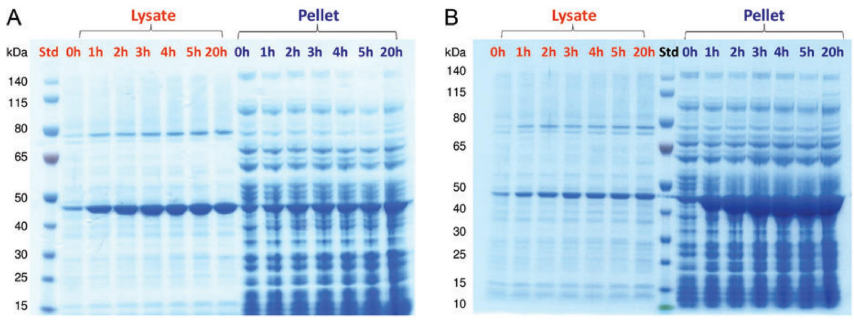

Fig. 2. Expression profiles of ∇3PdST (**A**) and PdST (**B**). The SDS polyacrylamide gels show cell lysate (red) and pellet (blue) after certain times of induction (0–20 h). The gels were stained with Coomassie brilliant blue.

vector, and expression was done in *E. coli* BL21-Gold(DE3) under well controlled and exactly comparable conditions in each case. Figure 2 shows time courses of expression of PdST and ∇3PdST analyzed by sodium dodecyl sulfate polyacrylamide gel electrophoresis (SDS–PAGE) of isopropyl-beta-D-thiogalactopyranoside (IPTG)-induced *E. coli* cell extracts. We were surprised that ∇3PdST was expressed by far better than PdST (Figure 2) and also ∇27PdST (data not shown). The protein amount recovered from a 1-L bacterial culture after two-step purification on HisTrap and HiTrap Q columns (Supplementary data, Figures S1 and S2) was 25 mg ∇3PdST, exceeding the corresponding amounts of PdST and ∇27PdST by ∼50-fold. Using SDS–PAGE, we determined a molecular mass of 50 kDa for purified ∇27PdST, consistent with the mass expected for the full-length protein of 412 amino acids plus His-tag (data not shown). Unlike full-length PmST1, ∇27PdST does not seem to be processed in *E. coli*. The purified ∇3PdST eluted in gel filtration chromatography in a single protein peak that contained all of the applied sialyltransferase activity and corresponded to an apparent mass of 47 kDa, suggesting that the enzyme is a functional monomer (Supplementary data, Figure S3). Purified preparations of PdST, ∇3PdST and ∇27PdST had similar specific activities of 5.5–6.0 U/mg, assayed with lactose as acceptor. All further studies were therefore performed with ∇3PdST.

Basic characterization of the sialyltransferase activity of ∇3PdST

The standard assay for enzyme activity involved enzymatic conversion of CMP-Neu5Ac in the presence of lactose as acceptor and the determination of the released CMP using high-performance liquid chromatography (HPLC). Applying ∇3PdST in a suitable concentration in the range 0.1–1 μM, we noticed that the CMP formation rate decreased rapidly with time even though the donor substrate was still present in excess. Addition of bovine serum albumin (BSA) (1 mg/mL) prevented the effect that was presumably caused by the inactivation of ∇3PdST at the high dilution of the enzyme. The specific activity of 5.7 U/mg thus obtained for ∇3PdST is lower, ∼10-fold, than the reported specific activity of PmST1 recorded with a similar assay but at 37°C (Yu et al. 2005). It is, however, on the same magnitude order as the reported specific activities of several α2,3- and α2,6-sialyltransferases of family GT-80 (Yamamoto et al. 1996, 2007; Tsukamoto et al. 2007).

We examined the acceptor substrate specificity of ∇3PdST using the standard activity assay, but replacing lactose with another potential substrate to become sialylated. Table II shows the results. Among several monosaccharides tested, only D-galactose was used in the enzymatic reaction. Several β-D-galactosides were sialylated with high activity and remarkable tolerance for structural variation in the non-galactosyl part of the acceptor molecule. Raffinose was, therefore, examined because it contains a terminal α-D-galactosyl residue. It was inactive. The high anomeric selectivity of ∇3PdST can be explained from results of structure modeling, as will be discussed later.

Activity of sialyltransferases is generally inhibited by the reaction product CMP, but also by cytidine-5′-triphosphate (CTP). The inhibitory effect is particularly strong in mammalian sialyltransferases of family GT-29 where CTP is even used to stop the enzymatic reaction (Scudder and Chantler 1981). We determined that ∇3PdST activity, measured in an assay that used ortho-nitrophenyl-β-D-galactopyranoside (oNP-βGal) as acceptor instead of lactose, was decreased by just 55% (20 mM CTP) and 32% (20 mM CMP) in the presence of a large excess of each compound over CMP-Neu5Ac (1 mM). Therefore, this implies that neither CMP nor CTP is a strong inhibitor of the enzyme which could present a significant advantage in the case that ∇3PdST was applied as catalyst for the synthesis of sialosides. Considering literature reports about the stimulation of sialyltransferase activity by salt and detergent (Mine et al. 2010), we examined the possible influence of NaCl (10–500 mM) and Triton X-100 (1–10 g/L) on ∇3PdST activity, but found none.

Regioselectivity of sialyltransfer and demonstration of catalytic multifunctionality of ∇3PdST

Using conditions of the standard assay, lactose was sialylated from CMP-Neu5Ac until ∼90% of the donor substrate was converted. The resulting mixture was subjected to a detailed product analysis using high-performance liquid chromatography electrospray ionization ion trap-mass spectrometr (HPLC-ESI-IT-MS) and high-performance anion exchange pulsed amperometric detection (HPAE-PAD). The MS data showed that roughly 70% of the initial lactose had become

Table II. Acceptor substrate specificity of ∇3PdST. CMP-Neu5Ac was used as donor substrate.

Acceptor	Linkage	Structure	Specific activity (U/mg)
Monosaccharides			
D-Galactose		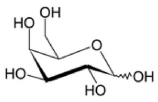	2.0
D-Glucose		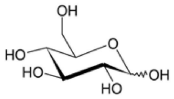	–
D-Mannose		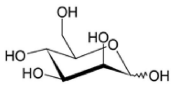	–
L-Fucose		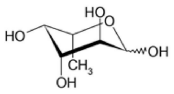	–
Di- and trisaccharides			
Lactose	β1,4	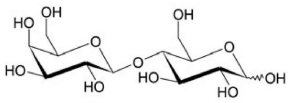	5.7
N-Acetyl-D-lactosamine	β1,4	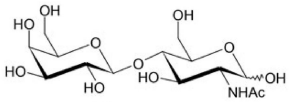	5.4
Lactulose	β1,4	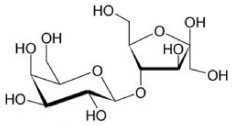	5.0
Sucrose	α1,2	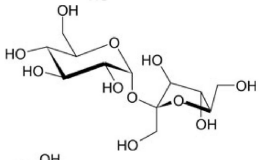	–
Raffinose	α1,6	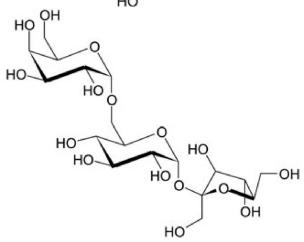	–
Labeled sugars			
oNP-Lactose	β1,4	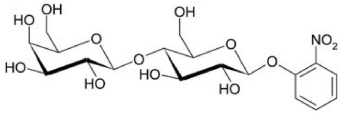	7.8
oNP-β-D-Galactose		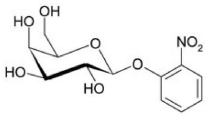	5.9

derivatized and that the enzymatic modification was a monosialylation. Multiple sialylation events on lactose were not observed above the detection limit (0.1%). The portion of CMP-Neu5Ac that was utilized in the reaction, but did not end up in sialylated lactose, was probably transformed via hydrolysis (see later). Authentic standards of 6′-sialyllactose and 3′-sialyllactose were applied to identify the sialyltransfer product(s) of ∇3PdST. The enzyme showed strong preference for the sialylation of the 3′-OH in lactose (≥95%). We were able to detect 6′-sialyllactose as reaction product, but this was formed in only very tiny amounts. Results on analysis by HPAE-PAD are shown in the Supplementary data, Figure S4. Therefore, we propose that ∇3PdST should be classified as α2,3-sialyltransferase.

Scheme 1 provided the frame of reference for examining ∇3PdST in respect to alternative reactions that the enzyme might catalyze. Reaction **1** is the normal sialyltransfer. We found ∇3PdST to possess α2,3-sialidase activity against 3′-sialyllactose (reaction **2**). The enzyme was also active as α2,3-trans-sialidase, transferring a sialyl residue from 3′-sialyllactose to an alternative acceptor (reaction **3**) which here was oNP-βGal. The linkage of the trans-sialylation product was assigned as α2,3 as it eluted identically as the Neu5Acα2,3Gal-oNP standard obtained from the normal sialyltransfer reaction (Supplementary data, Figure S5). The α2,3-sialidase and α2,3-trans-sialidase activities of ∇3PdST were affected strongly by pH, as shown in Table III. Hydrolysis of 3′-sialyllactose at pH 4.5 occurred at a 25-fold faster rate than at pH 8.0. 3′-Sialyllactose was stable throughout the experiment in the absence of enzyme. The α2,3-trans-sialidase activity of the enzyme, while being highly significant at pH 4.5, was completely lost at pH 8.0. We analyzed the regioselectivity in reactions **2** and **3**. Unlike 3′-sialyllactose, the 6′-regioisomeric substrate was not hydrolyzed by ∇3PdST, even at the low pH of 4.5 that was shown to favor a pronounced α2,3-sialidase activity (Table III). We also tested trans-sialylation from 6′-sialyllactose to oNP-βGal at both pH 4.5 and pH 8.0, but did not observe any. These findings imply a large preference of ∇3PdST for cleaving α2,3- when compared with α2,6-sialosidic linkages, fully consistent with the proposed categorization of the enzyme based on the regioselectivity of the sialyltransfer. Finally, when assayed in the absence of acceptor substrate, ∇3PdST displayed high activity for the hydrolysis of CMP-Neu5Ac (reaction **4**). Note that CMP-Neu5Ac was also hydrolyzed in the absence of enzyme. The enzymatic hydrolysis was, however, $>10^3$-fold increased compared with the uncatalyzed rate of $5.7 \cdot 10^{-5}$ mM/min.

The role of Thr-116 analyzed with site-directed mutagenesis

We built homology models of PdST in the apo-form and in a ternary complex with CMP-Neu5Ac and lactose bound. The model of the apo-form was obtained directly from the experimental structure of apo-PmST1 (M144D mutant; PDB code: 3S44). The model of the ternary complex was generated as a hybrid of several PmST1-ligand template structures (Supplementary data, Methods and Figure S7). Except for residue replacement at position 116, the modeled active sites of PdST in apo- and ligand-bound form superimpose almost perfectly with the corresponding active-site structures of PmST1 (Figure 3). The model also suggests that despite the presence of Thr^{116} PdST accommodates lactose and CMP-Neu5Ac in their respective binding sites in a highly similar way as PmST1.

To examine the biological significance of the Ser→Thr substitution within the natural YDDGS/T-motif of PdST, we reverted the amino acid exchange through creation of a T116S site-directed mutant of ∇3PdST. Residue numbering of PdST is used. The purified mutant was assayed in reactions **1** to **4** as described for the wild-time enzyme (see *Regioselectivity of sialyltransfer and demonstration of catalytic mutifunctionality of ∇3PdST*), and we summarize the results in Table III where specific activities of the two forms of ∇3PdST are compared. Even though differences between T116S mutant and the wild-type enzyme were rather subtle, it is clear from Table III that substitution of Thr^{116} by Ser was not functionally silent in ∇3PdST. The T116S mutant had a 1.6-fold lower sialyltransferase activity than the wild-type enzyme. Its α2,3-sialidase and α2,3-trans-sialidase activities, on the contrary, were enhanced substantially when compared with wild-type ∇3PdST. Taking the ratio between (trans)-sialidase (pH 4.5) and sialyltransferase (pH 8.0) activities as a parameter of enzyme selectivity, therefore, replacement of Thr^{116} resulted in a marked change in reaction preference so that the "side activity" was now equal to or even slightly favored over the canonical sialyltransferase activity in the mutated ∇3PdST. The CMP-Neu5Ac hydrolase activity was not affected by substitution of Thr^{116} by Ser. However, the overall picture emerging from Table III is that the T116 mutant is clearly a worse sialyltransferase than the wild-type enzyme, first of all because of its lower specific transferase activity, but secondly also because of a non-favorable change in reaction selectivity caused by the site-directed substitution. In terms of physiological function as α2,3-sialyltransferase, therefore, there might be good reason for PdST to have Thr^{116} instead of Ser. In terms of practical application, enzymatic synthesis of sialosides would also benefit from a biocatalyst whose main synthetic activity is not compromized by a variety of side

Table III. Specific activities of wild-type and T116S forms of ∇3PdST in different reactions catalyzed (Scheme 1)

	Donor	Acceptor	pH	∇3PdST (U/mg)	∇3PdST T116S (U/mg)
α2,3-Sialyltransferase activity	CMP-Neu5Ac	Lactose	8.0	5.7	3.5
α2,3-Sialyltransferase activity	CMP-Neu5Ac	oNP-βGal	8.0	5.9	3.8
Hydrolase activity	CMP-Neu5Ac	—	8.0	3.7	4.2
α2,3-Sialidase activity	3′-Sialyllactose	—	8.0	0.02	0.05
			4.5	0.5	1.3
α2,3-Trans-sialidase activity	3′-Sialyllactose	oNP-βGal	8.0	n.d.	n.d.
			4.5	1.0	4.0

n.d., not detectable

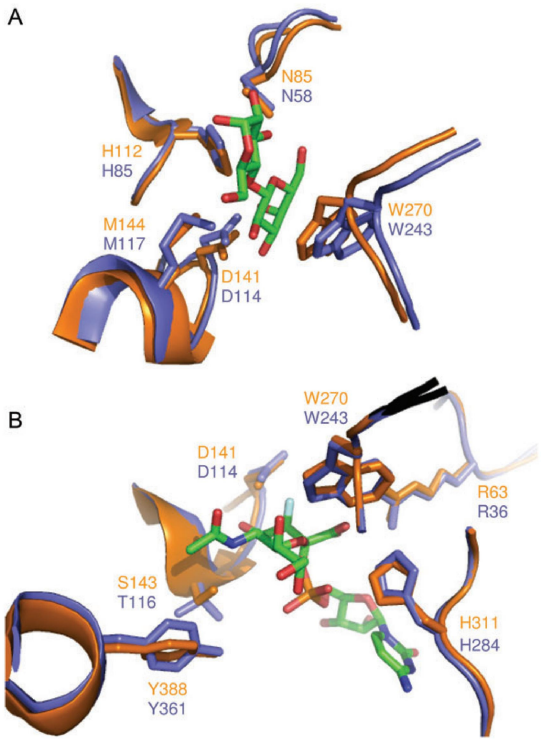

Fig. 3. Close-up views of the substrate-binding site in the modeled structure of PdST and in the experimental structure of PmST1. (**A**) Acceptor-binding site in an overlay of PdST (slate) and PmST1 (orange, PDB code 2ILV). Lactose is shown (colored by element). (**B**) Donor-binding site in an overlay of PdST (slate) and PmST1 (orange, PDB code 2IHJ). CMP-3F(a)Neu5Ac is shown (colored by element). The homology model of PdST is in the closed conformation and was obtained using structure modeling with the program YASARA. Residues, interacting with the ligands, are shown (Ni et al. 2007).

activities. Preference would therefore be given to wild-type ∇3PdST featuring a threonine as residue 116.

We determined apparent kinetic parameters (k_{cat}, K_M) of wild-type ∇3PdST and T116S mutant for sialyltransfer from CMP-Neu5Ac to oNP-βGal as acceptor. Initial rates were measured at pH 8.0 applying variable CMP-Neu5Ac concentration, while the oNP-βGal concentration was constant at 10.0 mM. The K_M of wild-type enzyme for CMP-Neu5Ac was 1.1 ± 0.1 mM, whereas that of T116S mutant was 0.25 ± 0.01 mM. The 4.5-fold increase in apparent affinity for CMP-Neu5Ac binding ($1/K_M$) caused by the mutation of Thr^{116} was contrasted by a decrease in similar magnitude (5.3-fold) in the catalytic constant k_{cat} which was 3 s^{-1} in the T116S mutant and 16 s^{-1} in the wild-type enzyme. Because effects of the mutation on k_{cat} and K_M compensate each other, the catalytic efficiency of CMP-Neu5Ac utilization (k_{cat}/K_M) remains largely unaltered by the site-directed substitution of Thr^{116}. What the mutation clearly does, however, is that it introduces a subtle change in the balance between tightness of substrate binding and speed of catalytic turnover in PdST. Optimization of k_{cat} and K_M at a given catalytic efficiency is considered to be important for the physiological function of enzymes under physiological boundary conditions (Fersht 1998). Looking at sialyltransferases of family GT-80 as a whole, two groups of enzymes can be distinguished according to K_M for CMP-Neu5Ac. The high-K_M low-affinity group comprises PdST as well as PmST1 (Yu et al. 2005) and the α2,6-sialyltransferases (Yamamoto et al. 1996, 2007; Sun et al. 2008; Mine et al. 2010). The high-affinity group comprises α2,3-sialyltransferases that show K_M values lowered by more than a magnitude order in comparison with the other enzyme group's typical K_M values (Li et al. 2007; Tsukamoto et al. 2007).

Enzyme application for synthesis: sialylation of oNP-βGal

We compared wild-type enzyme and T116S mutant as catalysts for the sialylation of oNP-βGal from CMP-Neu5Ac. All compounds involved in the reaction were analyzed, and Figure 4 shows the change of their concentrations over time. Reaction of wild-type ∇3PdST was characterized by fast consumption of the CMP-Neu5Ac donor substrate that was complete within ∼10 min. The utilization of CMP-Neu5Ac resulted in release of the equivalent amount of CMP. The oNP-βGal acceptor was also converted, however, to a lower completeness (∼80%) than CMP-Neu5Ac. A significant portion of CMP-Neu5Ac was therefore lost to non-productive transformation via hydrolysis. Concomitant with oNP-βGal consumption a new compound appeared whose experimental mass of 592 Da was consistent with a singly sialylated oNP-βGal molecule. Considering the clear separation of 3′- and 6′-sialyllactose in HPAE-PAD (Supplementary data, Figure S4), we think that had the sialylation of oNP-βGal resulted in formation of different product regioisomers, the applied analytical method would have detected it. However, this was not the case, and nuclear magnetic resonance (NMR) analysis (nuclear overhauser enhancement spectroscopy (NOESY) and heteronuclear multiple bond correlation (HMBC)) confirmed the sialylation product to be solely Neu5Acα2,3Gal-oNP (Supplementary data, Figure S6). Reactions of wild-type enzyme and T116S mutant yielded the same transfer product.

Figure 4 shows that conversion of CMP-Neu5Ac was slowed down under conditions in which wild-type enzyme had been replaced by T116S mutant in exactly the same molar concentration. Enzyme-specific activity, which is lower in T116S mutant when compared with wild-type ∇3PdST, provides a plausible explanation for the different transformation rates at reaction start. However, the reaction time course of the T116S mutant was furthermore distinct in that it featured a clear leveling-off in the transformation rate already at relatively low levels of conversion of CMP-Neu5Ac (∼50%). This kinetic behavior was clearly unexpected, considering that the mutant shows a comparably low K_M for CMP-Neu5Ac (see *The role of Thr-116 analyzed with site-directed mutagenesis* section). It could therefore indicate an issue of product inhibition in the mutant that is not present in wild-type enzyme. Another interesting consequence of substituting Thr^{116} by Ser was in lowering the yield of sialylation product, presumably due to enhanced utilization of the donor substrate for non-productive hydrolysis by the mutant when compared with the wild-type enzyme. Overall, the productivity of the wild-type enzyme in the sialylation of oNP-βGal was about three times that of the T116S mutant.

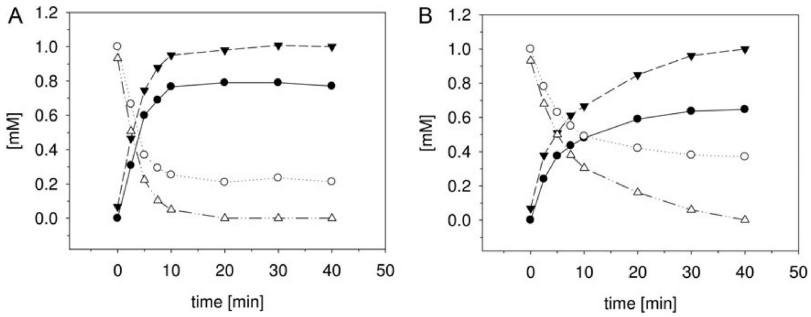

Fig. 4. Time course of the enzymatic synthesis of Neu5Acα2,3Gal-oNP using wild-type ∇3PdST (**A**) and the T116S mutant of the enzyme (**B**). The reaction mixture (20 µL), containing 1 mM CMP-Neu5Ac, 1 mM oNP-βGal, 0.5 µM enzyme, 15 µM bovine serum albumin (BSA) in 50 mM phosphate buffer, pH 8.0, was incubated at 25°C. The reaction in samples taken at certain times was stopped by addition of ice-cold acetonitrile (40 µL). After centrifugation, the samples were analyzed by reversed-phase ion-pairing chromatography (see *Materials and methods*). oNP-βGal, open circle; Neu5Acα2,3Gal-oNP, filled circle; CMP-Neu5Ac, open triangle; CMP, closed reverse triangle.

Two additional characteristics of the reaction time courses in Figure 4 are worth pointing out. First, the sialyltransfer product was not degraded, even at extended incubation times long after CMP-Neu5Ac had been used up. It seems, therefore, that under the applied conditions of pH 8.0, the enzymes' sialidase activity does not interfere with product stability. Second, the molar ratios of substrates consumed (CMP-Neu5Ac/oNP-βGal) and products formed (CMP/Neu5Acα2,3Gal-oNP) were constant throughout the course of reaction. The result implies that the ratio of sialyltransferase (r_{TR}) and donor substrate hydrolysis (r_H) rates was not variable with time or progress of the reaction. Competition between sialyltransfer and hydrolysis is therefore not determined at the level of binding of the oNP-βGal acceptor, as this would require that hydrolysis gradually gain in importance as lactose is depleted from the reaction. Rather unexpectedly, therefore, partial loss of CMP-Neu5Ac to reaction with water must probably be ascribed to an alternative "hydrolysis-only" mode of accommodation of CMP-Neu5Ac at the donor substrate-binding site of PdST. A recent study of PmST1 has shown that hydrolysis of CMP-Neu5Ac proceeded with two different, inverting and retaining, stereochemical outcomes in the Neu5Ac product. Therefore, this suggests that donor substrate hydrolysis might differ mechanistically from the "normal use" of CMP-Neu5Ac for sialyltransfer (Sugiarto et al. 2012).

Discussion

PdST: a new α2,3-selective sialyltransferase from P. dagmatis

Using sequence similarity to PmST1, we have identified a previously uncharacterized gene from *P. dagmatis* and show here that the protein encoded by it displays sialyltransferase activity. The enzyme PdST is regioselective for sialylating the 3-OH of D-galactose or of terminal β-galactosyl residues in different acceptor substrates using CMP-Neu5Ac as the donor. Only when the pH was decreased to pH 4.5, which is far below the optimum pH for sialyltransfer (pH 8.0), did the regioselectivity of PdST become slightly relaxed so that a small amount (5–7%) of α2,6-sialoside was also formed next to the predominant α2,3-sialosidic product. PdST is therefore different from PmST1 whose regioselectivity for the sialylation of the β-D-galactosyl moiety in a 4-methylumbelliferyl-β-D-lactoside acceptor (LacβMU) was reported to undergo complete switch from α2,3 to α2,6 on lowering the pH from 8.5 to 4.5 (Yu et al. 2005). Thr^{116} is the single "second-shell" residue in which the catalytic center of PdST differs from that of PmST1 (Figure 3B). Interestingly, therefore, substitution of Thr^{116} by Ser resulted in a four-fold enhancement of α2,6- when compared with α2,3-sialyltransfer at low pH. Crystal structures of PmST1 were determined only at pH conditions where the enzyme is exclusively active as α2,3-sialyltransferase, thus precluding a detailed structural interpretation of the pH-dependent switch in regioselectivity (Ni et al. 2006, 2007). However, we notice that His^{112} is a candidate residue in the PmST1-binding site for D-galactose/β-D-galactosyl (Figure 3A) that might undergo ionization in the relevant pH range (pH 4.5–6.5) and whose protonation state could decisively influence the positioning of the sialyl acceptor substrate. It was shown in the structure of PmST1 that His^{112} forms a hydrogen bond with the 4′-OH of β-D-galactosyl in lactose and that it is also within hydrogen bonding distance to Asp^{141} (Ni et al. 2007). The histidine was proposed to thus underpin the aspartate's catalytic function as the general base. The decrease in overall sialyltransferase activity in PmST1 and PdST in the pH range below 6.5 might, therefore, be explained by a pH effect on their respective Asp-His dyad in the active site (Figure 3A). From the crystal structure, it is also known, that in PmST1, Ser^{143} (equivalent to Thr^{116} of PdST) forms a hydrogen bond to the *N*-acetyl group of Neu5Ac (Figure 3B). Alteration of PdST regioselectivity in consequence of substitution of Thr^{116} by Ser supports the suggestion that positioning of the sialyl donor substrate also has an important influence on site preference of the enzymatic reaction.

Peculiarities of the acceptor substrate specificity of PdST appear to be largely due to Trp^{243}, which in structure model stacks against the B face of the β-galactosyl ring. D-Glucose is not an acceptor substrate, most probably because its equatorial 4-OH prevents the stacking interaction with Trp^{243}. The position of Trp^{243} is also not compatible with the accommodation of a bulky α-galactoside at the acceptor-binding site, consistent with the finding that α-D-galactosyl in raffinose is not sialylated

by the enzyme. However, the comparably small α-methyl-D-galactoside is a substrate of PmST1 (Yu et al. 2005). α/β-Galactoside α2,3-sialtransferases of family GT-80 lack the equivalent tryptophan in their sequences, as shown in Supplementary data, Figure S8. Unlike PdST and PmST1, these enzymes are unspecific with respect to the anomeric configuration of the sialylated galactoside and also show activity with D-glucose and D-glucosides as acceptors (Tsukamoto et al. 2007).

PdST is a multifunctional α2,3-sialyltransferase and a useful sialylation catalyst

Next to its major α2,3-sialyltransferase activity, PdST also displays pronounced hydrolase activity against CMP-Neu5Ac. Donor substrate hydrolysis occurs at a high rate when no acceptor substrate is present (Table III). It is somewhat attenuated, but still significant as a side reaction under conditions of sialyltransfer (Figure 4). PdST is also active as α2,3-sialidase and α2,3-trans-sialidase (Scheme 1, Table III). Each reaction catalyzed by PdST shows a distinct pH-dependency (Table III) which is consistent with reported evidence on other bacterial sialyltransferases (Yu et al. 2005; Cheng et al. 2010; Mine et al. 2010). Mechanistically, the catalytic multifunctionality of sialyltransferases is not fully understood and a catalytic nucleophile for the α2,3-trans-sialidase reaction, expected from studies of natural trans-sialidases (Schenkman et al. 1991; Damager et al. 2008), has so far remained elusive (Cheng et al. 2010). The exact role of key active-site residues might vary according to reaction catalyzed (Ni et al. 2007; Sugiarto et al. 2011). The microenvironment of the proposed general base catalyst (Asp^{141} in PmST1; Asp^{114} in PdST; Table I) might exercise control over both reactivity and selectivity. PdST is clearly a better sialyltransferase when the nearby residue 116 is a threonine, not a serine (Table III). The M144D mutant of PmST1 shows a drastically decreased α2,3-sialidase activity when compared with the wild-type enzyme (Sugiarto et al. 2012). Residues flanking the catalytic Asp might contribute to fine-tuning of enzyme function through their involvement in the large domain closure movement that occurs in PmST1 upon donor substrate binding and results in the development of a fully functional acceptor-binding site. In particular, Ser^{143} (equivalent to Thr^{116} in PdST) establishes a hydrogen bond with Tyr^{388} from the opposite domain in the closed protein conformation (Ni et al. 2006). Interestingly, the M144D mutant was "locked" in the open conformation even in the presence of the donor substrate (Sugiarto et al. 2012).

A major limitation on the application of bacterial sialyltransferases to the synthesis of sialosides is presented by the different hydrolysis side reactions catalyzed (Shaikh and Withers 2008). Using PdST, degradation of CMP-Neu5Ac affects the transformation efficiency much more than that of the sialyltransfer product(s) formed. High yields (≥80%) of selectively monosialylated oNP-βGal were nevertheless obtained through the proper selection of reaction conditions (high pH, short incubation times; Figure 4). However, analysis of the competition between utilization of CMP-Neu5Ac for sialyltransfer and hydrolysis in dependence of the reaction course in Figure 4 provides good evidence in support of the suggestion that reasonably complete suppression of donor substrate hydrolysis in PdST would probably be best achieved through targeted protein engineering rather than reaction optimization. Note that the sialidase activity of α2,3-sialyltransferase from *P. phosphoreum*, however, could be successfully controlled by the use of organic solvent (Nagashima et al. 2012). There are several reports on engineered variants of sialyltransferases with potentially improved properties for biocatalytic synthesis. The M144D mutant of PmST1 showed strongly reduced hydrolase activity (Sugiarto et al. 2012). And an E271F/R313Y double mutant of PmST1 was essentially devoid of sialidase activity (Sugiarto et al. 2011). A similar observation is reported for an E342A mutant of α2,3-sialyltransferase from *P. phosphoreum* (Kajiwara et al. 2012). Using the performance of the corresponding wild-type enzyme(s) as a benchmark (Yu et al. 2005; Yu, Chokhawala, et al. 2006; Yu, Huang, et al. 2006; Tsukamoto et al. 2007), protein engineering of sialyltransferases is presented with the challenge of avoiding trade-off between selectivity gain and activity loss. Evidence for PdST that a seemingly minor structural change caused by the substitution of Thr^{116} by Ser resulted in distinct properties during enzymatic synthesis (Figure 4) underscores the need to still explore a more comprehensive variety of enzyme mutants in the development of an "ideal" sialylation biocatalyst.

Considering that we have focused our analyses and discussions exclusively on sialyltransferases of family GT-80, it is important to emphasize that biocatalytic synthesis of sialosides has also been performed with enzymes of other GT families. For example, preparative synthetic use of sialyltransferases is by far not restricted to enzymes adopting the GT-B fold. Bacterial sialyltransferases from family GT-42 (Cheng et al. 2008; Schur et al. 2012) and GT-52 (Gilbert et al. 1996; Thon et al. 2011) have been applied. Members of family GT-42 display a GT-A fold (Chiu et al. 2004), whereas members of family GT-52 have a unique GT-B fold featuring a novel domain swap to create a functional homodimeric form (Lin et al. 2011). Moreover, mammalian sialyltransferases from family GT-29 have also been employed for synthesis (Blixt et al. 2002; Yu, Chokhawala, et al. 2006). All the different enzymes have their individual advantages and limitations (e.g. donor and acceptor substrate tolerance, enzyme expression level and enzyme stability) for producing glycoconjugates and sialosides (Watson et al. 2011; Malekan et al. 2013). Together, they provide access to a broad portfolio of natural and non-natural carbohydrate structures. However, also from this perspective, there is still need to broaden the current selection of sialylation biocatalysts. As the use of glycosyltransferases is currently gaining a strong momentum (Palcic 2011; Bojarova et al. 2013), a detailed understanding of structure–function relationships will be of great importance for their further development.

Summarizing, we have presented a multifunctional, yet regioselective α2,3-sialyltransferase from *P. dagmatis*. PdST is the first sialyltransferase to carry a threonine instead of a serine in the highly conserved YDDGS-motif, and this natural mutation is shown to be beneficial for high-yielding synthesis of α2,3-sialosides.

Materials and methods

Chemicals

Ampicillin, IPTG, imidazole, BSA and acetonitrile were from Carl-Roth (Austria). CMP-Neu5Ac, lactose, D-galactose,

D-glucose, D-mannose, lactulose, sucrose and raffinose were obtained from Sigma-Aldrich (Austria) in the highest purity available. Moreover, ammonium acetate, tetrabutylammonium hydrogen sulfate, NaOH solution (50% in H_2O) and sodium acetate in the HPLC grade were also from Sigma-Aldrich oNP-lactose, oNP-β-D-galactose (oNP-βGal), L-fucose, *N*-acetyl lactosamine and 3′- and 6′-sialyllactose sodium salt were from Carbosynth (UK).

DNA techniques

The synthetic gene (∇27PdST, Mr Gene GmbH, Germany) coding for the conserved hypothetical protein from *P. dagmatis* strain ATCC43325 (PdST) and an N-terminal elongation of 27 amino acids was cloned through the *Nde*I and *Hin*dIII restriction sites into pET23a(+) (Novagen, Germany) yielding the plasmid pET23a(+)_∇27PdST. For rapid purification, a hexahistidine-tag was C-terminally fused over a 7 amino acid linker region to the protein. PdST and ∇3PdST, which codes for PdST and an N-terminal elongation of 3 amino acids, were amplified from pET23a(+)_∇27PdST. The genomic DNA from *P. dagmatis* was ordered from DSMZ (DSM No. 22969).

Protein expression and purification

The protein expression started by addition of IPTG after the culture reached an optical density of 1.0 and was cooled down to 30°C. Cells were harvested 4.5 h after the induction. Cell pellet was resuspended in binding buffer (30 mM sodium phosphate, 300 mM NaCl, 15 mM imidazol, 10% glycerol, pH 7.4) and disrupted by sonication. The cell lysate was cleared by centrifugation and filtration. The protein was purified in two steps: HisTrap HP FF and HiTrap Q HP FF (GE Healthcare, Germany). Purified enzyme was aliquoted and stored at −70°C. Gel filtration analysis was performed on a Superose 6, 10/300 GL column (GE Healthcare) using a multicomponent buffer system (L-malic acid, MES, Tris) at 0.1 M and pH 6.5 which was supplemented with 1% glycerol and 10 mM NaCl (Newman 2004).

Standard sialyltransferase activity assay

The reaction mixture consisted of 1 mM CMP-Neu5Ac, 1 mM of lactose and enzyme solution in 20 µL of 50 mM sodium phosphate buffer, pH 8.0, containing 15 µM BSA. The enzymatic reaction was carried out at 25°C and 400 rpm. All assays were performed in duplicate. The enzymatic reaction was stopped after 2 min of incubation by quenching on ice and addition of 40 µL of ice-cold acetonitrile. After dilution, 10 µL were analyzed by reverse-phase ion-pair HPLC on an Agilent Technologies 1200 series system (see Supplementary data, Methods for more details).

Analysis of acceptor substrate specificity and influence of additives on the sialyltransferase activity

Unless otherwise mentioned, the enzymatic reaction and analysis were carried out as described for the standard sialyltransferase activity assay. D-Galactose, D-glucose, D-mannose, L-fucose, lactose, *N*-acetyl-D-lactosamine, lactulose, sucrose, raffinose, oNP-βGal and oNP-lactose were tested as acceptor substrates. The reaction mixture consisted of 1 mM CMP-Neu5Ac, 1 mM acceptor substrate and 1 µM purified sialyltransferase (∇3PdST) in 50 mM sodium phosphate buffer, pH 8.0, containing 15 µM BSA. The influence of Triton X-100 (0–1%), NaCl (0–500 mM), CMP (0–20 mM) and CTP (0–20 mM) on the enzymatic activity was investigated. The apparent kinetic parameters for CMP-Neu5Ac were determined using 0.1–10 mM CMP-Neu5Ac, 10 mM oNP-βGal and 0.7 µM of purified sialyltransferase (∇3PdST variant) in 20 µL of 50 mM sodium phosphate buffer, pH 8.0, containing 15 µM BSA.

Identification of sialyltransferase assay products by HPLC-ESI-IT-MS, HPAE-PAD and NMR

The sialyltransferase assay products (3′- and/or 6′-sialyllactose and Neu5Acα2,3Gal-oNP) were identified by HPLC-ESI-IT-MS on an Agilent Technologies 1100 Series system equipped with a ZIC®-HILIC column (100 × 4.6 mm, 5 µm; dichrom GmbH, Germany). Negative ionization mode and single ion monitoring at 631 and 592 Da, respectively, were used for detection. 3′- and 6′-sialyllactose sodium salt (Carbosynth) were used as standards. Furthermore, 3′- and 6′-sialyllactose were separated and quantified by HPAE chromatography on a Dionex BioLC system equipped with a CarboPac® PA200 column (3 × 250 mm; Thermo Fisher Scientific Inc., Dionex). NOESY1D and HMBC spectra were recorded to determine the regioselectivity of Neu5Acα2,3Gal-oNP (see Supplementary data, Methods for more details).

CMP-Neu5Ac hydrolase, α2,3-sialidase and α2,3-trans-sialidase activity measurement

The reaction mixture for the determination of CMP-Neu5Ac hydrolase activity consisted of 1.0 mM CMP-Neu5Ac with or without 0.5 µM purified enzyme (∇3PdST variant) in 50 mM sodium phosphate buffer, pH 8.0, containing 15 µM BSA. Reactions were allowed to proceed for 0, 5, 10, 15, 30 and 60 min. The reaction products were analyzed by HPLC as described for the standard sialyltransferase activity assay.

The reaction mixture for the determination of α2,3-sialidase activity consisted of 1.5 mM 3′-sialyllactose with or without 1 µM purified enzyme (∇3PdST variant) in buffer containing 15 µM BSA. 50 mM citric buffer and 50 mM sodium phosphate buffer was used at pH 4.5 and 8.0, respectively. The reaction products were analyzed by HPAE chromatography on a Dionex BioLC system (see *Identification of sialyltransferase assay products by HPLC-ESI-IT-MS, HPAE-PAD and NMR*).

The reaction mixture for the determination of α2,3-trans-sialidase activity consisted of 1.58 mM 3′-sialyllactose as donor, 1.58 mM oNP-βGal as an acceptor and 1 µM purified enzyme (∇3PdST variant) in buffer containing 15 µM BSA. 50 mM citric buffer and 50 mM sodium phosphate buffer was used at pH 4.5 and 8.0, respectively. The reaction products were analyzed by HPLC as described for the standard sialyltransferase activity assay, whereas the decrease in the substrate (oNP-βGal) and the increase in product were followed.

Structural modeling of PdST

Homology models were built using the program YASARA (www.yasara.org; Krieger et al. 2002, 2004). Initially, the PdST sequence was submitted to modeling in a fully automated procedure using the provided hm_build macro. A total of seven

suitable templates were identified and used during the modeling. Due to the low quality of the hybrid model, the final homology model was based on a single template structure (PDB code 3S44, *z*-score: 0.388). In order to generate a closed conformation model, a set of templates (PDB codes: 2IHJ, 2IHK, 2IHZ, 2ILV, 2Z4T) with ligand(s) and/or substrate(s) bound in the active site was directly submitted to YASARA. A single template model based on the PDB code 2IHJ template was the best scoring model in this round (*z*-score: 0.294).

Supplementary Data

Supplementary data for this article is available online at http://glycob.oxfordjournals.org/.

Funding

This work was supported by the Federal Ministry of Economy, Family and Youth (BMWFJ), the Federal Ministry of Traffic, Innovation and Technology (BMVIT), the Styrian Business Promotion Agency, SFG, the Standortagentur Tirol and ZIT-Technology Agency of the City of Vienna through the COMET-Funding Programme managed by the Austrian Research Promotion Agency FFG.

Acknowledgements

The authors gratefully acknowledge Dr. Hansjörg Weber from the Graz University of Technology for the NMR analysis.

Conflict of interest

None declared.

Abbreviations

BSA, bovine serum albumin; CMP, cytidine-5′-monophosphate; CTP, cytidine-5'-triphosphate; ESI, electrospray ionization; HMBC, heteronuclear multiple bond correlation; HPAE, high-performance anion exchange; HPAE-PAD, high-performance anion exchange pulsed amperometric detection (HPAE-PAD); HPLC, high-performance liquid chromatography; HPLC-ESI-IT-MS, high-performance liquid chromatography electrospray ionization ion trap-mass spectrometry; IPTG, isopropyl-beta-D-thiogalactopyranoside; IT-MS, ion trap-mass spectrometry; MS, mass spectrometry; Neu5Ac, N-acetyl-neuraminic; NMR, nuclear magnetic resonance; NOESY, nuclear overhauser enhancement spectroscopy; OD, optical density; PAD, pulsed amperometric detection; SDS-PAGE, sodium dodecyl sulfate polyacrylamide gel electrophoresis.

References

Blixt O, Allin K, Pereira L, Datta A, Paulson JC. 2002. Efficient chemoenzymatic synthesis of O-linked sialyl oligosaccharides. *J Am Chem Soc*. 124:5739–5746.

Bojarova P, Rosencrantz RR, Elling L, Kren V. 2013. Enzymatic glycosylation of multivalent scaffolds. *Chem Soc Rev*. 42:4774–4797.

Cheng J, Huang S, Yu H, Li Y, Lau K, Chen X. 2010. Trans-sialidase activity of *Photobacterium damselae* α2,6-sialyltransferase and its application in the synthesis of sialosides. *Glycobiology*. 20:260–268.

Cheng J, Yu H, Lau K, Huang S, Chokhawala H, Li Y, Kumar V, Chen X. 2008. Multifunctionality of *Campylobacter jejuni* sialyltransferase CstII: Characterization of GD3/GT3 oligosaccharide synthase, GD3 oligosaccharide sialidase, and trans-sialidase activities. *Glycobiology*. 18:686–697.

Chiu CP, Watts AG, Lairson LL, Gilbert M, Lim D, Wakarchuk WW, Withers SG, Strynadka NCJ. 2004. Structural analysis of the sialyltransferase CstII from *Campylobacter jejuni* in complex with a substrate analog. *Nature Struct Mol Biol*. 11:163–170.

Coutinho PM, Deleury E, Davies GJ, Henrissat B. 2003. An evolving hierarchical family classification for glycosyltransferases. *J Mol Biol*. 328:307–317.

Damager I, Buchini S, Amaya MF, Buschiazzo A, Alzari P, Frasch AC, Watts A, Withers SG. 2008. Kinetic and mechanistic analysis of *Trypanosoma cruzi* trans-sialidase reveals a classical Ping-Pong mechanism with acid/base catalysis. *Biochemistry*. 47:3507–3512.

Fersht A. 1998. *Structure and Mechanism in Protein Science: A Guide to Enzyme Catalysis and Protein Folding*. 1st ed. New York: Freeman, W.H. & Company.

Gilbert M, Watson DC, Cunningham AM, Jennings MP, Young NM, Wakarchuk WW. 1996. Cloning of the lipooligosaccharide α2,3-sialyltransferase from the bacterial pathogens *Neisseria meningitidis* and *Neisseria gonorrhoeae*. *J Biol Chem*. 271:28271–28276.

Iwatani T, Okino N, Sakakura M, Kajiwara H, Takakura Y, Kimura M, Ito M, Yamamoto T, Kakuta Y. 2009. Crystal structure of α/β-galactoside α-2,3-sialyltransferase from a luminous marine bacterium, *Photobacterium phosphoreum*. *FEBS Lett*. 583:2083–2087.

Kajiwara H, Katayama S, Kakuta Y, Okino N, Ito M, Mine T, Yamamoto T. 2012. Loss-of-function mutation in bi-functional marine bacterial sialyltransferase. *Biosci Biotechnol Biochem*. 76:1639–1644.

Kakuta Y, Okino N, Kajiwara H, Ichikawa M, Takakura Y, Ito M, Yamamoto T. 2008. Crystal structure of Vibrionaceae *Photobacterium* sp. JT-ISH-224 α-2,6-sialyltransferase in a ternary complex with donor product CMP and acceptor substrate lactose: Catalytic mechanism and substrate recognition. *Glycobiology*. 18:66–73.

Kondadi PK, Rossi M, Twelkmeyer B, Schur MJ, Li J, Schott T, Paulin L, Auvinen P, Hänninen ML, Schweda EKH, et al. 2012. Identification and characterization of a lipopolysaccharide α2,3-sialyltransferase from the human pathogen *Helicobacter bizzozeronii*. *J Bacteriol*. 194:2540–2550.

Krieger E, Darden T, Nabuurs SB, Finkelstein A, Vriend G. 2004. Making optimal use of empirical energy functions: Force-field parameterization in crystal space. *Proteins*. 57:678–683.

Krieger E, Koraimann G, Vriend G. 2002. Increasing the precision of comparative models with YASARA NOVA-a self-parameterizing force field. *Proteins*. 47:393–402.

Lau K, Yu H, Thon V, Khedri Z, Leon ME, Tran BK, Chen X. 2011. Sequential two-step multienzyme synthesis of tumor-associated sialyl T-antigens and derivatives. *Org Biomol Chem*. 9:2784–2789.

Li Y, Chen X. 2012. Sialic acid metabolism and sialyltransferases: natural functions and applications. *Appl Microbiol Biotechnol*. 94:887–905.

Li Y, Sun M, Huang S, Yu H, Chokhawala HA, Thon V, Chen X. 2007. The Hd0053 gene of *Haemophilus ducreyi* encodes an α2,3-sialyltransferase. *Biochem Biophys Res Commun*. 361:555–560.

Lin LYC, Rakic B, Chiu CPC, Lameignere E, Wakarchuk WW, Withers SG, Strynadka NCJ. 2011. Structure and mechanism of the lipooligosaccharide sialyltransferase from *Neisseria meningitidis*. *J Biol Chem*. 286:37237–37248.

Malekan H, Fung G, Thon V, Khedri Z, Yu H, Qu J, Li Y, Ding L, Lam KS, Chen X. 2013. One-pot multi-enzyme (OPME) chemoenzymatic synthesis of sialyl-Tn-MUC1 and sialyl-T-MUC1 glycopeptides containing natural or non-natural sialic acid. *Bioorg Med Chem*. 21:4778–4785.

Milac AL, Buchete NV, Fritz TA, Hummer G, Tabak LA. 2007. Substrate-induced conformational changes and dynamics of UDP-N-acetylgalactosamine: polypeptide N-acetylgalactosaminyltransferase-2. *J Mol Biol*. 373:439–451.

Mine T, Katayama S, Kajiwara H, Tsunashima M, Tsukamoto H, Takakura Y, Yamamoto T. 2010. An α2,6-sialyltransferase cloned from *Photobacterium leiognathi* strain JT-SHIZ-119 shows both sialyltransferase and neuraminidase activity. *Glycobiology*. 20:158–165.

Nagashima I, Mine T, Yamamoto T, Shimizu H. 2012. Efficiency of organic solvents on the ability of α2,3-sialyltransferase from *Photobacterium* sp. JT-ISH-224 to control a hydrolysis side reaction. *Carbohydr Res*. 358:31–36.

Newman J. 2004. Novel buffer systems for macromolecular crystallization. *Acta Crystallogr Sect D*. 60:610–612.

Ni L, Chokhawala HA, Cao H, Henning R, Ng L, Huang S, Yu H, Chen X, Fisher AJ. 2007. Crystal structures of *Pasteurella multocida* sialyltransferase complexes with acceptor and donor analogues reveal substrate binding sites and catalytic mechanism. *Biochemistry*. 46:6288–6298.

Ni L, Sun M, Yu H, Chokhawala H, Chen X, Fisher AJ. 2006. Cytidine 5′-monophosphate (CMP)-induced structural changes in a multifunctional sialyltransferase from *Pasteurella multocida*. *Biochemistry*. 45:2139–2148.

Oh TJ, Kim DH, Kang SY, Yamaguchi T, Sohng JK. 2011. Enzymatic synthesis of vancomycin derivatives using galactosyltransferase and sialyltransferase. *J Antibiot*. 64:103–109.

Palcic MM. 2011. Glycosyltransferases as biocatalysts. *Curr Opin Chem Biol*. 15:226–233.

Qasba PK, Ramakrishnan B, Boeggeman E. 2005. Substrate-induced conformational changes in glycosyltransferases. *Trends in Biochemical Sciences*. 30:53–62.

Schauer R. 2009. Sialic acids as regulators of molecular and cellular interactions. *Curr Opin Struct Biol*. 19:507–514.

Schenkman S, Jiang MS, Hart GW, Nussenzweig V. 1991. A novel cell surface trans-sialidase of *Trypanosoma cruzi* generates a stage-specific epitope required for invasion of mammalian cells. *Cell*. 65:1117–1125.

Schur MJ, Lameignere E, Strynadka NC, Wakarchuk WW. 2012. Characterization of α2,3- and α2,6-sialyltransferases from *Helicobacter acinonychis*. *Glycobiology*. 22:997–1006.

Scudder PR, Chantler EN. 1981. Glycosyltransferases of the human cervical epithelium II. Characterization of a CMP-*N*-acetylneuraminate: Galactosylglycoprotein sialyltransferase. *Biochim Biophys Acta Enzymol*. 660:136–141.

Shaikh FA, Withers SG. 2008. Teaching old enzymes new tricks: engineering and evolution of glycosidases and glycosyl transferases for improved glycoside synthesis. *Biochem Cell Biol*. 86:169–177.

Sugiarto G, Lau K, Li Y, Khedri Z, Yu H, Le DT, Chen X. 2011. Decreasing the sialidase activity of multifunctional *Pasteurella multocida* α2–3-sialyltransferase 1 (PmST1) by site-directed mutagenesis. *Mol BioSyst*. 7:3021–3027.

Sugiarto G, Lau K, Qu J, Li Y, Lim S, Mu S, Ames JB, Fisher AJ, Chen X. 2012. A sialyltransferase mutant with decreased donor hydrolysis and reduced sialidase activities for directly sialylating Lewis^{x}. *ACS Chem Biol*. 7:1232–1240.

Sun M, Li Y, Chokhawala HA, Henning R, Chen X. 2008. N-Terminal 112 amino acid residues are not required for the sialyltransferase activity of *Photobacterium damselae* α-2,6-sialyltransferase. *Biotechnol Lett*. 30:671–676.

Takakura Y, Tsukamoto H, Yamamoto T. 2007. Molecular cloning, expression and properties of an α/β-galactoside α2,3-sialyltransferase from *Vibrio* sp. JT-FAJ-16. *J Biochem*. 142:403–412.

Thon V, Lau K, Yu H, Tran BK, Chen X. 2011. PmST2: A novel *Pasteurella multocida* glycolipid α2,3-sialyltransferase. *Glycobiology*. 21:1206–1216.

Tsukamoto H, Takakura Y, Mine T, Yamamoto T. 2008. *Photobacterium* sp. JT-ISH-224 produces two sialyltransferases, α/β-galactoside α2,3-sialyltransferase and β-galactoside α2,6-sialyltransferase. *J Biochem*. 143: 187–197.

Tsukamoto H, Takakura Y, Yamamoto T. 2007. Purification, cloning, and expression of an α/β-galactoside α-2,3-sialyltransferase from a luminous marine bacterium, *Photobacterium phosphoreum*. *J Biol Chem*. 282:29794–29802.

Varki A. 2008. Sialic acids in human health and disease. *Trends Mol Med*. 14:351–360.

Watson DC, Leclerc S, Wakarchuk WW, Young NM. 2011. Enzymatic synthesis and properties of glycoconjugates with legionaminic acid as replacement for neuraminic acid. *Glycobiology*. 21:99–108.

Yamamoto T, Hamada Y, Ichikawa M, Kajiwara H, Mine T, Tsukamoto H, Takakura Y. 2007. A β-galactoside α2,6-sialyltransferase produced by a marine bacterium, *Photobacterium leiognathi* JT-SHIZ-145, is active at pH 8. *Glycobiology*. 17:1167–1174.

Yamamoto T, Ichikawa M, Takakura Y. 2008. Conserved amino acid sequences in the bacterial sialyltransferases belonging to glycosyltransferase family 80. *Biochem Biophys Res Commun*. 365:340–343.

Yamamoto T, Nakashizuka M, Kodama H, Kajihara Y, Terada I. 1996. Purification and characterization of a marine bacterial β-galactoside α2,6-sialyltransferase from *Photobacterium damselae* JT0160. *J Biochem*. 120:104–110.

Yamamoto T, Takakura Y, Tsukamoto H. 2006. Bacterial sialyltransferases. *Trends Glycosci Glycotechnol*. 18:253–265.

Yu H, Chokhawala HA, Huang S, Chen X. 2006. One-pot three-enzyme chemoenzymatic approach to the synthesis of sialosides containing natural and non-natural functionalities. *Nat Protocols*. 1:2485–2492.

Yu H, Chokhawala H, Karpel R, Yu H, Wu B, Zhang J, Zhang Y, Jia Q, Chen X. 2005. A multifunctional *Pasteurella multocida* sialyltransferase: A powerful tool for the synthesis of sialoside libraries. *J Am Chem Soc*. 127:17618–17619.

Yu H, Huang S, Chokhawala H, Sun M, Zheng H, Chen X. 2006. Highly efficient chemoenzymatic synthesis of naturally occurring and non-natural α-2,6-linked sialosides: A *P. damselae* α-2,6-sialyltransferase with extremely flexible donor−substrate specificity. *Angew Chem Int Ed*. 45:3938–3944.

Zhuo Y, Bellis SL. 2011. Emerging role of α2,6-sialic acid as a negative regulator of galectin binding and function. *J Biol Chem*. 286:5935–5941.

Supporting Information

Characterization of a multifunctional α2,3-sialyltransferase from *Pasteurella dagmatis*

Katharina Schmölzer[1], Doris Ribitsch[1], Tibor Czabany[2], Christiane Luley-Goedl[1], Deja Kokot[2], Andrzej Lyskowski[1], Sabine Zitzenbacher[1], Helmut Schwab[1,3], Bernd Nidetzky[1,2]

[1]*Austrian Centre of Industrial Biotechnology, Petersgasse 14, 8010 Graz, Austria*

Table of contents

General recombinant DNA techniques S3

Cloning, amplification from genomic DNA, sequencing, alignment S3-S4

Expression and purification S5-S6

Standard sialyltransferase activity assay S6

Acceptor substrate specificity, influence of additivies S7

Identification of sialyltransfer products by HPLC-ESI-IT-MS, HPAE-PAD and NMR S8

CMP-Neu5Ac hydrolase, α2,3-sialidase and α2,3-trans-sialidase activity S9

Figure S1. Chromatogram of purification of ∇3PdST via HisTrap HP FF. S11

Figure S2. Chromatogram of purification of ∇3PdST via HiTrap Q HP FF. S11

Figure S3. Gel filtration analysis of ∇3PdST. S12

Figure S4. Separation of 3'- and 6'-sialyllactose by HPAE chromatography. S13

Figure S5. HPLC analysis and UV-detection of acceptor substrate (oNP-βGal) and product (Neu5Acα2,3Gal-oNP) from a sialyltransferase and a trans-sialidase reaction. S14

Figure S6. NOESY1D spectrum and 1H spectrum of Neu5Acα2,3Gal-oNP. S15

Figure S7. Comparison of open and closed conformation model of PdST. S16

Figure S8. Structural interpretation of the specificity towards α- and/or β-galactosides. S17

Methods

General recombinant DNA techniques

All DNA manipulations described in this work were performed by standard methods (Sambrook et al 1989). The PCR was performed in a Gene Amp® PCR 2200 thermocycler (Applied Biosystems, USA). Digestion of DNA with restriction endonucleases (New England Biolabs, USA), dephosphorylation with alkaline phosphatase (Roche, Germany) and ligation with T4 DNA-ligase (Fermentas, Germany) were performed in accordance to the manufacturer's instructions. Plasmid Mini Kit from Qiagen (Germany) was used to prepare plasmid DNA. Plasmids and DNA fragments were purified by Qiagen DNA purification kits (Qiagen, Germany).

Cloning and modification of PdST

The synthetical gene (∇27PdST, Mr. Gene GmbH, Germany) coding for the conserved hypothetical protein from *Pasteurella dagmatis* strain ATCC 43325 (PdST) and an N-terminal elongation of 27 AA, was cloned through the *Nde*I and *Hind*III restriction sites into pET23a(+) (Novagen, Germany) yielding the plasmid pET23a(+)_mPdST2. For rapid purification, a 6xHisTag was C-terminally fused over a 7 AA linker region to the protein. PdST and ∇3PdST, which codes for PdST and an N-terminal elongation of 3 AA, were amplified from pET23a(+)_mPdST2. The PCR was carried out in 50 µL using 0.5 µM forward (5'-AGATACTCATATGACAATCTATTTAGATCCTGCTTCATTACCCAC-3' or 5'-AGATACTCATATGAAAACAATCACAATCTATTTAGATCCTGCTTCATT-3', respectively) and reverse primer (5'-CTGGAGAAGCTTTAACTGTTTTAAACTATCCCAAAAAATAATTTGAGATTTATC-3'), 0.2 mM dNTP-mix, 1.0 U Phusion DNA Polymerase

(Finnzymes, Finnland) and 1x reaction buffer provided by the supplier. The DNA amplification was performed in 25 cycles according to the instructions for the DNA polymerase. The PCR products were gel-purified and subcloned into the pJET1/blunt cloning vector (Fermentas, Germany). For expression in *E. coli*, the subcloned inserts were restricted with *Nde*I and *Hind*III and ligated into pET23a(+). The plasmids were confirmed by DNA sequencing and transformed into *E. coli* BL21_Gold(DE3).

Amplification of PdST from the genomic DNA

The genomic DNA from *P. dagmatis* was ordered from DSMZ (DSM No. 22969). The PCR was carried out in 50 µL using 0.5 µM forward (5'-AGATACTCATATGAACAAA AGCTCTCTCTCTCTTAAACTTATC-3') and reverse primer (5'-CTGGAGAAGCTT TAACTGTTTTAAACTATCCCAAAAAATAATTTGAGATTTATC-3'), 0.2 mM dNTP-mix, 1.0 U Phusion DNA Polymerase (Finnzymes, Finnland) and 1x reaction buffer provided by the supplier. The DNA amplification was performed in 30 cycles according to the instructions for the DNA polymerase.

DNA sequencing, alignments and deposition of sequence data

DNA was sequenced as custom service by Agowa (Germany). DNA analysis was performed with Vector NTI Suite 10 (Invitrogen, USA). BLAST search was carried out by the ExPASy (Expert Protein Analysis System) proteomics server of the Swiss Institute of Bioinformatics, and sequences of related proteins were aligned using the Clustal W program (Swiss EMBnet node server). The nucleotide sequence of PdST has been deposited in the GenBank database under accession number JX870648.

Protein expression and purification

50 mL LB-medium supplemented with 115 mg/L ampicillin were inoculated with freshly transformed cells and incubated overnight at 37 °C and 130 rpm on a rotary shaker (Certomat® BS-1 incubator, Sartorius). 10 ml of the overnight culture were transferred to a 1-L baffled shaking flask containing 200 mL of the same liquid medium and incubated at 37 °C, 130 rpm until an optical density (600 nm) of approximately 1.0 was reached. The culture was cooled down to 30 °C and protein production was induced by addition of IPTG at a final concentration of 0.1 mM. After a certain time of incubation (1 - 20 h) the cells were harvested by centrifugation at 4 °C, 5000 rpm for 15 min and stored at -20 °C. For protein purification, cell pellet from 1-L cell culture was resuspended in 10 mL binding buffer (30 mM sodium phosphate, 300 mM NaCl, 15 mM imidazol, 10% glycerol, pH 7.4) and disrupted by sonication using three-times 30-s pulses under ice cooling (cell disruptor from BRANSON Ultrasonics). The cell lysate was centrifuged at 13,000 rpm for 30 min and filtered *via* 0.45 µm and 0.2 µm filters. In a first step, the cleared cell lysate was loaded onto a HisTrap HP FF 5 mL column (GE Healthcare, Germany) at a flow rate of 2 mL/min. The column had been equilibrated with binding buffer. After a washing step of 10 column volumes, the enzyme was eluted with a linear gradient of 15 - 300 mM imidazol within 10 column volumes. Fractions of 3-mL were collected and analyzed by SDS-PAGE. Sialyltransferase containing fractions were pooled and dialyzed overnight against 20 mM Tris/HCl, 50 mM NaCl, pH 8.5. The enzyme solution was further applied onto a HiTrap Q HP FF 2x1 mL column (GE Healthcare, Germany) at a flow rate of 1 mL/min. The column had been equilibrated with 20 mM Tris/HCl, 50 mM NaCl, pH 8.5. After a washing step of 10 column volumes, the enzyme was eluted with a linear gradient of 0.05 – 1.0 M NaCl within 10 column volumes. Fractions of 1-mL were collected and analyzed by SDS-PAGE. Sialyltransferase

containing fractions were pooled and buffer was exchanged to 20 mM Tris/HCl, 150 mM NaCl, pH 7.5 using PD-10 desalting columns (GE Healthcare, Germany). Purified enzymes were aliquoted and stored at -70 °C. Gel filtration analysis was performed on a Superose 6, 10/300 GL column (GE Healthcare, Germany) using a multi-component buffer system (L-malic acid, MES, Tris) at 0.1 M and pH 6.5 which was supplemented with 1% glycerol and 10 mM NaCl (Newman 2004).

Standard sialyltransferase activity assay

The standard reaction was performed as described below. The reaction mixture consisted of 1 mM of CMP-Neu5Ac, 1 mM of lactose and enzyme solution in 20 µL of 50 mM sodium phosphate buffer, pH 8.0 containing 15 µM BSA. The enzymatic reaction was carried out at 25 °C and 400 rpm. All assays were performed in duplicate. The enzymatic reaction was stopped after 2 min of incubation by quenching on ice and addition of 40 µL of ice-cold acetonitrile. The reaction mixture was centrifuged at 4 °C, 13,000 rpm for 3 min to remove precipitated protein. After appropriate dilution, 10 µL were injected to HPLC analysis using a Chromolith® Performance RP-18 (100 x 4.6 mm; Merck Chemicals, Germany) column in reversed phase ion-pairing mode on an Agilent Technologies 1200 Series system. The column was equilibrated with 20 mM phosphate buffer, pH 6.8 containing 2 mM tetrabutylammonium at a flow rate of 2 mL/min. A temperature control unit maintained 30 °C throughout the analysis. Samples were eluted with a linear gradient from 0 – 2% acetonitrile in 3 min followed by 2 - 25% acetonitrile in 7 min and detected by UV at 254 nm. The release of CMP (CMP_{Total}) was determined and the amount of transferred Neu5Ac ($CMP_{Transfer}$) was calculated according to Eqn.1. CMP_{Blank} is a

substrate blank. One unit (1 U) was defined as the amount of enzyme that could transfer 1 µmol of sialic acid per min to lactose under the conditions described above.

$$CMP_{Transfer} = CMP_{Total} - CMP_{Blank} \quad \text{(Eqn. 1)}$$

Analysis of acceptor substrate specificity and influence of additives on the sialyltransferase activity

Unless otherwise mentioned, the enzymatic reaction and analysis were carried out as described for the standard sialyltransferase activity assay. D-Galactose, D-glucose, D-mannose, L-fucose, lactose, *N*-acetyl-D-lactosamine, lactulose, sucrose, raffinose, oNP-βGal and oNP-lactose were tested as acceptor substrates. The reaction mixture consisted of 1 mM of CMP-Neu5Ac, 1 mM of acceptor substrate and 1 µM of purified sialyltransferase (∇3PdST) in 20 µL of 50 mM sodium phosphate buffer, pH 8.0 containing 15 µM BSA. The influence of TritonX-100 (0 – 1%), NaCl (0 – 500 mM), CMP (0 – 20 mM) and CTP (0 – 20 mM) on the enzymatic activity was investigated. The reaction mixture consisted of 1 mM of CMP-Neu5Ac, 1 mM *o*NP-Gal and 1 µM of purified sialyltransferase (∇3PdST) in 20 µL of 50 mM sodium phosphate buffer, pH 8.0 containing 15 µM BSA. The enzymatic reaction was stopped after 10 min of incubation. The synthesis of Neu5Acα2,3Gal-oNP was recorded in a time span of 0 - 40 min. The reaction mixture consisted of 1 mM of CMP-Neu5Ac, 1 mM of oNP-βGal and 0.5 µM of purified sialyltransferase (∇3PdST variant) in 20 µL of 50 mM sodium phosphate buffer, pH 8.0 containing 15 µM BSA. The apparent kinetic parameters for CMP-Neu5Ac were determined using 0.1 – 10 mM CMP-Neu5Ac, 10 mM oNP-βGal and 0.7 µM of purified sialyltransferase (∇3PdST variant) in 20 µL of 50 mM sodium phosphate buffer, pH 8.0 containing 15 µM BSA. The enzymatic reaction was stopped after 2.5 min of incubation.

Identification of sialyltransferase assay products by HPLC-ESI-IT-MS, HPAE-PAD and NMR

The sialyltransferase assay products (3'- and/or 6'-sialyllactose and Neu5Acα2,3Gal-oNP) were identified by HPLC-ESI-IT-MS on an Agilent Technologies 1100 Series system equipped with a ZIC®-HILIC column (100 x 4.6 mm, 5 µm; dichrom GmbH, Germany). The column was equilibrated with 85% (v/v) acetonitrile and 15% (v/v) 20 mM ammonium acetate, pH 8.5 at a flow rate of 1 mL/min. 20 µL of sample were injected and eluted using a linear gradient from 0 - 20% of 20 mM ammonium acetate, pH 8.5 in 20 minutes. The MS unit was equipped with an electrospray ionization (ESI) and an ion trap (IT) compartment. Negative ionization mode and single ion monitoring (SIM) at 633 and 592 Da, respectively were used for detection. 3'- and 6'-sialyllactose sodium salt (Carbosynth, UK) were used as standards. Furthermore, 3'- and 6'-sialyllactose were also successfully separated and quantified by High-Performance Anion-Exchange chromatography (HPAE). A Dionex BioLC system equipped with a CarboPac® PA200 column (3 x 250 mm; Thermo Fisher Scientific Inc., Dionex) and a CarboPac® guard column was used. 25 µL of sample were injected and eluted using an isocratic concentration of 100 mM NaOH with 40 mM sodium acetate and a flow rate of 0.5 mL/min at 30 °C. An ED50 electrochemical detector with a carbohydrate certified gold working electrode was used for pulsed amperometric detection (PAD) in the carbohydrate waveform (as recommended from the supplier). The α2,3-regioselectivity of the Neu5Acα2,3Gal-oNP product was proven by NMR spectroscopy. 1H NMR (500 MHz) and 13C NMR (125 MHz) spectra were recorded on a Varian INOVA 500 MHz spectrometer equipped with a 5 mm Indirect Detection probe. The product mixture (60% CMP, 5% oNP-βGal and 35% Neu5Acα2,3Gal-oNP) was dissolved in D_2O and 1H spectra were recorded with

presaturation of the residual water signal. The HMBC spectrum was measured with 128 scans per increment and adiabatic carbon 180° pulses. A NOESY1D spectrum was acquired with DPFGSE excitation of the proton at C-3 of Neu5Ac to reveal an NOE to the proton at C-3 of galactose (see Supporting Information Figure S6).

CMP-Neu5Ac Hydrolase, α2,3-sialidase and α2,3-trans-sialidase activity measurement

Unless otherwise mentioned, the enzymatic reaction was carried out as described for the standard sialyltransferase activity assay. The reaction mixture for determination of CMP-Neu5Ac hydrolase activity consisted of 1.0 mM of CMP-Neu5Ac with or without 0.5 µM of purified enzyme (∇3PdST variant) in 20 µL of 50 mM sodium phosphate buffer, pH 8.0 containing 15 µM BSA. Reactions were allowed to proceed for 0, 5, 10, 15, 30 and 60 min. The reaction products were analyzed by HPLC as described for the standard sialyltransferase activity assay.

The reaction mixture for determination of α2,3-sialidase activity consisted of 1.5 mM of 3'-sialyllactose with or without 1 µM of purified enzyme (∇3PdST variant) in 20 µL of buffer containing 15 µM BSA. 50 mM citric buffer and 50 mM sodium phosphate buffer was used at pH 4.5 and 8.0, respectively. Reactions were allowed to proceed for 90 min. The reaction products were analyzed by HPAE chromatography on a Dionex BioLC system as described above.

The reaction mixture for determination of α2,3-trans-sialidase activity consisted of 1.58 mM of 3'-sialyllactose as donor, 1.58 mM of oNP-βGal as acceptor and 1 µM of purified enzyme (∇3PdST variant) in 20 µL of buffer containing 15 µM BSA. 50 mM citric buffer and 50 mM sodium phosphate buffer was used at pH 4.5 and 8.0, respectively. Reactions were allowed to proceed for up to 45 min. The reaction

products were analyzed by HPLC as described for the standard sialyltransferase activity assay whereas the decrease of substrate (oNP-βGal) and the increase of product was followed.

S10

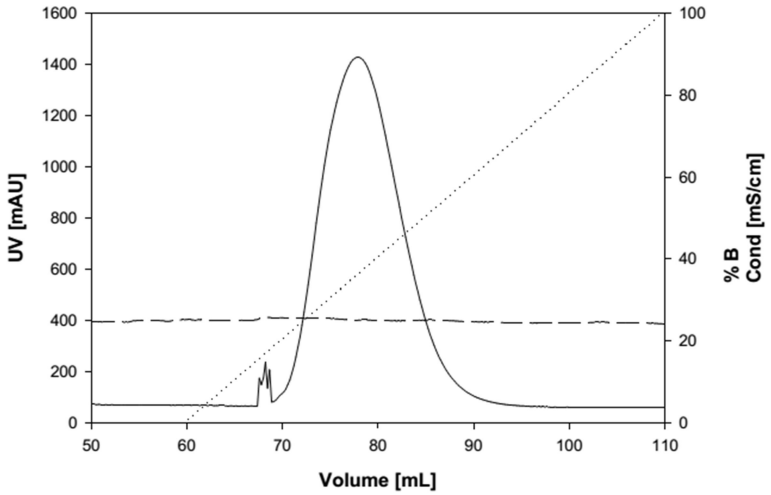

Fig. S1. Chromatogram of purification of ∇3PdST via HisTrap HP FF 5 mL column. Solid line, UV signal (mAU); dotted line, percentage of buffer B; dashed line, conductivity (mS/cm).

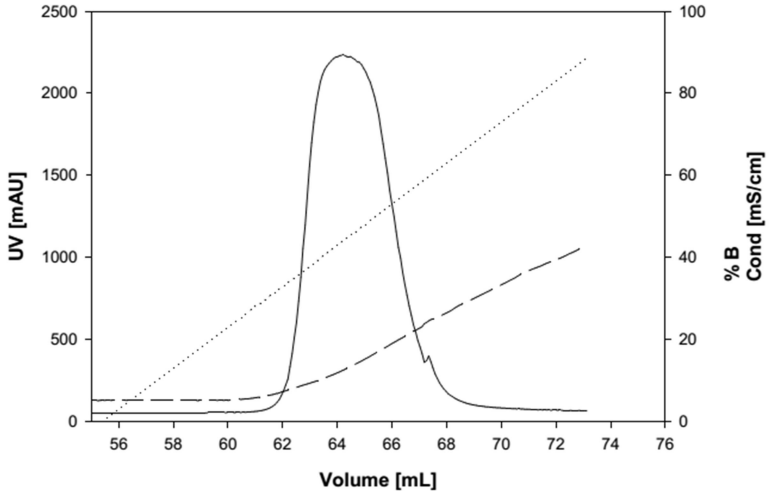

Fig. S2. Chromatogram of purification of ∇3PdST via HiTrap Q HP FF 2x1 mL column. Solid line, UV signal (mAU); dotted line, percentage of buffer B; dashed line, conductivity (mS/cm).

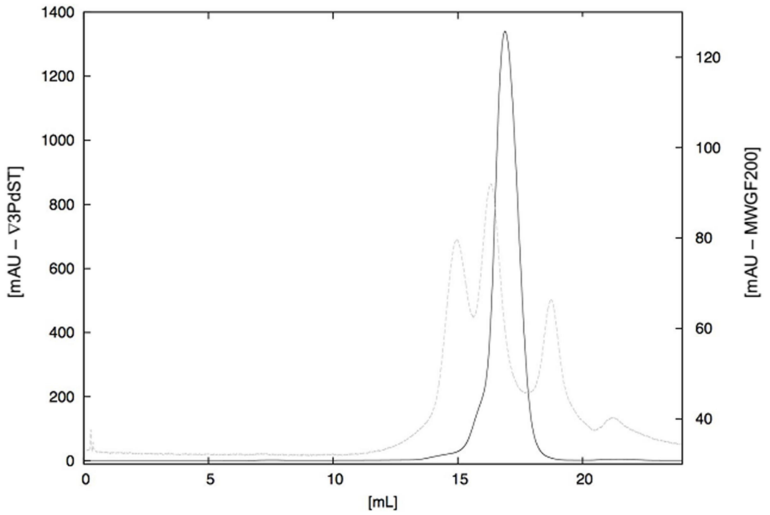

Fig. S3. Gel filtration analysis of ∇3PdST. The components of the Sigma MWGF200 Gel Filtration Molecular Weight Markers Kit (dashed line) and the ∇3PdST sample (solid line) were analyzed on a Superose 6 10/300 GL column (GE Healthcare). The components of the Sigma MWGF200 eluted at the following volumes: 14.94 mL, β-Amylase (200.0 kDa); 16.36 mL, BSA (66.0 kDa); 18.74 mL, Cytochrome C (12.4 kDa). The elution volume of ∇3PdST was 16.89 mL which corresponds to a molecular mass of 46.9 kDa.

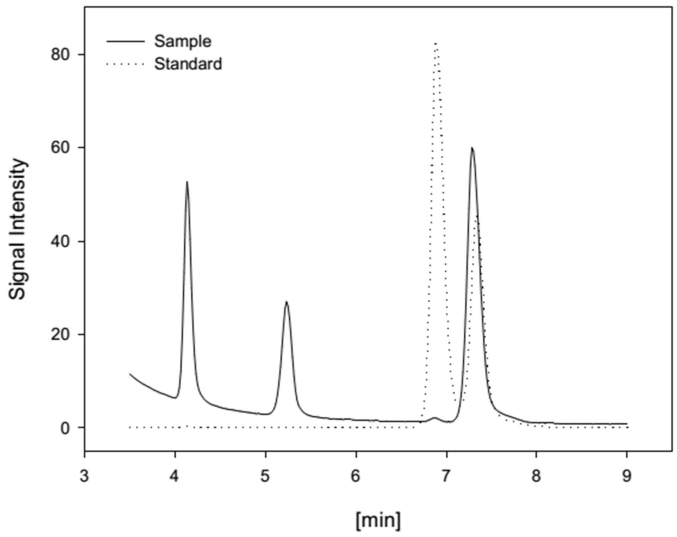

Fig. S4. Separation of 3'- and 6'-sialyllactose by High Performance Anion Exchange chromatography (HPAE). Dotted line, standard of 3'- and 6'-sialyllactose with retention times of 7.3 and 6.9 min, respectively; solid line, standard sialyltransferase reaction mixture (2.0 min, lactose (not shown); 4.2 min, CMP-Neu5Ac; 5.3 min, sialic acid ; 6.9 min, 6'-sialyllactose and 7.3 min, 3'-sialyllactose).

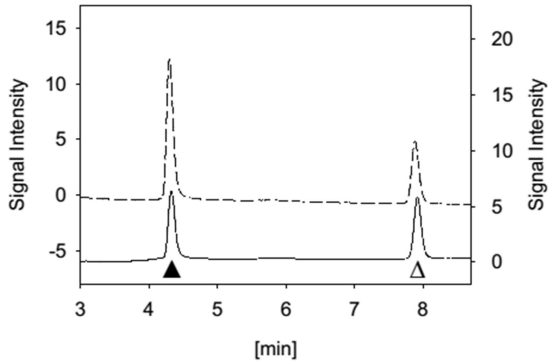

Fig. S5. HPLC analysis and UV-detection of acceptor substrate (oNP-βGal, ▲) and product (Neu5Acα2,3Gal-oNP, Δ) from a sialyltransferase reaction (solid line) and a trans-sialidase reaction (dashed line) with CMP-Neu5Ac (1 mM) and 3'-sialyllactose (1.58 mM) as donor, respectively. Reactions were incubated at 25°C, 400 rpm in the presence of 1 µM enzyme for 8 and 45 min, respectively. Both reactions yield the same product. Chromatograms were recorded on a Chromolith® Performance RP-18 column.

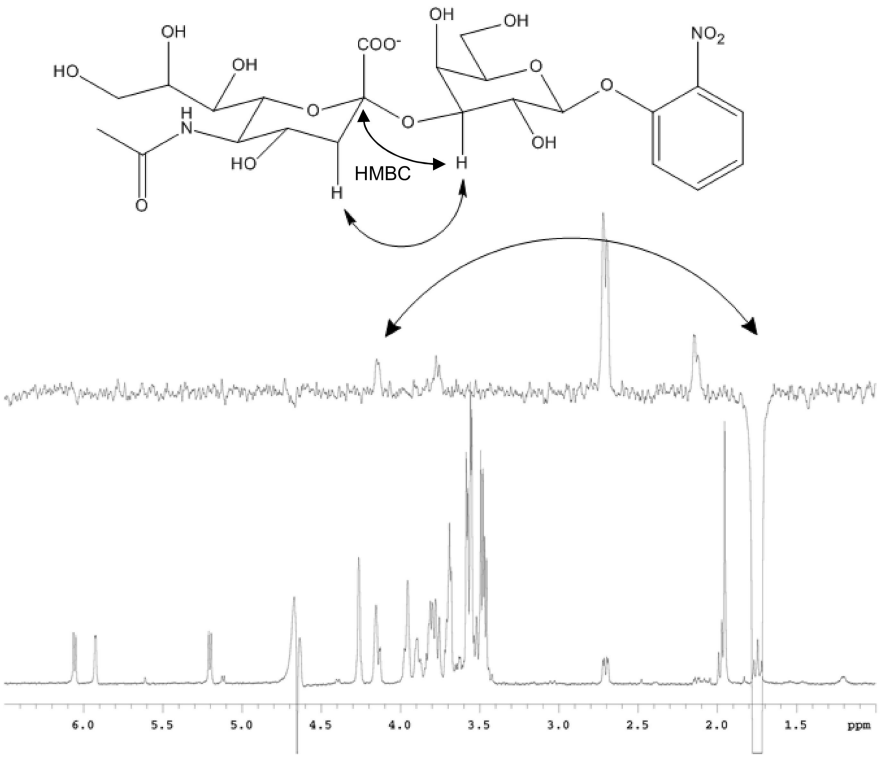

Fig. S6. NOESY1D spectrum (upper panel) and 1H spectrum (lower panel) of Neu5Acα2,3Gal-oNP with selective excitation of the proton at C-3 of Neu5Ac (the mixing time was 500 ms). In addition, an HMBC correlation could be found between the proton at C-3 of galactose and the quaternary carbon-2 of Neu5Ac supporting the substitution pattern of galactose.

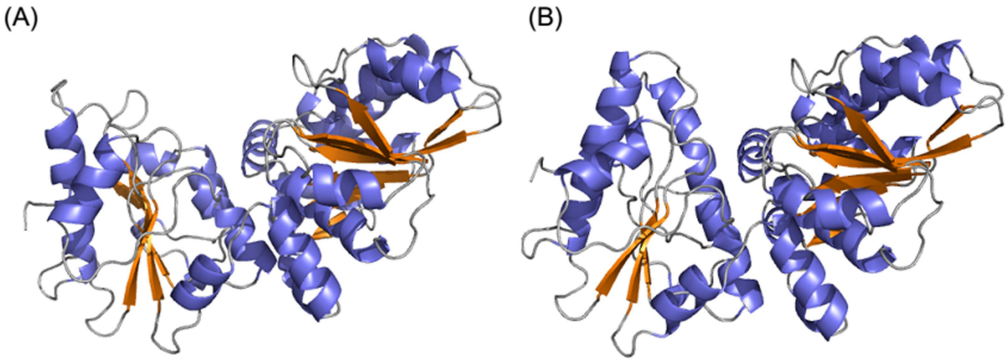

Fig. S7. Comparison of (A) open and (B) closed conformation model of PdST. Homology modeling was done with YASARA Structure. The open conformation model is based on PmST1 M144D (PDB code 3S44). A set of homologous experimental structures (PDB codes: 2IHJ, 2IHK, 2IHZ, 2ILV, 2Z4T) was used as template to obtain the closed conformation model.

(A)

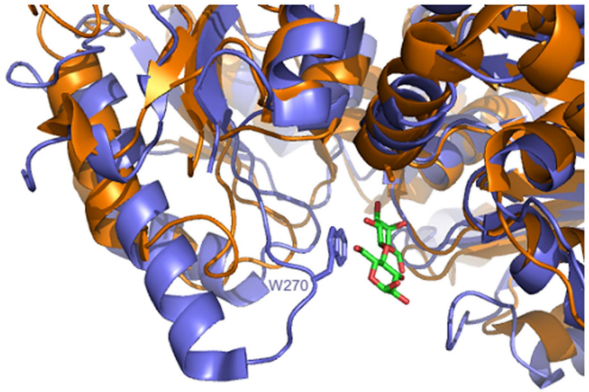

(B)

Sialyltransferase		Accession number	Residues around Trp270
P. multocida	a2,3/a2,6	AAY89061	GTTTWEGNTDVREYYAQQQ
P. dagmatis	a2,3	ZP_05920895	GTTTWEGNTDIREYYAKQQ
P. damselae	a2,6	BAA25316	GTTTWAG-GETKEYYAQQQ
P. leiognathi	a2,6	BAF91416	GTTTWAG-GETKEYYAQQQ
P. phosphoreum	a2,3	BAF63530	GTNSGT-------ATAEQQ
Vibrio sp.	a2,3	BAF91160	GSNSAT-------ATAEEQ
H. ducreyi	a2,3	AAP95068	GTTAFNLDQEKLDLLTQLH

Fig. S8. Structural interpretation of the specificity towards α- and/or β-galactosides. (A) Overlay of α2,3/α2,6-sialyltransferase from *Pasteurella multocida* (PDB code 2ILV, slate) and α/β-galactoside α2,3-sialyltransferase from *Photobacterium phosphoreum* (PDB code 2ZWI, orange). Lactose (bound to 2ILV, coloured by element) is displayed. (B) Partial sequence alignment of GT-80 sialyltransferases, showing residues around Trp270 where the numbering corresponds to PmST1.

Mechanistic study of CMP-Neu5Ac hydrolysis by α2,3-sialyltransferase from *Pasteurella dagmatis*

Katharina Schmölzer[1], Christiane Luley-Goedl[1], Tibor Czabany[2], Doris Ribitsch[1], Helmut Schwab[1,4], Hansjörg Weber[3], Bernd Nidetzky[1,2]

[1]Austrian Centre of Industrial Biotechnology, Petersgasse 14, 8010 Graz, Austria
[2]Institute of Biotechnology and Biochemical Engineering, Graz University of Technology, Petersgasse 12/I, 8010 Graz, Austria
[3]Institute of Organic Chemistry, Graz University of Technology, Stremayrgasse 9, 8010 Graz, Austria
[4]Institute of Molecular Biotechnology, Graz University of Technology, Petersgasse 14, 8010 Graz, Austria

Corresponding author: bernd.nidetzky@tugraz.at; Phone: +43 316 873 8400; FAX: +43 316 873 8434
Proofs and reprints should be addressed to Bernd Nidetzky.

Accepted for publication in FEBS Letters (FEBSLETTERS-D-14-00775R1).

Supporting Information: General methods; ^{1}H NMR spectrum of Neu5Ac; uncatalyzed CMP-Neu5Ac hydrolysis rates; time-course of uncatalyzed CMP-Neu5Ac hydrolysis; time-course of wild-type PdST catalyzed CMP-Neu5Ac hydrolysis; time-resolved ^{1}H NMR analysis of uncatalyzed CMP-Neu5Ac hydrolysis; time-resolved ^{1}H NMR analysis of wild-type PdST catalyzed CMP-Neu5Ac hydrolysis.

Keywords: bacterial sialyltransferase / glycosyltransferase family GT-80 / donor substrate hydrolysis / *in situ* ^{1}H NMR analysis / inverting mechanism / His^{284} mutants

Abbreviations: Neu5Ac, *N*-acetylneuraminic acid; oNP-βGal, 2-nitrophenyl-β-D-galactopyranoside.

Highlights

- Hydrolysis of CMP-Neu5Ac by *Pasteurella dagmatis* α2,3-sialyltransferase studied.
- Reaction monitored with *in situ* proton NMR.
- Enzymatic hydrolysis with inversion of the configuration at the anomeric center.
- Single displacement-like reaction mechanism proposed.
- His^{284} substituted by Asn, Tyr, or Asp, and enzyme variants characterized.
- His^{284} proposed to facilitate the departure of the CMP leaving group.

Abstract

Bacterial sialyltransferases of glycosyltransferase family GT-80 exhibit pronounced hydrolase activity toward CMP-activated sialyl donor substrates. Using *in situ* proton NMR, we show that hydrolysis of CMP-Neu5Ac by *Pasteurella dagmatis* α2,3-sialyltransferase (PdST) occurs with axial-to-equatorial inversion of the configuration at the anomeric center to release α-Neu5Ac product. We propose catalytic reaction through a single displacement-like mechanism where water replaces sugar substrate as sialyl group acceptor. PdST variants having His^{284} in the active site replaced by Asn, Asp or Tyr showed up to 10^4-fold reduced activity, but catalyzed CMP-Neu5Ac hydrolysis with analogous inverting stereochemistry. The proposed catalytic role of His^{284} in the PdST hydrolase mechanism is to facilitate departure of the CMP leaving group.

1 Introduction

Attachment of sialic acid residue(s) is a key final step in the biosynthesis of complex oligosaccharides, mostly on glycoproteins and gangliosides. Sialic acid-capped oligosaccharide structures are central elements of cellular recognition [1,2]. Sialyltransferases are glycosyltransferases (EC 2.4.99) that utilize a CMP-activated donor substrate, typically CMP-*N*-acetylneuraminic acid (CMP-Neu5Ac), to catalyze sialylation of nascent oligosaccharide acceptors [3,4]. Sialyltransferases are widely distributed in animal tissues [5-7], but are also present in other organisms including yeasts [8] and bacteria [9].

Chemically, the sialyltransferase reaction involves nucleophilic substitution at the C2 of the transferred sialyl residue and proceeds with axial-to-equatorial inversion of the anomeric configuration [10,11]. A single displacement-type catalytic mechanism via an oxocarbenium ion-like transition state has been proposed (Figure 1A) [12]. In this mechanism, a general catalytic base on the enzyme facilitates attack of the acceptor substrate on the reactive C2, and departure of the CMP leaving group is assisted from another enzyme group through electrostatic stabilization (Figure 1B) or partial protonation [13-15].

A common feature of glycosyltransferase active site function is effective exclusion of water nucleophile from the catalytic center, thus reducing the possibility for "error hydrolysis" during the reaction [16-18]. Bacterial sialyltransferases differ from their counterpart enzymes from mammalian sources, and they are also unusual among the glycosyltransferases in general, in that they often exhibit pronounced hydrolase activity toward their nucleotide-activated donor substrate [19-23]. Sialyltransferases of family GT-80 are effective CMP-Neu5Ac hydrolases in particular. Studies of *Pasteurella* sp. sialyltransferases from family GT-80 reveal that hydrolysis of CMP-Neu5Ac occurs in the absence, but also in the presence of acceptor substrate [21-24].

The catalytic mechanism by which sialyltransferases hydrolyze their donor substrate is not completely clear, and this study was performed to obtain deepened understanding. A highly probable hydrolase mechanism is one of single displacement-like reaction (Figure 1A) where water replaces sugar substrate as sialyl group acceptor. However, a recent study of *P. multocida* sialyltransferase PmST1 suggested the possibility of a more plastic mechanism of CMP-Neu5Ac hydrolysis [23]. Using *in situ* monitoring of the hydrolysis reaction with proton NMR, Chen and colleagues showed that donor substrate hydrolysis by PmST1 occurred with either one of the possible stereochemical outcomes, that is, the formation of both α- and β-Neu5Ac [23] (Figure 1C). Different stereochemical courses of the reaction necessitate distinct catalytic mechanisms [11]. Elucidation of how a single sialyltransferase active site might be able to promote hydrolysis with

inversion and retention at the same time presents an interesting mechanistic problem. The type of stereochemical "promiscuity" suggested for PmST1 lacks precedence among glycosyltransferases. Herein we report the stereochemical course of CMP-Neu5Ac hydrolysis catalyzed by wild-type and mutated α2,3-sialyltransferases PdST from *P. dagmatis*. PdST shares with PmST1 the common membership to glycosyltransferase family GT-80 [25] and is about 70% identical to it in amino acid sequence [22]. Using *in situ* reaction monitoring by proton NMR under conditions that rigorously eliminate possible interference from Neu5Ac mutarotation, we show that PdST exhibits absolute stereochemical fidelity in acting as an inverting CMP-Neu5Ac hydrolase. Variants of the enzyme in which the catalytic His^{284} was replaced by Asn, Asp or Tyr exhibited strongly decreased activity compared to wild-type PdST, but catalyzed donor substrate hydrolysis also with inversion of anomeric configuration. A catalytic mechanism for CMP-Neu5Ac hydrolysis by PdST is proposed. A possible role of His^{284} as catalytic nucleophile in enzymatic trans-sialylation reaction with retention of equatorial anomeric configuration was investigated.

2 Materials and methods

2.1 *Chemicals*

Neu5Ac was from Carbosynth (Compton, Berkshire, UK). All other materials are described elsewhere [22].

2.2 *Site-directed mutagenesis*

Mutations to replace His^{284} by Asn (H284N), Asp (H284D) or Tyr (H284Y) were introduced by two-stage PCR [26] where a pET23a(+) expression vector encoding ∇3PdST (variant of wild-type PdST elongated by three amino acids at the N-terminus [22]) was used as template. Full experimental details are summarized in Supplementary information. All inserts were confirmed by DNA sequencing.

2.3 *Protein expression and purification*

Protein expression in *E. coli* and preparation of the cell lysate were done as previously described [22]. Target proteins were purified via their C-terminal His-tag, as described under Supplementary information. SDS PAGE was used to confirm purity of enzyme preparations.

2.4 *Sialyltransferase and CMP-Neu5Ac hydrolase activity*

α2,3-Sialyltransferase activity was assayed in a total volume of 20 µL using 50 mM sodium phosphate buffer, pH 8.0. Reaction mixture contained 1 mM CMP-Neu5Ac, 1 mM acceptor (2-nitrophenyl-β-D-galactopyranoside; oNP-βGal), 5 µM enzyme, and 1 mg/mL BSA. Enzymatic conversion was carried out at 25°C and agitation rate of 400 rpm using a Thermomixer comfort (Eppendorf, Germany). All assays were performed in duplicate. Reactions were stopped at certain times by adding 40 µL of ice-cold acetonitrile. Mixtures were incubated on ice for 10 min and centrifuged to remove precipitated protein. Samples were analyzed by reverse phase ion-pair HPLC (see the Supplementary information).

CMP-Neu5Ac hydrolase activity was assayed under exactly the same conditions just described, except that no oNP-βGal was present in the reaction. Sampling and sample analysis were also carried out as described above (Supplementary information).

2.5 *In situ ^{1}H NMR measurements*

A Varian (Agilent) INOVA 500-MHz spectrometer (Agilent Technologies, Santa Clara United States) was used for NMR measurements at the indicated temperatures in D_2O/H_2O solutions employing VNMRJ 2.2D software. ^{1}H NMR spectra were measured at 499.98MHz on a 5 mm indirect detection PFG-probe. Enzymatic reactions were performed at 5°C (wild-type) or 28°C (His^{284} mutants) in a total volume of 600 µL in sodium tartrate buffer (50 mM, pH 5.5) containing 1 or 2 mM CMP-Neu5Ac, enzyme (5 µM of wild-type PdST; 43 µM of H284N; 8.5 µM of H284Y; 61 µM of H284D) and 1 mg/mL BSA. ^{1}H NMR spectra were recorded with pre-saturation of the water signal by a shaped pulse. Standard pre-saturation sequence was used: relaxation delay 2 s; 90° proton pulse; acquisition time 2.048 s; spectral width 8 kHz; number of points 32 k. Between 8 to 64 scans were accumulated depending on the rate of the enzymatic reaction. Arrayed spectra were acquired with an array of pre-acquisition delay of 60 s.

2.6 *Trans-sialylation assay*

α2,3-Trans-sialylation activity was assayed in a total volume of 20 µL using 50 mM citric buffer, pH 5.5. Reaction mixture contained 1.58 mM 3´-sialyllactose, 1.58 mM oNP-βGal, 1 (wild-type) or 5 µM (His^{284} mutants) enzyme, and 1 mg/mL BSA. Reactions were performed with and without 1 mM CMP. Enzymatic conversion was carried out at 25°C and agitation rate of 400 rpm using a Thermomixer comfort (Eppendorf, Germany). Sampling and sample analysis were carried out as

described above for sialyltransferase assay (also see Supplementary information). The decrease in the substrate (oNP-βGal) and the increase in product were followed.

3 Results and discussion

3.1 *Stereochemical course of hydrolysis of CMP-Neu5Ac by wild-type PdST*

Hydrolysis of CMP-Neu5Ac by wild-type PdST was analyzed with time-resolved *in situ* ^{1}H NMR spectroscopy, focusing on determination of the anomeric configuration of the released Neu5Ac product in particular. However, mutarotation of Neu5Ac was a problem, necessitating optimization of reaction conditions so that the enzymatic reaction was appreciably faster than spontaneous equilibration of Neu5Ac anomeric forms. It was known from literature [27-31] and was verified herein (Figure S1, Supplementary information) that β-Neu5Ac (~92%) strongly prevails over α-Neu5Ac (≤ 8%) at mutarotation equilibrium. Therefore, this result suggested special caution in the product analysis. Uncatalyzed hydrolysis of CMP-Neu5Ac was shown to be slow enough to not interfere with the enzymatic conversion in the time span of the experiment.

Reaction at pH 5.5 and 5°C was chosen based on results of preliminary experiments (Figure S2 – S4, Supplementary information) and literature [27,28,32-34]. Conversion of CMP-Neu5Ac and formation of hydrolysis product, α-Neu5Ac or β-Neu5Ac, were tracked by the equatorial and axial H-3 proton signals of each of the Neu5Ac species, which are discriminated in the aliphatic region of the ^{1}H NMR spectrum. Figure 2 shows a stack plot of spectra recorded at different reaction times. Already the first spectrum, which was obtained after 2 min, revealed a characteristic signal for the H_{3eq} proton of α-Neu5Ac (H_{3eq} = 2.86 ppm). Note that the H_{3ax} signal of α-Neu5Ac was not resolved due to spectral overlap with the corresponding H_{3ax} from CMP-Neu5Ac (1.74 ppm). Reaction progress was reflected clearly in signal intensity increase from the H_{3eq} of α-Neu5Ac. By contrast, signal from β-Neu5Ac was not detectable, even after extended incubation times of up to 26 min (Figure 2). Advance of the mutarotation was noticeable only later, β-Neu5Ac appeared after 40 min. Conversion of CMP-Neu5Ac was complete after about 1 h.

These results provide clear evidence of an axial-to-equatorial inverting stereochemical course of CMP-Neu5Ac conversion by PdST that yields α-Neu5Ac as the sole hydrolysis product. From the complete absence of β-Neu5Ac in the product mixture within 26 min, we conclude that the alternate (axial-to-axial retaining) stereochemical course was not utilized in the catalytic reaction of PdST. Stereochemical promiscuity in the hydrolysis of CMP-Neu5Ac, observed for PmST1 [23], is therefore not a common feature of catalytic function of family GT-80 sialyltransferases.

Mechanistically, hydrolysis of CMP-Neu5Ac with inversion might occur through a single displacement-like catalytic process (Figure 1A), where water substitutes the carbohydrate acceptor substrate of the canonical sialyltransferase reaction. In this scenario, "error hydrolysis" would result from competition between carbohydrate and water acting as nucleophiles of the reaction (Figure 1A).

3.2 *Consequences of site-directed replacements of His^{284}*

Rationale for choosing amino acid residues to replace His^{284} was first of all to eliminate potential general acid catalysis to CMP-Neu5Ac hydrolysis (His→Asn; H284N) because unlike the original histidine (Figure 1A and 1B), Asn^{284} is not a competent proton donor to the phosphodiester group of the donor substrate. The canonical sialyltransfer and also CMP-Neu5Ac hydrolysis were therefore likely to be affected by the substitution His→Asn. Secondly, we wanted to introduce potentially acidic and at the same time also nucleophilic residues (His→Tyr, H284Y; His→Asp; H284D) in the active site. While it is highly improbable that CMP-Neu5Ac hydrolysis receives catalytic support from a nucleophilic residue at position 284, PdST catalyzes an additional reaction, the so-called trans-sialylation, where Neu5Ac is transferred from sialylated carbohydrate donor substrate (e.g. 3'-sialyllactose) to a carbohydrate acceptor (e.g. oNP-βGal) [22]. The reaction proceeds through an equatorial-to-equatorial retaining stereochemical course, giving Neu5Acα2,3Gal-oNP as the product [22]. Possible participation of an enzyme nucleophile (His^{311}) in the trans-sialylation reaction of sialyltransferase PmST1 has been considered in an earlier study [12]. It was therefore interesting to examine CMP-Neu5Ac hydrolysis and also trans-sialylation activities of the PdST mutants. Note that retaining sialidases and trans-sialidases were previously shown to utilize tyrosine for nucleophilic catalysis [35-41]. Asp or Glu are common catalytic nucleophiles in retaining glycoside hydrolases [42]. The three PdST variants (H284N, H284Y, H284D) were obtained as highly purified protein preparations from *E. coli* overexpression cultures (data not shown).

Table 1 summarizes specific sialyltransferase and CMP-Neu5Ac hydrolase activities of the PdST variants along with the corresponding specific activities of the wild-type enzyme. Exchange of His^{284} resulted in up to 10^4-fold decrease in activity for sialylation of oNP-βGal, indicating high importance of the histidine for catalytic function of PdST. Interestingly, replacement of the homologous His^{311} by Ala in PmST1 had a comparably small effect (13.5-fold decrease) on the catalytic rate (k_{cat}) of CMP-Neu5Ac utilization [21]. Here, specific activity for CMP-Neu5Ac hydrolysis in the absence of acceptor substrate was also decreased, up to 10^3-fold, in the PdST variants. To express change in apparent reaction selectivity brought about by substitution of His^{284},

we define the selectivity parameter R_{TH}, which is the ratio of the specific activity of the canonical sialyltransfer from CMP-Neu5Ac to oNP-βGal and the specific activity of CMP-Neu5Ac donor substrate hydrolysis in the absence of acceptor substrate. Note that R_{TH} is not an expression of the intrinsic enzyme selectivity. Under the conditions used, R_{TH} also includes effects on acceptor substrate binding. In wild-type PdST, R_{TH} had a value of 1.6, indicating that sialyltransfer was preferred over hydrolysis. R_{TH} was lowered drastically as consequence of substitution of His^{284}, as shown in Table 1. From its R_{TH} value of 0.028, the H284D variant of PdST could no longer be considered a sialyltransferase, but rather behaved as a major CMP-Neu5Ac hydrolase. More detailed investigations of the molecular basis of R_{TH} and the effect of substitution of His^{284} on R_{TH} were beyond the scope of the study and were left for consideration in the future.

All PdST mutants lacked trans-sialylation activity above detection limit with the methods used (2×10^{-4} U/mg). By way of comparison, the wild-type enzyme exhibited a specific trans-sialylation activity of 0.15 U/mg. CMP (1 mM) stimulated the activity of wild-type PdST (0.90 U/mg), and it also elicited a tiny amount of trans-sialylation activity in the H284N mutant ($\sim 5 \times 10^{-4}$ U/mg). The trans-sialylation product of the H284N reaction co-eluted in HPLC with authentic Neu5Acα2,3Gal-oNP standard. Therefore, this suggested a stereochemical course of the enzymatic transformation where the equatorial anomeric configuration of substrate was retained in product. The H284Y and H284D mutants were completely inactive even in the presence of CMP. Overall, these results do not support a role of His^{284} as nucleophile in the retaining trans-sialylation reaction catalyzed by PdST. However, more research will be needed to clarify the enzymatic mechanism of trans-sialylation with retention of configuration.

Effect of enhanced hydrolase activity in PdST variants was evaluated in “synthesis experiments” where sialylation of oNP-βGal from CMP-Neu5Ac was the target reaction. Figure S5 (Supplementary information) compares reaction time courses for the PdST variants to that of the wild-type enzyme. All reactant concentrations except that of Neu5Ac were observed analytically, and results are reported on the basis of verified mass balance for the overall conversion. Previous study of wild-type PdST has shown that enzymatic transformation of oNP-βGal is completely regioselective and gives Neu5Acα2,3Gal-oNP as sole sialyltransfer product [22]. Figure 3A shows superimposition of HPLC elution profiles of samples from the different enzymatic reactions. Only a single sialyltransfer product was formed in each reaction, and this product co-eluted with authentic Neu5Acα2,3Gal-oNP standard, providing strong evidence in support of product identity. We therefore concluded that regioselectivity of sialylation of oNP-βGal was not changed as result of substitution of His^{284}. The result also implies sialyltransfer by the PdST variants according to the same axial-to-equatorial inverting stereochemical course as that of the wild-type enzyme.

Figure 3 (panels B and C) displays time-dependent formation of Neu5Acα2,3Gal-oNP in the different conversions. It also shows the release of CMP for reference to the progress of donor substrate utilization. The H284N and H284Y variants converted CMP-Neu5Ac fully in the time span of the experiment. Reaction was substantially slower with the H284D variant. Error hydrolysis of CMP-Neu5Ac was the predominant way of donor substrate conversion with each enzyme, however, especially with the H284D variant. Yields of the Neu5Acα2,3Gal-oNP product did not exceed 40% based on CMP-Neu5Ac converted in the reactions of the PdST variants (Figure 3C) whereas in reaction of the wild-type enzyme under otherwise identical conditions, the yield was ~80% (Figure 3B, 3C and S5, panel A, Supplementary information) [22]. Donor substrate conversion by H284D variant occurred almost exclusively via hydrolysis, with a maximum yield of Neu5Acα2,3Gal-oNP well below 10%.

3.3 *Stereochemical course of CMP-Neu5Ac hydrolysis by PdST variants*

Low specific activities of the PdST variants necessitated that *in situ* proton NMR analyses of the stereochemical course of CMP-Neu5Ac hydrolysis were performed under conditions different from the ones used with the wild-type enzyme. Temperature was increased to 28°C, and enzyme concentration was also raised by up to ten-fold. Spectra were recorded every 5 min, and characteristic spectrum at representative time from each reaction is shown in Figure 4. With each PdST variant, enzymatic conversion of CMP-Neu5Ac resulted in release of mainly α-Neu5Ac while the corresponding β-anomer was detectable only in tiny amounts. The presence of β-Neu5Ac can be explained by slow mutarotation of the α-Neu5Ac formed in the enzymatic reaction. The alternative scenario where α-Neu5Ac is generated via mutarotation of enzymatically formed β-anomer is clearly not possible due to position of the mutarotation equilibrium (see 3.1 *Stereochemical course of hydrolysis of CMP-Neu5Ac by wild-type PdST*). Relevant controls performed under otherwise identical conditions, however, in the absence of enzyme showed that uncatalyzed hydrolysis of CMP-Neu5Ac occurred at a rate about 15 to 110-fold slower than the enzymatic rates, and that its main reaction end-product was actually β-Neu5Ac in accordance with results of earlier studies [34] (Figure S6, Supplementary information). Therefore, these results are consistent with an axial-to-equatorial (β-to-α) inverting stereochemical course of CMP-Neu5Ac hydrolysis by each of the three PdST variants.

3.4 *Mechanistic implications for PdST-catalyzed hydrolysis of CMP-Neu5Ac*

Crystal structure of PmST1 in complex with the catalytically incompetent donor substrate analogue CMP-3F(a)Neu5Ac [21] (Figure 1B) shows that His^{311} is in a position to establish a tight hydrogen

bond with a non-bridging oxygen atom of the CMP's phosphate group. This would allow the histidine to (partially) protonate the glycosidic oxygen in CMP-Neu5Ac, as required if its catalytic function were that of a Brønsted acid. However, the relevant pK_a of CMP is low (6.19 [43]), and there is the question, therefore, whether Brønsted catalysis would be particularly effective in facilitating the leaving group departure. Supported by crystallographic observations (Figure 1B), a plausible alternative scenario of catalytic function is that His^{311}, and the homologous His^{284} in PdST, provide simply electrostatic stabilization to the departing CMP moiety in the transition state of the single displacement-like catalytic reaction. Decrease in reaction rate of H284N variant by about 100-fold compared to the reaction rate of the wild-type enzyme (Table 1) implies loss of 11.4 kJ/mol of transition state stabilization energy as result of the site-directed substitution. The observed amount of transition state destabilization in the H284N variant lies at the lower end of, but is clearly within the expected range of the energetic consequences of removal of a charged hydrogen bond [44].

Replacement of His^{284} by Asp is expected to be more difficult to accommodate by PdST than the corresponding Asn or Tyr replacement, due to the drastic change in active-site electrostatics that it produces under the assumption that the Asp is ionized. Coherently, the H284D variant was by far the least active among the PdST variants studied. Finally, positioning of donor and acceptor substrate relative to each other is also critical in the reaction of PdST, and a water nucleophile can probably tolerate site-directed replacements by far more easily than a carbohydrate acceptor. Each site-directed substitution of His^{284}, however, especially the substitution with Asp, resulted in substantial decrease in R_{TH} to progressively (Asn < Tyr < Asp) favor hydrolysis over sialyltransfer.

The relatively high level of hydrolase activity in the family GT-80 sialyltransferases PdST [22] and PmST1 [23] remains somewhat enigmatic, particularly in light of bacterial sialyltransferases of family GT-42 and GT-52, which utilize different active-site structures to achieve the same axial-to-equatorial inverting sialyltransfer at however relatively scant donor substrate hydrolysis [19,20,45]. Note, the higher activities of family GT-80 STs compared to other GT families may also contribute to the increased hydrolysis to sialyltransfer ratio. How sialyltransferases fine-tune their catalytic center interactions to prevent erroneous reaction with water is an interesting, yet still elusive problem of both fundamental and applied importance in the field.

4 Conclusions

In summary, we demonstrate herein that CMP-Neu5Ac hydrolysis by PdST proceeds with axial-to-equatorial configuration inversion, presumably as result of a single displacement reaction, just like the canonical sialyltransfer to carbohydrate acceptors catalyzed by this enzyme. Stereochemical

promiscuity indicated by formation of inversion and retention product simultaneously, as reported for PmST1 from the same family GT-80 [23], was ruled out rigorously for PdST. Substitution of active-site His^{284} by Asn, Tyr or Asp had no impact on the donor hydrolysis mechanism: each PdST variant catalyzed CMP-Neu5Ac conversion with analogous inverting stereochemistry. Furthermore, mutational studies of PdST support a catalytic role of His^{284} in donor substrate hydrolysis, which is to facilitate the departure of the CMP leaving group probably through electrostatic interactions (Figure 1B). A possible role of His^{284} as catalytic nucleophile in enzymatic trans-sialylation with retention of equatorial anomeric configuration is not supported.

Acknowledgements

This work was supported by the Federal Ministry of Economy, Family and Youth (BMWFJ), the Federal Ministry of Traffic, Innovation and Technology (BMVIT), the Styrian Business Promotion Agency, SFG, the Standortagentur Tirol and ZIT-Technology Agency of the City of Vienna through the COMET-Funding Programme managed by the Austrian Research Promotion Agency FFG.

5 References

[1] Schauer, R. (2009). Sialic acids as regulators of molecular and cellular interactions. Curr. Opin. Struct. Biol. 19, 507-514.

[2] Varki, A. (2008). Sialic acids in human health and disease. Trends Mol. Med. 14, 351-360.

[3] Chen, X. and Varki, A. (2009). Advances in the biology and chemistry of sialic acids. ACS Chem. Biol. 5, 163-176.

[4] Audry, M., Jeanneau, C., Imberty, A., Harduin-Lepers, A., Delannoy, P. and Breton, C. (2011). Current trends in the structure–activity relationships of sialyltransferases. Glycobiology 21, 716-726.

[5] Harduin-Lepers, A., Vallejo-Ruiz, V., Krzewinski-Recchi, M.-A., Samyn-Petit, B., Julien, S. and Delannoy, P. (2001). The human sialyltransferase family. Biochimie 83, 727-737.

[6] Lowe, J.B. and Marth, J.D. (2003). A genetic approach to mammalian glycan function. Annu. Rev. Biochem. 72, 643-691.

[7] Harduin-Lepers, A., Mollicone, R., Delannoy, P. and Oriol, R. (2005). The animal sialyltransferases and sialyltransferase-related genes: a phylogenetic approach. Glycobiology 15, 805-817.

[8] Rodrigues, M.L., Dobroff, A.S., Couceiro, J.N., Alviano, C.S., Schauer, R. and Travassos, L.R. (2002). Sialylglycoconjugates and sialyltransferase activity in the fungus *Cryptococcus neoformans*. Glycoconjugate J. 19, 165-173.

[9] Yamamoto, T., Takakura, Y. and Tsukamoto, H. (2006). Bacterial sialyltransferases. Trends Glycosci. Glyc. 18, 253-265.

[10] Buschiazzo, A. and Alzari, P.M. (2008). Structural insights into sialic acid enzymology. Curr. Opin. Chem. Biol. 12, 565-572.

[11] Lairson, L.L., Henrissat, B., Davies, G.J. and Withers, S.G. (2008). Glycosyltransferases: structures, functions, and mechanisms. Annu. Rev. Biochem. 77, 521-555.

[12] Sugiarto, G., Lau, K., Li, Y., Khedri, Z., Yu, H., Le, D.-T. and Chen, X. (2011). Decreasing the sialidase activity of multifunctional *Pasteurella multocida* α2,3-sialyltransferase 1 (PmST1) by site-directed mutagenesis. Mol. Biosyst. 7, 3021-3027.

[13] Breton, C., Fournel-Gigleux, S. and Palcic, M.M. (2012). Recent structures, evolution and mechanisms of glycosyltransferases. Curr. Opin. Struct. Biol. 22, 540-549.

[14] Clarke, A.J., Hurtado-Guerrero, R., Pathak, S., Schüttelkopf, A.W., Borodkin, V., Shepherd, S.M., Ibrahim, A.F.M. and van Aalten, D.M.F. (2008). Structural insights into mechanism and specificity of *O*-GlcNAc transferase. EMBO J. 27, 2780-2788.

[15] Lazarus, M.B., Nam, Y., Jiang, J., Sliz, P. and Walker, S. (2011). Structure of human *O*-GlcNAc transferase and its complex with a peptide substrate. Nature 469, 564-567.

[16] Goedl, C. and Nidetzky, B. (2008). The phosphate site of trehalose phosphorylase from *Schizophyllum commune* probed by site-directed mutagenesis and chemical rescue studies. FEBS J. 275, 903-913.

[17] Gutmann, A. and Nidetzky, B. (2012). Switching between *O*- and *C*-glycosyltransferase through exchange of active-site motifs. Angew. Chem. Int. Ed. 51, 12879-12883.

[18] Persson, K., Ly, H.D., Dieckelmann, M., Wakarchuk, W.W., Withers, S.G. and Strynadka, N.C.J. (2001). Crystal structure of the retaining galactosyltransferase LgtC from *Neisseria meningitidis* in complex with donor and acceptor sugar analogs. Nat. Struct. Mol. Biol. 8, 166-175.

[19] Chiu, C.P.C., Lairson, L.L., Gilbert, M., Wakarchuk, W.W., Withers, S.G. and Strynadka, N.C.J. (2007). Structural analysis of the α2,3-sialyltransferase Cst-I from *Campylobacter jejuni* in apo and substrate-analogue bound forms. Biochemistry 46, 7196-7204.

[20] Chiu, C.P.C., Watts, A.G., Lairson, L.L., Gilbert, M., Lim, D., Wakarchuk, W.W., Withers, S.G. and Strynadka, N.C.J. (2004). Structural analysis of the sialyltransferase CstII from *Campylobacter jejuni* in complex with a substrate analog. Nat. Struct. Mol. Biol. 11, 163-170.

[21] Ni, L. et al. (2007). Crystal structures of *Pasteurella multocida* sialyltransferase complexes with acceptor and donor analogues reveal substrate binding sites and catalytic mechanism. Biochemistry 46, 6288-6298.

[22] Schmölzer, K. et al. (2013). Characterization of a multifunctional α2,3-sialyltransferase from *Pasteurella dagmatis*. Glycobiology 23, 1293-1304.

[23] Sugiarto, G. et al. (2012). A sialyltransferase mutant with decreased donor hydrolysis and reduced sialidase activities for directly sialylating Lewis^x. ACS Chem. Biol. 7, 1232-1240.

[24] Ni, L., Sun, M., Yu, H., Chokhawala, H., Chen, X. and Fisher, A.J. (2006). Cytidine 5'-monophosphate (CMP)-induced structural changes in a multifunctional sialyltransferase from *Pasteurella multocida*. Biochemistry 45, 2139-2148.

[25] Yamamoto, T., Ichikawa, M. and Takakura, Y. (2008). Conserved amino acid sequences in the bacterial sialyltransferases belonging to glycosyltransferase family 80. Biochem. Biophys. Res. Commun. 365, 340-343.

[26] Wang, W. and Malcolm, B.A. (1999). Two-stage PCR protocol allowing introduction of multiple mutations, deletions and insertions using QuikChange site-directed mutagenesis. BioTechniques 26, 680-682.

[27] Chan, J., Sandhu, G. and Bennet, A.J. (2011). A mechanistic study of sialic acid mutarotation: implications for mutarotase enzymes. Org. Biomol. Chem. 9, 4818-4822.

[28] Friebolin, H., Kunzelmann, P., Supp, M., Brossmer, R., Keilich, G. and Ziegler, D. (1981). ^{1}H-NMR-spektroskopische Untersuchungen zur Mutarotation der *N*-Acetyl-D-neuraminsäure-ph-Abhängigkeit der Mutarotationsgeschwindigkeit. Tetrahedron Lett. 22, 1383-1386.

[29] Jaques, L.W., Brown, E.B., Barrett, J.M., Brey, W.S., Jr. and Weltner, W., Jr. (1977). Sialic acid. A calcium-binding carbohydrate. J. Biol. Chem. 252, 4533-4538.

[30] Klepach, T., Carmichael, I. and Serianni, A.S. (2008). 13C-labeled N-acetyl-neuraminic acid in aqueous solution: detection and quantification of acyclic keto, keto hydrate, and enol forms by 13C NMR spectroscopy. J. Am. Chem. Soc. 130, 11892-11900.

[31] Moustafa, I., Connaris, H., Taylor, M., Zaitsev, V., Wilson, J.C., Kiefel, M.J., von Itzstein, M. and Taylor, G. (2004). Sialic acid recognition by *Vibrio cholerae* neuraminidase. J. Biol. Chem. 279, 40819-40826.

[32] Beau, J.-M., Schauer, R., Haverkamp, J., Kamerling, J.P., Dorland, L. and Vliegenthart, J.F.G. (1984). Chemical behaviour of cytidine 5′-monophospho-*N*-acetyl-*β*-D-neuraminic acid under neutral and alkaline conditions. Eur. J. Biochem. 140, 203-208.

[33] Comb, D.G., Watson, D.R. and Roseman, S. (1966). The sialic acids: IX. Isolation of cytidine 5'-monophospho-N-acetylneuramininic acid from *Escherichia coli* K-235. J. Biol. Chem. 241, 5637-5642.

[34] Kajihara, Y., Nishigaki, S., Hanzawa, D., Nakanishi, G., Okamoto, R. and Yamamoto, N. (2011). Unique self-anhydride formation in the degradation of cytidine-5′-monophosphosialic acid (CMP-Neu5Ac) and cytidine-5′-diphosphosialic acid (CDP-Neu5Ac) and its application in CMP-sialic acid analogue synthesis. Chem. Eur. J. 17, 7645-7655.

[35] Amaya, M.F. et al. (2004). Structural insights into the catalytic mechanism of *Trypanosoma cruzi* trans-sialidase. Structure 12, 775-784.

[36] Damager, I., Buchini, S., Amaya, M.F., Buschiazzo, A., Alzari, P., Frasch, A.C., Watts, A. and Withers, S.G. (2008). Kinetic and mechanistic analysis of *Trypanosoma cruzi* trans-sialidase reveals a classical ping-pong mechanism with acid/base catalysis. Biochemistry 47, 3507-3512.

[37] Newstead, S.L., Potter, J.A., Wilson, J.C., Xu, G., Chien, C.-H., Watts, A.G., Withers, S.G. and Taylor, G.L. (2008). The structure of *Clostridium perfringens* NanI sialidase and its catalytic intermediates. J. Biol. Chem. 283, 9080-9088.

[38] Watts, A.G., Damager, I., Amaya, M.L., Buschiazzo, A., Alzari, P., Frasch, A.C. and Withers, S.G. (2003). *Trypanosoma cruzi* trans-sialidase operates through a covalent sialyl−enzyme intermediate: tyrosine is the catalytic nucleophile. J. Am. Chem. Soc. 125, 7532-7533.

[39] Watts, A.G., Oppezzo, P., Withers, S.G., Alzari, P.M. and Buschiazzo, A. (2006). Structural and kinetic analysis of two covalent sialosyl-enzyme intermediates on *Trypanosoma rangeli* sialidase. J. Biol. Chem. 281, 4149-4155.

[40] Watts, A.G. and Withers, S.G. (2004). The synthesis of some mechanistic probes for sialic acid processing enzymes and the labeling of a sialidase from *Trypanosoma rangeli*. Can. J. Chem. 82, 1581-1588.

[41] Watson, J.N., Dookhun, V., Borgford, T.J. and Bennet, A.J. (2003). Mutagenesis of the conserved active-site tyrosine changes a retaining sialidase into an inverting sialidase. Biochemistry 42, 12682-12690.

[42] Rye, C.S. and Withers, S.G. (2000). Glycosidase mechanisms. Curr. Opin. Chem. Biol. 4, 573-580.

[43] Massoud, S.S. and Sigel, H. (1988). Metal ion coordinating properties of pyrimidine-nucleoside 5'-monophosphates (CMP, UMP, TMP) and of simple phosphate monoesters,

including D-ribose 5'-monophosphate. Establishment of relations between complex stability and phosphate basicity. Inorg. Chem. 27, 1447-1453.

[44] Fersht, A.R. et al. (1985). Hydrogen bonding and biological specificity analysed by protein engineering. Nature 314, 235-238.

[45] Lin, L.Y.-C., Rakic, B., Chiu, C.P.C., Lameignere, E., Wakarchuk, W.W., Withers, S.G. and Strynadka, N.C.J. (2011). Structure and mechanism of the lipooligosaccharide sialyltransferase from *Neisseria meningitidis*. J. Biol. Chem. 286, 37237-37248.

Legends to figures

Fig. 1. (A) Proposed single displacement-like axial-to-equatorial inverting mechanism of the catalytic reaction of family GT-80 bacterial sialyltransferases. The ROH acceptor is the nucleophile of the reaction. While in the "normal" sialyltransferase reaction, ROH is a carbohydrate, typically D-galactose or D-galactoside, the same mechanism might result in CMP-Neu5Ac donor substrate hydrolysis when water replaces ROH. (B) Key active-site residues in crystallographic and biochemical studies of PmST1 (pink, PDB code 2IHZ) and corresponding residues in the modeled structure of PdST (grey, homology model [22]). CMP-3F(a)Neu5Ac (drawn with green-colored carbon atoms) and lactose (drawn with yellow-colored carbon atoms) are shown. (C) Products of inverting (α-Neu5Ac) and retaining (β-Neu5Ac) CMP-Neu5Ac hydrolysis.

Fig. 2. Time-resolved ^{1}H NMR (500 MHz) analysis of wild-type PdST (5 µM) catalyzed CMP-Neu5Ac hydrolysis. For reaction conditions, see the Methods. The initial CMP-Neu5Ac concentration was 1.0 mM.

Fig. 3. (A) Superimposition of HPLC elution profiles of samples from sialylation of oNP-βGal catalyzed by wild-type PdST and His^{284} variants thereof. Authentic Neu5Acα2,3Gal-oNP elutes with a retention time of 8.7 min. Retention times of the other components in the sialyltransferase reaction mixture are 1.4 min (CMP), 2.1 min (CMP-Neu5Ac) and 4.5 min (oNP-βGal). (B) Time course of the enzymatic synthesis of Neu5Acα2,3Gal-oNP. H284N (●, ○); H284Y (■, □); H284D (▲, Δ); and WT (♦, ◊); closed symbols, Neu5Acα2,3Gal-oNP; open symbols, CMP. 0.5 µM (wild-type) and 5 µM (His^{284} variants) of enzyme were used. (C) Neu5Acα2,3Gal-oNP yields (black bars) after complete conversion of CMP-Neu5Ac and the corresponding ratios of donor substrate hydrolysis to sialyltransfer under "synthesis conditions" (grey bars), when acceptor substrate (oNP-βGal) was present in the reactions. Note therefore that the ratios given here are not simply the reciprocal R_{TH} values shown in Table 1, even though $1/R_{TH}$ reflects the trend seen in synthesis experiments.

Fig. 4. ^{1}H NMR (500 MHz) spectra of samples from hydrolysis reactions catalyzed by H284N, H284Y, and H284D variant of PdST are shown. For reaction conditions, see the Methods. The initial CMP-Neu5Ac concentration was 2.0 mM.

Figure 1

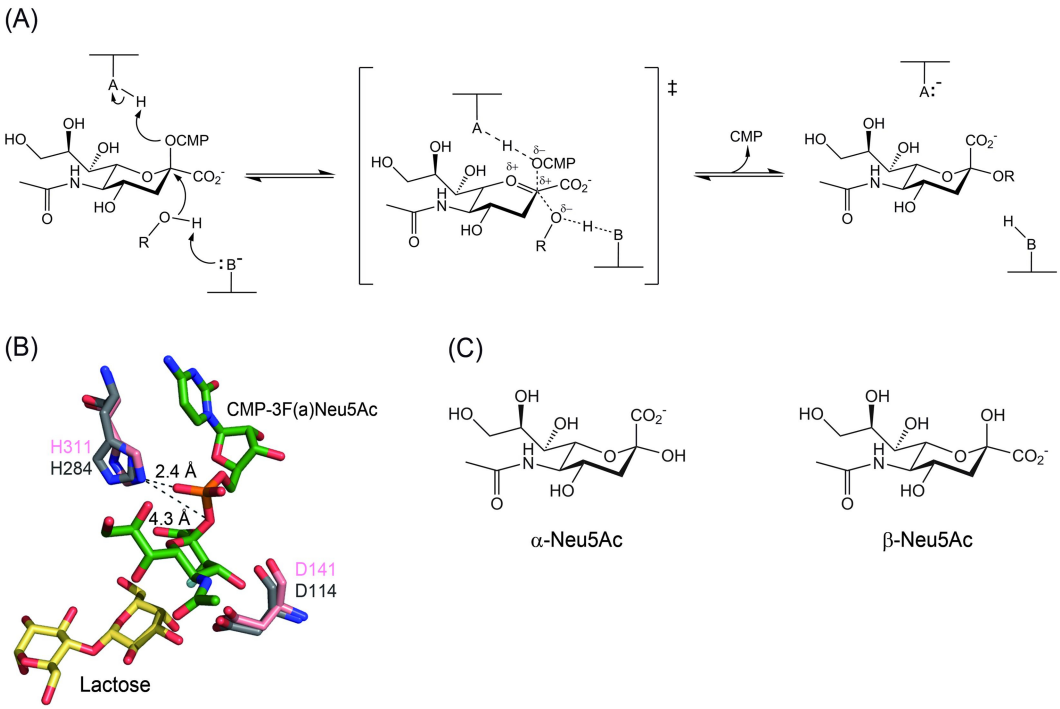
(A)
(B)
CMP-3F(a)Neu5Ac
H311
H284
2.4 Å
4.3 Å
D141
D114
Lactose
(C)
α-Neu5Ac
β-Neu5Ac

Figure 2

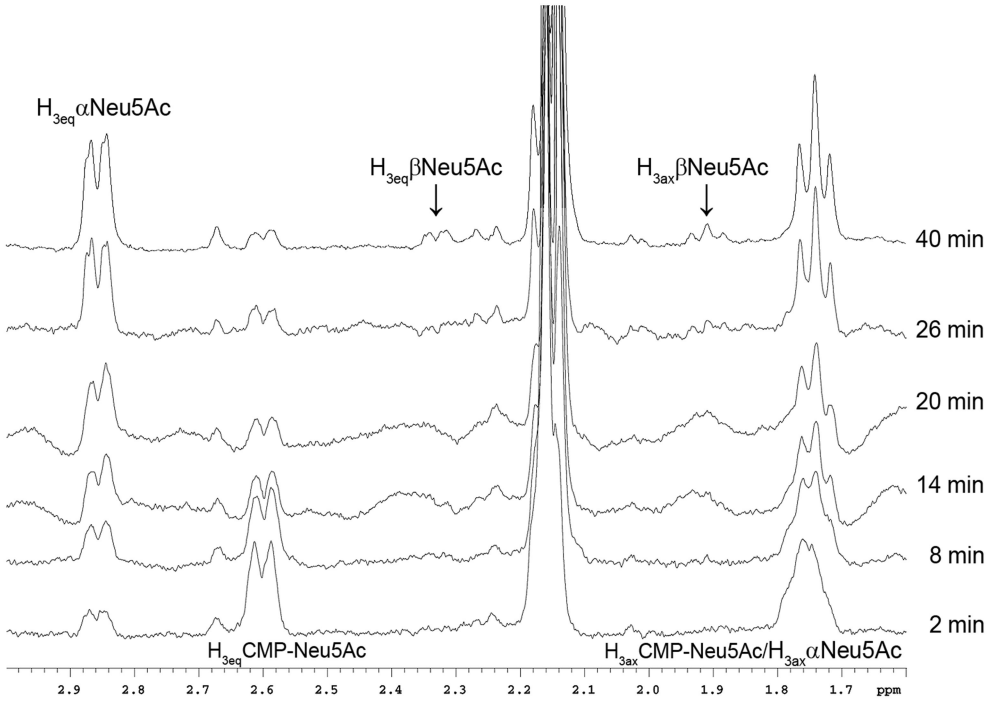
H3eqαNeu5Ac
H3eqβNeu5Ac
H3axβNeu5Ac
40 min
26 min
20 min
14 min
8 min
2 min
H3eqCMP-Neu5Ac
H3axCMP-Neu5Ac/H3axαNeu5Ac
2.9 2.8 2.7 2.6 2.5 2.4 2.3 2.2 2.1 2.0 1.9 1.8 1.7 ppm

Figure 3

(A)

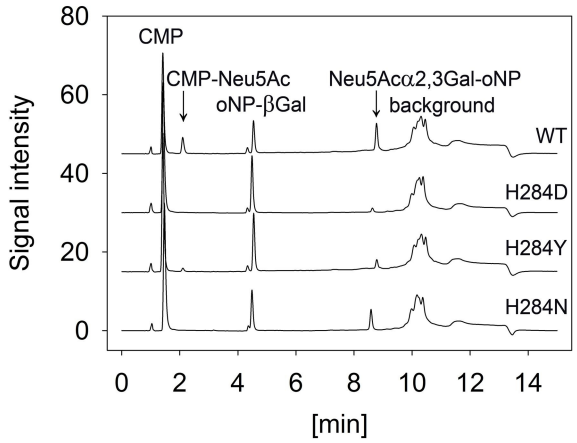
CMP
CMP-Neu5Ac
oNP-βGal
Neu5Acα2,3Gal-oNP
background
WT
H284D
H284Y
H284N
Signal intensity
[min]

(B)

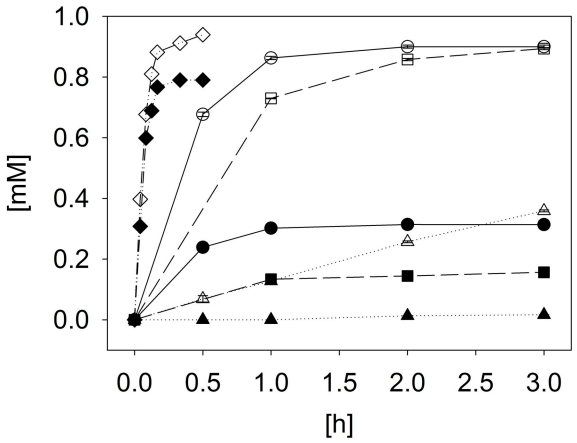
[mM]
[h]

(C)

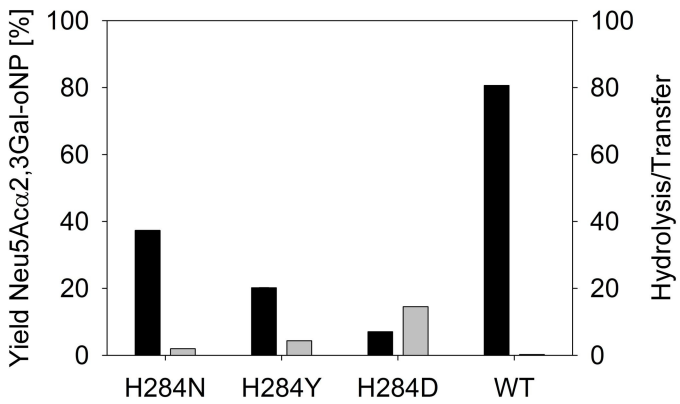
Yield Neu5Acα2,3Gal-oNP [%]
Hydrolysis/Transfer
H284N
H284Y
H284D
WT

Figure 4

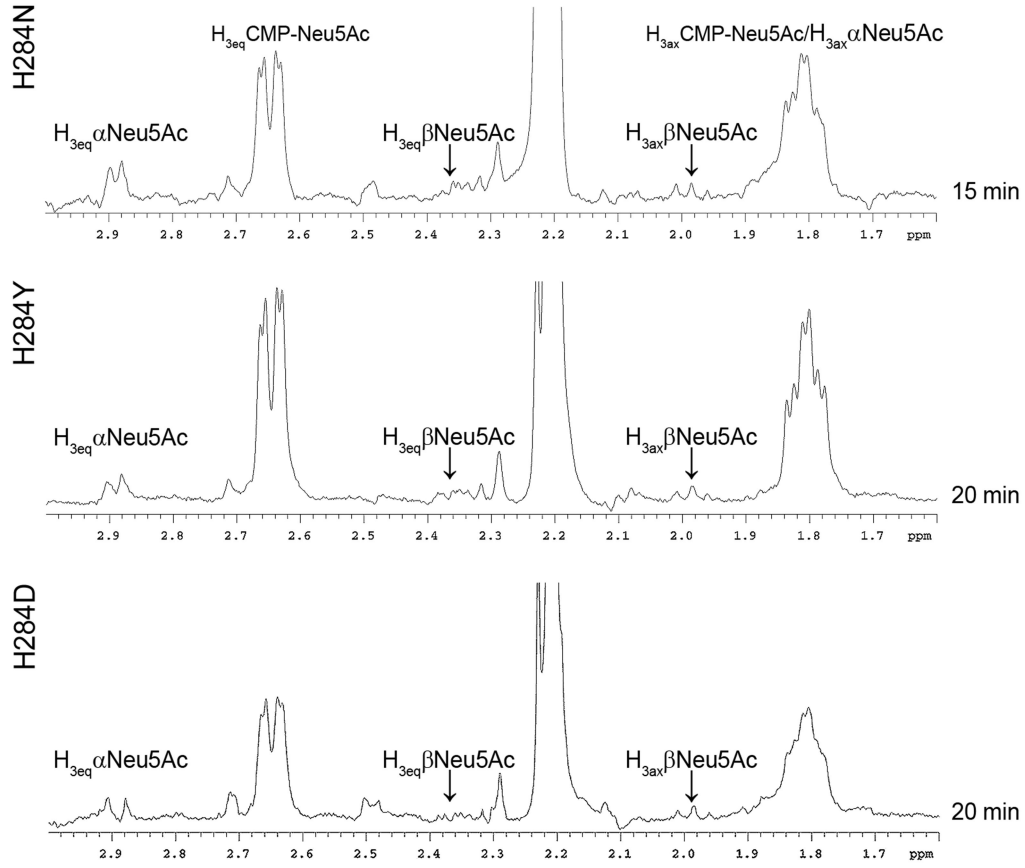
H284N
H3eqCMP-Neu5Ac
H3axCMP-Neu5Ac/H3axαNeu5Ac
H3eqαNeu5Ac
H3eqβNeu5Ac
H3axβNeu5Ac
15 min
2.9 2.8 2.7 2.6 2.5 2.4 2.3 2.2 2.1 2.0 1.9 1.8 1.7 ppm
H284Y
H3eqαNeu5Ac
H3eqβNeu5Ac
H3axβNeu5Ac
20 min
2.9 2.8 2.7 2.6 2.5 2.4 2.3 2.2 2.1 2.0 1.9 1.8 1.7 ppm
H284D
H3eqαNeu5Ac
H3eqβNeu5Ac
H3axβNeu5Ac
20 min
2.9 2.8 2.7 2.6 2.5 2.4 2.3 2.2 2.1 2.0 1.9 1.8 1.7 ppm

Table 1. Specific sialyltransferase and hydrolase activities of wild-type PdST and His^{284} variants thereof.

	Sialyltransferase [a] (U/mg)	CMP-Neu5Ac hydrolase (U/mg)	R_{TH} [b]
WT	5.9	3.7	1.6
H284D	$2.1 \cdot 10^{-4}$	$7.6 \cdot 10^{-3}$	$2.8 \cdot 10^{-2}$
H284Y	$9.4 \cdot 10^{-3}$	$4.8 \cdot 10^{-2}$	$2.0 \cdot 10^{-1}$
H284N	$3.4 \cdot 10^{-2}$	$5.6 \cdot 10^{-2}$	$6.1 \cdot 10^{-1}$

The S.D. for specific activities was equal or smaller than 6% of the reported values.
[a]Acceptor: oNP-βGal, product: Neu5Acα2,3Gal-oNP; see the Methods for the assays used.
[b]R_{TH} is the ratio of specific activities of sialyltransfer to donor substrate hydrolysis in the absence of acceptor substrate.

Supplementary information

Mechanistic study of CMP-Neu5Ac hydrolase activity of the multifunctional α2,3-sialyltransferase from *Pasteurella dagmatis* PdST

Katharina Schmölzer[1], Christiane Luley-Goedl[1], Tibor Czabany[2], Doris Ribitsch[1], Helmut Schwab[1,4], Hansjörg Weber[3], Bernd Nidetzky[1,2]

[1]Austrian Centre of Industrial Biotechnology, Petersgasse 14, 8010 Graz, Austria

[2]Institute of Biotechnology and Biochemical Engineering, Graz University of Technology, Petersgasse 12/I, 8010 Graz, Austria

[3]Institute of Organic Chemistry, Graz University of Technology, Stremayrgasse 9, 8010 Graz, Austria

[4]Institute of Molecular Biotechnology, Graz University of Technology, Petersgasse 14, 8010 Graz, Austria

Table of contents

Site-directed mutagenesis S3

Protein purification S4

Sialyltransferase activity assay S5

CMP-Neu5Ac hydrolase activity assay S5

Trans-sialylation assay S6

Figure S1. ^{1}H NMR analysis of Neu5Ac at equilibrium S8

Figure S2. Uncatalyzed CMP-Neu5Ac hydrolysis rates
at different pH values and temperatures S9

Figure S3. Time course of the uncatalyzed CMP-Neu5Ac hydrolysis
at pH 5.5 and 5°C . S10

Figure S4. Time course of the wild-type PdST catalyzed
CMP-Neu5Ac hydrolysis at pH 5.5 and 5°C S11

Figure S5. Time course of the enzymatic synthesis of Neu5Acα2,3Gal-oNP
using wild-type, H284D, H284Y, and H284N variants of PdST S12

Figure S6. Time-resolved ^{1}H NMR (500 MHz) analysis of uncatalyzed
CMP-Neu5Ac hydrolysis at pH 5.5 and 28°C S13

Figure S7. Time-resolved ^{1}H NMR (500 MHz) analysis of wild-type PdST
catalyzed CMP-Neu5Ac hydrolysis at pH 5.5 and 5°C S14

Figure S8. Superimposition of HPLC elution profiles of samples from sialylation of
oNP-βGal catalyzed by wild-type PdST and His^{284} variants thereof S15

Methods

Site-directed mutagenesis

A pair of complementary oligonucleotide primers, each introducing the desired site-directed substitution at the protein level, was used. The mismatched bases are underlined.

H284N forward:

5´-CAATATAAAATCTATTTCAAAGGTAACCCAAGAGGTGGAGATATCAATGAT-3´

H284N reverse:

5´-ATCATTGATATCTCCACCTCTTGGGTTACCTTTGAAATAGATTTTATATTG-3´

H284Y forward:

5´-CAATATAAAATCTATTTCAAAGGTTATCCAAGAGGTGGAGATATCAATGAT-3´

H284Y reverse:

5´-ATCATTGATATCTCCACCTCTTGGATAACCTTTGAAATAGATTTTATATTG-3´

H284D forward:

5´-CAATATAAAATCTATTTCAAAGGTGACCCAAGAGGTGGAGATATCAATGAT-3´

H284D reverse:

5´-ATCATTGATATCTCCACCTCTTGGGTCACCTTTGAAATAGATTTTATATTG-3´

The PCR was performed in a Gene Amp® PCR 2200 thermocycler (Applied Biosystems, USA). The PCR was carried out in 50 µL using 0.3 µM forward and reverse primer, 0.2 mM dNTP-mix, 3.6 U Pfu DNA Polymerase (Promega, USA) and 1x reaction buffer provided by the supplier. The two-stage protocol involved in the first step two separate PCR reactions with the forward and reverse primers. These reactions consisted of a preheating step at 95°C for 60 s followed by 4 reaction cycles (95°C, 50 s; 55°C, 50 s; 72°C, 10 min). After this first step both PCR reactions

were mixed together in a 1:1 ratio followed by second standard mutagenesis PCR reaction using the same temperature program (95°C, 50 s; 55°C, 50 s; 72°C, 10 min) for 18 cycles. The amplification product was subjected to parental template digest by *Dpn*I (Fermentas, Germany) in accordance to the manufacturer's instructions and transformed into electro-competent *E. coli* BL21_Gold(DE3) cells. All inserts were sequenced as custom service by Agowa (Germany). Wizard® Plus SV Minipreps Kit from Promega (USA) was used to prepare plasmid DNA. DNA analysis was performed with Vector NTI Suite 10 (Invitrogen, USA).

Protein purification

Protein expression and preparation of the cell lysate were done as previously described [21]. The proteins were purified using an ÄKTAprime plus system (GE Healthcare, Germany). The cleared cell lysate was loaded onto two HisTrap HP FF 5 mL columns (GE Healthcare, Germany) at a flow rate of 2 mL/min. The columns had been equilibrated with binding buffer (30 mM potassium phosphate, 300 mM NaCl, 15 mM imidazol, 10% glycerol, pH 7.4). After a washing step of 10 column volumes, the enzyme was eluted with a linear gradient of 15 - 300 mM imidazol within 10 column volumes. Fractions of 3 mL were collected and analyzed by SDS-PAGE. Sialyltransferase containing fractions were pooled and dialyzed overnight against 20 mM Tris/HCl, 150 mM NaCl, pH 7.5. Purified enzymes were aliquoted and stored at -70°C.

Sialyltransferase activity assay

The reactions were performed in duplicate in a total volume of 20 µL in 50 mM sodium phosphate buffer, pH 8.0 containing 1 mM CMP-Neu5Ac, 1 mM oNP-βGal, 5 µM enzyme and 1 mg/mL BSA. The enzymatic reaction was carried out at 25°C and agitation rate of 400 rpm using a Thermomixer comfort (Eppendorf, Germany). The enzymatic reactions were stopped at certain time points of incubation by addition of 40 µL of ice-cold acetonitrile. The reaction mixtures were incubated on ice for 10 min and centrifuged at 4°C, 13,000 rpm for 10 min to remove precipitated protein. For time course experiments the same conditions were used and reactions were stopped after 0, 0.5, 1, 2, 3 and 22 h. After appropriate dilution, 5 µL were injected to HPLC analysis using a Chromolith® Performance RP-18 (100 x 4.6 mm; Merck Chemicals, Germany) column in reversed phase ion-pairing mode on an Agilent Technologies 1200 Series system. The column was equilibrated with 20 mM phosphate buffer, pH 6.8 containing 2 mM tetrabutylammonium at a flow rate of 2 mL/min. A temperature control unit maintained 30°C throughout the analysis. Samples were eluted with a linear gradient from 0 – 25% acetonitrile in 11 min and detected by UV at 254 nm. All compounds involved in the reaction were analyzed. One unit (1 U) was defined as the amount of enzyme that could transfer 1 µmol of sialic acid per min to oNP-βGal under the conditions described above.

CMP-Neu5Ac hydrolase activity measurement

The reactions were performed in duplicate in a total volume of 20 µL in 50 mM sodium phosphate buffer, pH 8.0 containing 1 mM CMP-Neu5Ac, 5 µM enzyme and 1 mg/mL BSA. The enzymatic reaction was carried out at 25°C and agitation rate of 400 rpm using a Thermomixer comfort (Eppendorf, Germany). The enzymatic

reactions were stopped at certain time points of incubation by addition of 40 µL of ice-cold acetonitrile. The reaction mixtures were incubated on ice for 10 min and centrifuged at 4°C, 13,000 rpm for 10 min to remove precipitated protein. For time course experiments the same conditions were used and reactions were stopped after 0, 0.5, 1, 2, 3 and 22 h. The reaction products were analyzed by HPLC as described above for the sialyltransferase activity assay.

Trans-sialylation assay

The reactions were performed in duplicate in a total volume of 20 µL in 50 mM citric buffer, pH 5.5 containing 1.58 mM 3´-sialyllactose, 1.58 mM oNP-βGal, 1 (wild-type) or 5 µM (His^{284} mutants) enzyme and 1 mg/mL BSA. Reactions were performed with and without 1 mM CMP. The enzymatic reaction was carried out at 25°C and agitation rate of 400 rpm using a Thermomixer comfort (Eppendorf, Germany). The enzymatic reactions were stopped after 0, 2.5, 5, 7.5, 10, 15, 30, and 45 min (wild-type) and 0, 0.25, 0.5, 1, 2, 3, 4, 5 and 22 h (His^{284} mutants) by addition of 40 µL of ice-cold acetonitrile. The reaction mixtures were incubated on ice for 10 min and centrifuged at 4°C, 13,000 rpm for 10 min to remove precipitated protein. After appropriate dilution, 5 µL were injected to HPLC analysis using a Synergi™ 4 µm Hydro-RP 80 Å (150 x 2 mm; Phenomenex, USA) column in reversed phase ion-pairing mode on an Agilent Technologies 1200 Series system. The column was equilibrated with 20 mM phosphate buffer, pH 6.8 containing 2 mM tetrabutylammonium at a flow rate of 0.5 mL/min. A temperature control unit maintained 30°C throughout the analysis. Samples were eluted with 0% acetonitrile in 3 min followed by a linear gradient from 0 – 25% acetonitrile in 10 min and detected by UV at 254 nm. The decrease in the substrate (oNP-βGal) and the

increase in product were followed. One unit (1 U) was defined as the amount of enzyme that could transfer 1 μmol of sialic acid per min to oNP-βGal under the conditions described above.

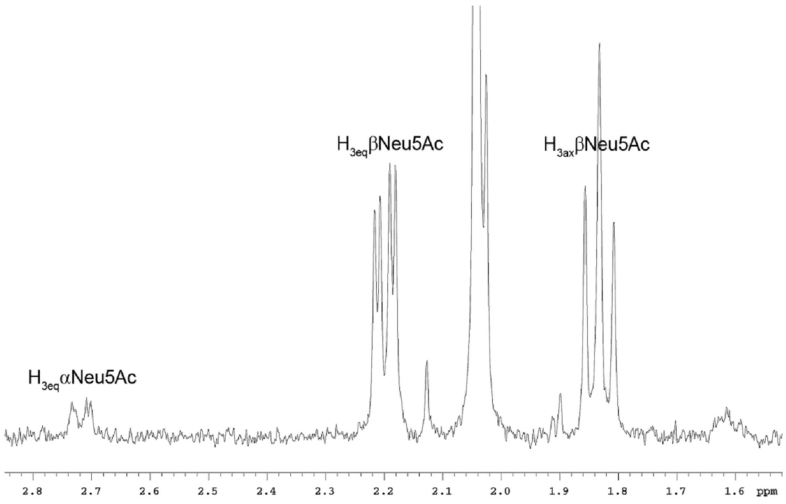

Fig. S1. ^{1}H NMR (500 MHz) analysis of Neu5Ac at equilibrium. Neu5Ac was incubated at room temperature and pH 8.0 overnight before NMR measurement. Integration of the peaks showed that the equilibrium mixture consists of ~90% β-anomer and ~10% α-anomer.

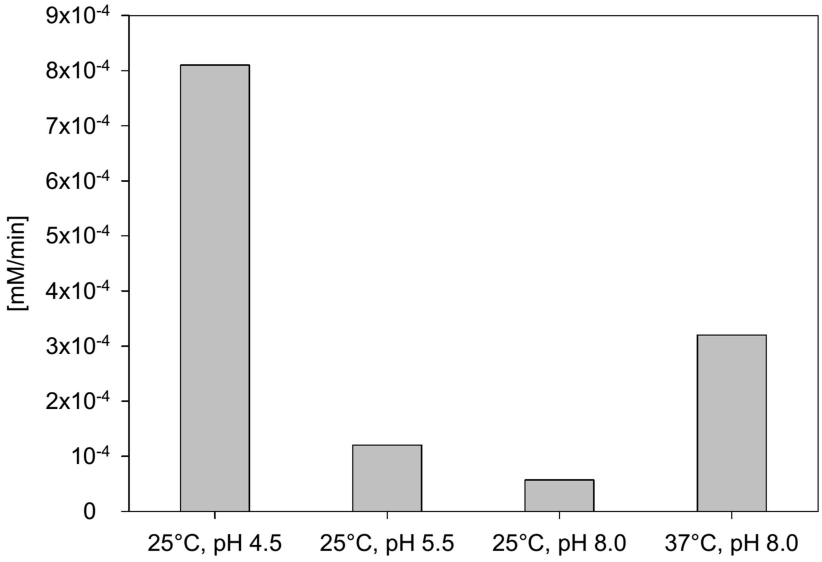

Fig. S2. Uncatalyzed CMP-Neu5Ac hydrolysis rates at different pH values and temperatures. The reaction mixture (20 µL), containing 1 mM CMP-Neu5Ac in 50 mM buffer was incubated at 25°C or 37°C and 400 rpm. A sodium citrate buffer was used at pH 4.5 and 5.5 and a sodium phosphate buffer was used at pH 8.0.

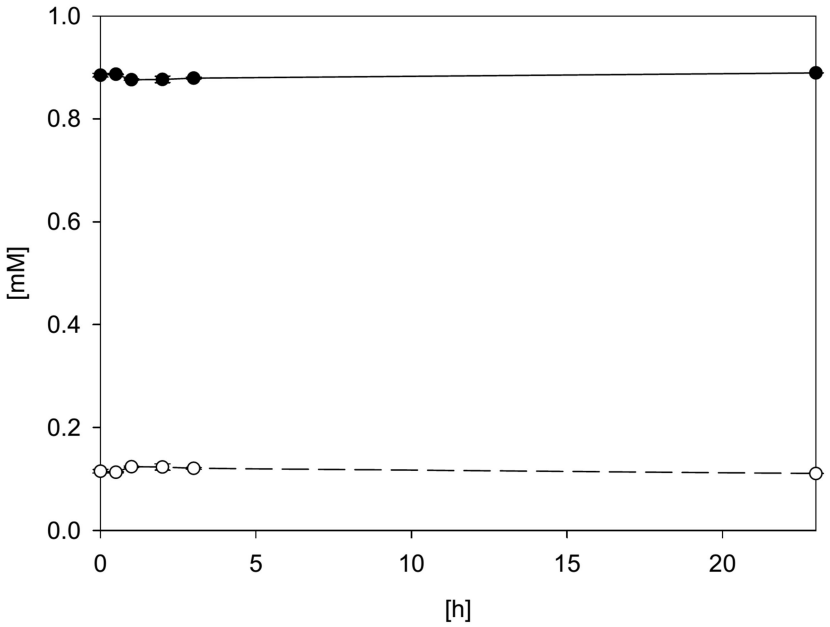

Fig. S3. Time course of the uncatalyzed CMP-Neu5Ac hydrolysis at pH 5.5 and 5°C. The reaction mixture (20 µL), containing 1 mM CMP-Neu5Ac in 50 mM sodium citrate buffer, pH 5.5, was incubated at 5°C and 0 rpm. Reactions were stopped after 0, 0.5, 1, 2, 3, and 22 h by addition of ice-cold acetonitrile (40 µL).The samples were analyzed by HPLC as described for the sialyltransferase activity assay. CMP-Neu5Ac (●, solid line); released CMP (○, dashed line).

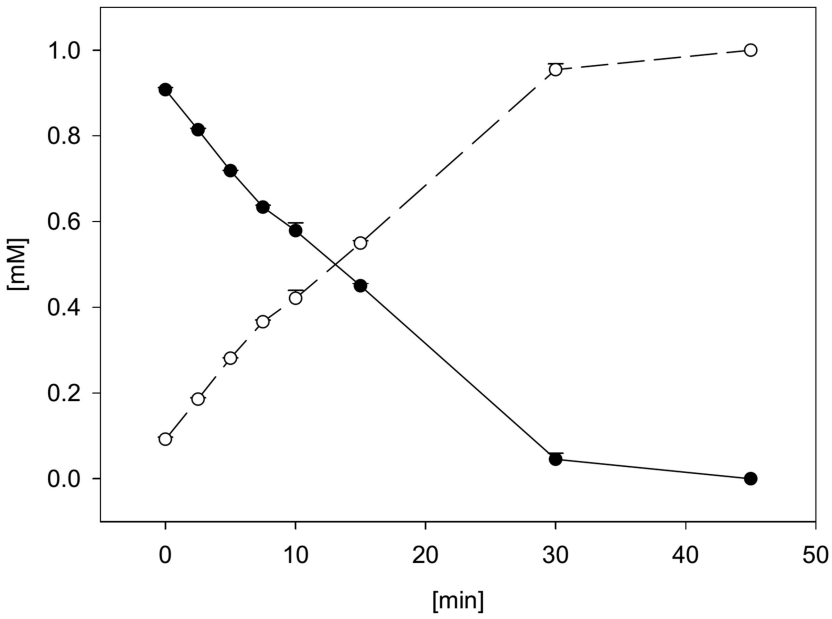

Fig. S4. Time course of the wild-type PdST catalyzed CMP-Neu5Ac hydrolysis at pH 5.5 and 5°C. The reaction mixture (20 µL), containing 1 mM CMP-Neu5Ac, 5 µM enzyme, 1 mg/mL BSA in 50 mM sodium citrate buffer, pH 5.5, was incubated at 0 rpm and 5°C. Reactions were stopped after 0, 2.5, 5, 7.5, 10, 15, 30 and 45 min by addition of ice-cold acetonitrile (40 µL). The samples were analyzed by HPLC as described for the sialyltransferase activity assay. CMP-Neu5Ac (●, solid line); released CMP (○, dashed line).

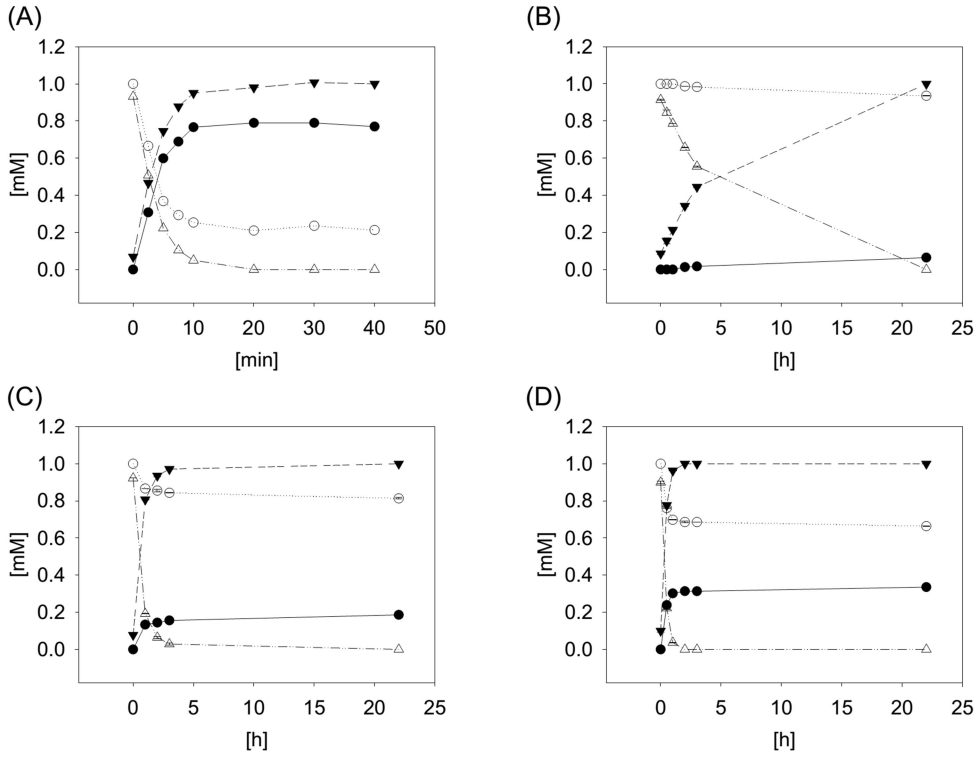

Fig. S5. Time course of the enzymatic synthesis of Neu5Acα2,3Gal-oNP using wild-type (A) [21], H284D (B), H284Y (C) and H284N (D) variants of PdST. oNP-βGal, open circle; Neu5Acα2,3Gal-oNP, filled circle; CMP-Neu5Ac, open triangle; CMP, closed reverse triangle. The reaction mixture (20 µL), containing 1 mM CMP-Neu5Ac, 1 mM oNP-βGal, 0.5 µM (wild-type) or 5 µM (His^{284} variants) enzyme, 1 mg/mL BSA in 50 mM sodium phosphate buffer, pH 8.0, was incubated at 25°C. Sampling and sample analysis are described in *Materials and methods*.

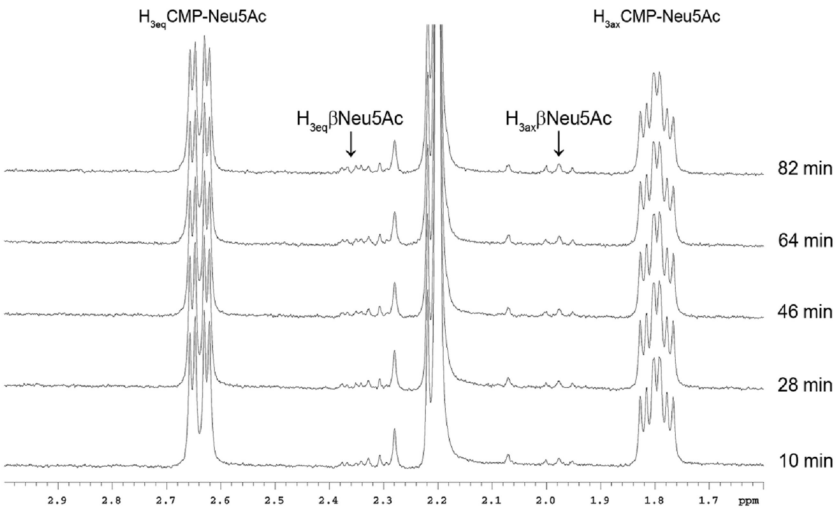

Fig. S6. Time-resolved ^{1}H NMR (500 MHz) analysis of uncatalyzed CMP-Neu5Ac hydrolysis. The reaction was performed at 28°C in a total volume of 600 µL in sodium tartrate buffer (50 mM, pH 5.5) containing 5 mM CMP-Neu5Ac.

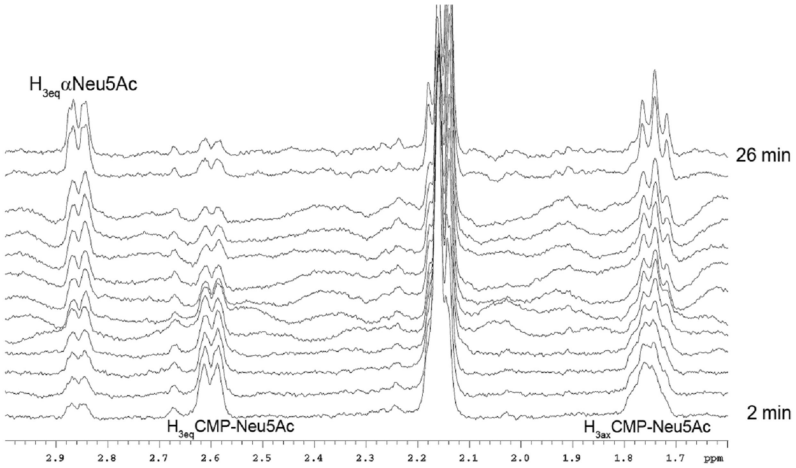

Fig. S7. Time-resolved ^{1}H NMR (500 MHz) analysis of wild-type PdST catalyzed CMP-Neu5Ac hydrolysis. The reaction was performed at 5°C in a total volume of 600 µL in sodium tartrate buffer (50 mM, pH 5.5) containing 1 mM CMP-Neu5Ac, 1 mg/mL BSA and 5 µM enzyme. Spectral data were acquired every 2 min.

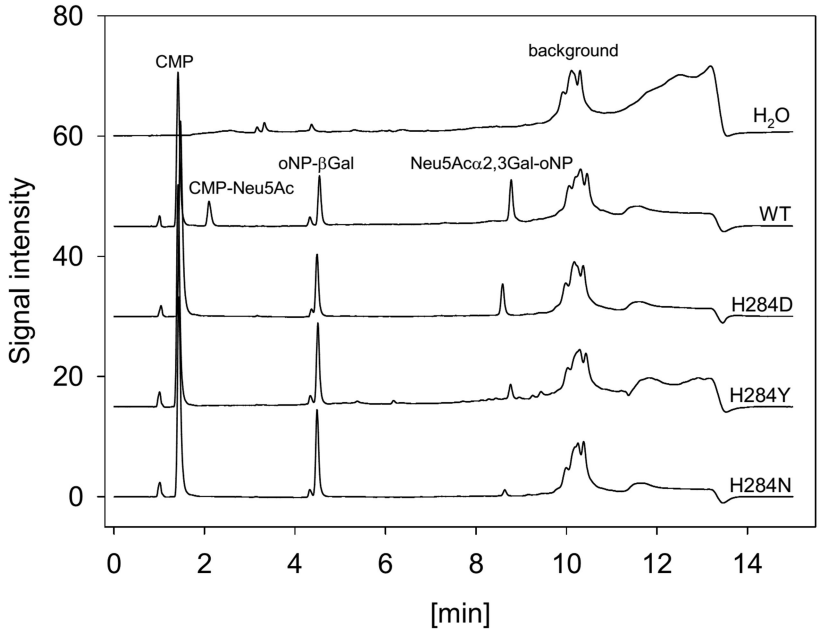

Fig. S8. Superimposition of HPLC elution profiles of samples from sialylation of oNP-βGal catalyzed by wild-type PdST and His^{284} variants thereof. Authentic Neu5Acα2,3Gal-oNP elutes with a retention time of 8.7 min. Retention times of the other components in the sialyltransferase reaction mixture are 1.4 min (CMP), 2.1 min (CMP-Neu5Ac) and 4.5 min (oNP-βGal), and 10.1 min background.

Complete Switch from α2,3- to α2,6-Regioselectivity in *Pasteurella dagmatis* β-D-Galactoside Sialyltransferase by Active-Site Redesign

Katharina Schmölzer,[†] Tibor Czabany,[‡] Christiane Luley-Goedl,[†] Doris Ribitsch,[†] Helmut Schwab,[†,§] Bernd Nidetzky[†,‡,*]

†Austrian Centre of Industrial Biotechnology, Petersgasse 14, 8010 Graz

‡Institute of Biotechnology and Biochemical Engineering, Graz University of Technology, Petersgasse 12/I, 8010 Graz, Austria

§Institute of Molecular Biotechnology, Graz University of Technology, Petersgasse 14, 8010 Graz, Austria

In preparation.

ABSTRACT: We report structure-guided active-site redesign of β-D-galactoside sialyltransferase (from *Pasteurella dagmatis*) to change enzyme regioselectivity from α2,3 in wild type to α2,6 in a P7H-M117A double mutant. The two sialyltransferases are used for alternative 3'- or 6'-sialylation of two synthetically important β-D-galactoside acceptor substrates, lactose and protein asialo-*N*-glycans. At pH 8.0 where enzymes are highly active and sialosides exhibit high stability, reactions from CMP-Neu5Ac donor substrate gave product yields of ≥ 70%.

Human milk oligosaccharides (HMOs) are a structurally distinct group of bioactive glycans unique to human milk.[1] Nearly 16% of the total HMOs comprise sialic acid[2], and sialyllactose is one of their main components[3]. Sialylated HMOs contain *N*-acetylneuraminic acid (Neu5Ac) attached to D-galactosyl or *N*-acetyl-D-galactosaminyl residues through α2,3- or α2,6-linkage (Scheme 1). Interest in sialylated HMOs is high due to their important roles in the development and health protection of newborn infants.[1,4] Since natural availability of sialylated HMOs is limited, synthetic sialyloligosaccharides (e.g. sialyllactose) are in great demand as infant formula[5,6] and neutraceutical ingredients[7,8].

Stereo- and regiocontrol are problems requiring special attention when installing a sialyl group on a nascent oligosaccharide. Selective biocatalytic sialylation avoids use of protecting group chemistry and therefore presents a highly attractive route for sialylated HMO synthesis. Sialyltransferases (STs; EC 2.4.99) catalyze transfer of a Neu5Ac residue from CMP-Neu5Ac to an acceptor oligosaccharide. Lactose is an expedient and also inexpensive acceptor, and its transformation into α2,3- or α2,6-sialyllactose (Scheme 1) has attracted considerable[9,10], in fact commercial interest. Although both sialyllactose regioisomers are biologically active[8,11], it is nevertheless important to have synthetic access to α2,3- and α2,6-sialoside products separately. Complementarily regioselective ST catalysts are needed for this purpose and ideally, one would use a pair of "ST twins" that differ in regioselectivity, but otherwise have completely uniform synthesis conditions and substrate specificities.

Scheme 1. Enzymatic Synthesis of α2,3- and α2,6-Sialyl- HMOs by Sialyltransferases with CMP-Neu5Ac and β-D-Galactoside substrates

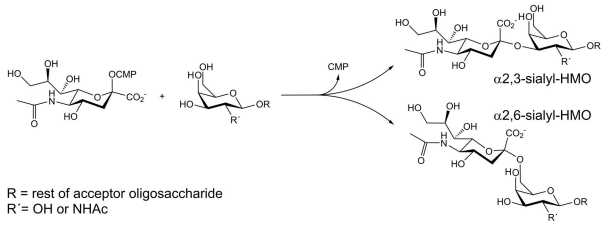

Only a relatively small number of natural α2,3- and α2,6-STs have been characterized so far, and the known enzymes exhibit strongly varying activity and stability properties. In particular, most STs are best active in an acidic pH range 5.0 – 6.0 [12-15]. However, sialoside synthesis takes place preferably at neutral to slightly alkaline pH (≈ 7.5 – 8.5) where spontaneous decomposition of CMP-Neu5Ac is minimized[16]. Product inhibition by CMP is pronounced in certain, especially mammalian STs.[15,17,18] Enzyme-catalyzed hydrolysis of CMP-Neu5Ac can also be a problem, particularly with bacterial STs.[19-22] Remedy is to a certain extent possible in all instances, but the clear drawback is that each enzyme requires extensive optimization individually. Being able to toggle between α2,3- or α2,6-sialylation with only minimal change in the biocatalytic system

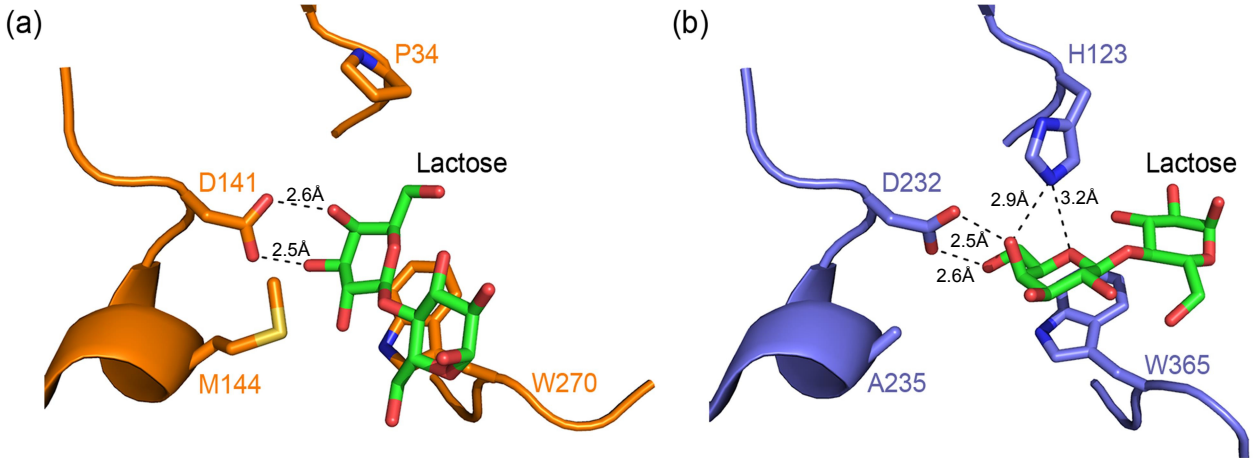

Figure 1. Acceptor-binding site comparison of family GT-80 α2,3- and α2,6-sialytransferases. (a) α2,3/α2,6-sialyltransferase from *P. multocida* PmST1 (PDB code 2ILV)[25]. (b) α2,6-sialyltransferase from *Photobacterium* sp. JT-ISH-224 (PDB code 2Z4T)[26].

used would therefore present a clear advantage.

We have focused in this study on glycosyltransferase family GT-80 that is rendered conspicuous among the known ST families by the broad variety of enzyme regioselectivities, namely α2,3-, α2,6-, and also mixed α2,3/α2,6, its members comprise[21,23,24]. STs of family GT-80 are furthermore characterized by high specific activity and broad acceptor substrate scope, which typically includes lactose. Active site remodeling of the naturally α2,3-selective β-D-galactoside ST from *Pasteurella dagmatis* (PdST)[19] was used to create the corresponding completely α2,6-selective counterpart enzyme. The desired biocatalytic toolbox for alternative α2,3- or α2,6-sialoside synthesis was thus provided and its application to sialylation of lactose at the preferred pH of 8.0 (which is also the optimum pH for sialyltransfer by PdST)[19] was demonstrated. Flexible α2,3- or α2,6-selective sialyltransfer was furthermore shown on a complex protein asialo-*N*-glycan substrate.

Design of the α2,6-selective PdST was developed from two family GT-80 protein structures that delineate distinct modes of accommodation of lactose at the acceptor binding sites of α2,3/α2,6-selective ST from *Pasteurella multocida* (PmST1) and α2,6-selective ST from *Photobacterium sp.* JT-ISH-224, as shown in Figure 1. PdST is 70% identical in amino acid sequence to PmST1, and residues of their acceptor binding sites (Figure 1a) are completely identical. Different orientations of the lactose β-D-galactosyl moiety relative to the catalytic base on the enzyme (Asp^{141}, Asp^{232}), such that either the 3-OH (Figure 1a) or the 6-OH (Figure 1b) is brought into a reactive position, appeared to have been evoked by a two amino acid residue substitution where Pro^{34} and Met^{144} in PmST1 are exchanged to, respectively, His^{123} and Ala^{235} in *Photobacterium* ST. Family-wide sequence comparison revealed clear sub-categorization of protein members of family GT-80 according to a highly conserved Pro/Met or His/Ala sequence pattern [see Table S1 in the Supporting Information (SI)] that was therefore hypothesized to be decisive for α2,3 compared to α2,6 ST regioselectivity. To graft α2,6-selective ST activity on PdST, the relevant residues Pro^{7} and Met^{117} were replaced to generate P7H single and P7H-M117A double variants of the naturally α2,3-selective wild-type enzyme. Biochemical data demonstrate an utterly successful active-site redesign.

Purified preparations of wild type and variant PdST were obtained from *Escherichia coli* overexpression culture producing target protein equipped with a C-terminal His_6-tag for purification by metal chelate chromatography. Specific activity for sialyltransfer to lactose (1 mM) from CMP-Neu5Ac (1 mM) was determined at pH 8.0, measuring the consumption of CMP-Neu5Ac and the release of CMP by HPLC, and the formation of sialyllactose by HPAEC-PAD (high-performance anion exchange chromatography with pulsed amperometric detection). The specific activity of P7H mutant was identical (5.7 U/mg protein) to that of the wild-type enzyme. The specific activity of the P7H-M117A double mutant was slightly lowered in comparison (2.2 U/mg). Sialyllactose regioisomers formed in the different enzymatic reactions were identified from their elution in HPAEC-PAD referenced against authentic standards of 3′- and 6′-sialyllactose, as shown in Figure 2. The wild-type enzyme produced 3′-sialyllactose exclusively. Single mutation of Pro^{7} to His drastically changed enzyme regioselectivity, so that 6'-sialylation of lactose was now strongly favored. However, 3′- sialyllactose was still present to ~4% of total transfer product (Figure 2), indicating that α2,3-ST activity had not been completely abolished in the P7H mutant. The double mutant P7H-M117A, by contrast, featured complete α2,3 to α2,6 switch in ST regioselectivity. No 3'-sialyllactose was detectable (≤ 1%) next to 6'-sialyllactose as product of the enzymatic sialyltransfer (Figure 2). These results suggest distinct and divergingly

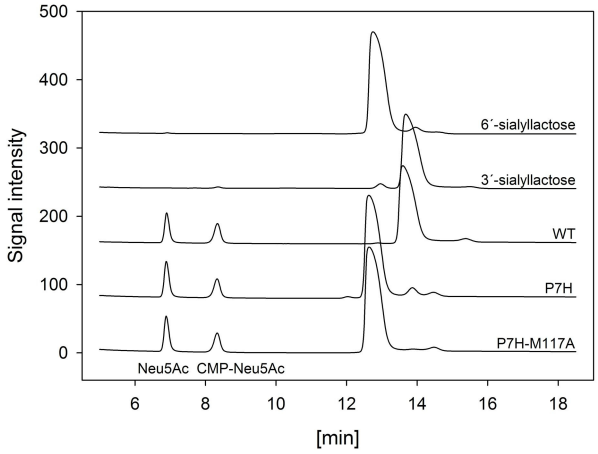

Figure 2. Gradual change from α2,3- to α2,6-regioselective sialyltransfer from CMP-Neu5Ac to lactose, resulting from substitution of Pro[7] by His and from additional substitution of Met[117] by Ala in PdST. Traces of HPAEC-PAD analysis of samples from different enzymatic reactions are superimposed along with traces of authentic 3'- and 6'-sialyllactose standards. The concentration of sialyllactose in each sample was approximately 0.7 mM. First 5 minutes omitted for clarity, shown in Figure S1 in the Supporting Information (SI).

important roles for His and Ala in conferring α2,6-regioselectivity to STs of family GT-80. While the His is clearly essential, the Ala seems to fulfil an auxiliary function in the fine-tuning of enzyme selectivity. Consistent with this notion, a single M117A mutant of PdST did not show significant change in regioselectivity as compared to wild-type enzyme (data not shown).

In a consequent next step, PdST and the mutants thereof were compared as biocatalysts for sialyllactose synthesis from CMP-Neu5Ac. Time courses of wild-type PdST and P7H-M117A variant are shown in Figure 3. The time-courses exactly reflect the mass balance. The two PdST enzymes yielded ≥ 70% of the alternative α2,3- or α2,6-sialyllactose regioisomers. Moreover, no product degradation was observed during the examined time period. Replacement by P7H single mutant led to identical yields of 6′-siallyllactose, but as discussed above, 3′-sialyllactose was produced as a side product [see Figure S2 in the Supporting Information (SI)]. The P7H-M117A double mutant of PdST features complete switch in regioselectivity, while preserving the basic properties of wild-type PdST, and is hence a perfect α2,6-ST.

P. multocida α2,3/α2,6-ST[23] and the *Photobacterium damselae* α2,6-ST[27] have been successfully applied in one-pot three enzyme synthesis of α2,3- and α2,6-linked sialosides, respectively, where appropriate conditions, suitable for each enzyme (sialic acid aldolase, CMP-sialic acid synthetase, ST), are strictly necessary. Our PdST enzyme toolbox provides the clear advantage of easy replaceability of the PdST variants for each other for

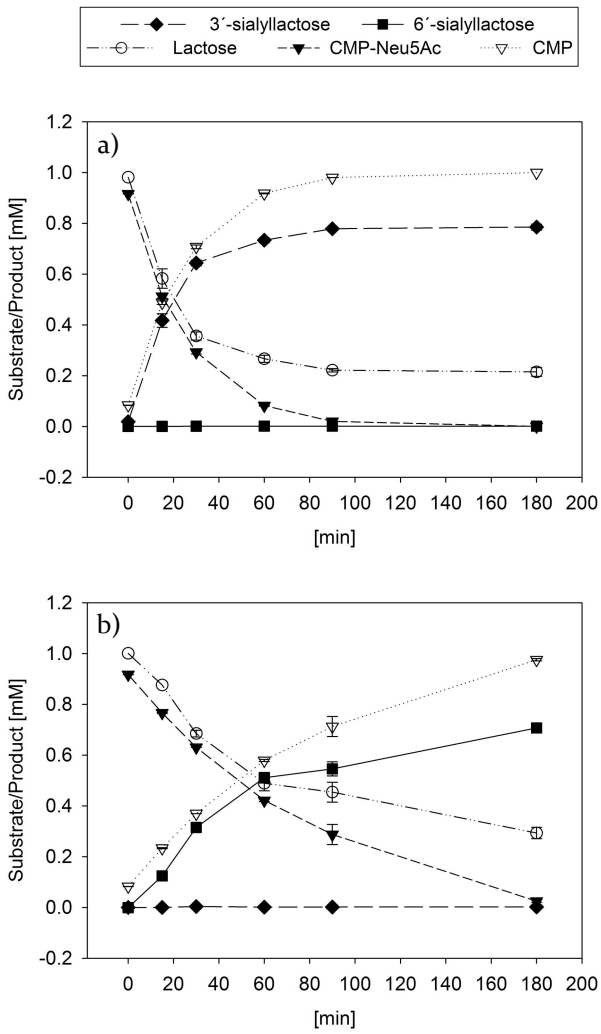

Figure 3. Time-courses of enzymatic synthesis of sialyllactose at pH 8.0 using 0.1 μM wild-type (a) and P7H-M117A variant (b) of PdST.

α2,3- or α2,6-linked sialoside synthesis, without further optimization of reaction conditions. Complete change from α2,3- to α2,6-regioselectivity was also reported for *P. multocida* PmST1 through lowering the pH from 8.5 to 4.5, however, only poor yields (5.5%) of α2,6-linked sialosides could be obtained at pH 5.5.[23] In a recent study, PmST1 catalyzed trans-sialylation of lactose from casein glycomacropeptide (cGMP) resulted in production of both 3′- and 6′-sialyllactose in a total yield of 45% and 35% at two distinct optimum conditions, but a concomitant by-product formation of ~20% (6′- or 3′-sialyllactose) could not be prevented even by careful control of pH and reaction time.[10] Moreover, several enzymatic methods employing trans-sialidases and sialidases have been described. Product hydrolysis is a severe drawback of applying sialidases, necessitating a strict control of the reaction time.[28-30] Sialidase activity of *Arthrobacter urefaciens* caused a sialyllactose loss of ~20% within 30 min and after 2 h

almost no product was left at pH 5.0.[28] In general, sialidases from different sources lack high yields, generally barely exceeding 13%.[28,31,32] The hydrolytic activity of a modified sialidase from *Trypanosoma rangeli* with enhanced trans-sialidase activity could also not be fully eliminated. Under optimized conditions (pH, temperature, reaction time, acceptor and donor concentrations) a 50% yield of 3′-sialyllactose was achieved from cGMP.[33] Implementation of higher 3′-sialyllactose yields using this engineered sialidase from *Trypanosoma rangeli* (≤ 70%) necessitated elaborate optimization of trans-sialylation versus hydrolysis activity (e.g. co-solvents[30], membrane-systems[34]). Another disadvantage of using sialidases in the transfer reactions is the need for a high excess of acceptor substrate (acceptor to donor ratio up to ~45:1)[29,30,33,34] to repress hydrolysis, which is especially relevant when working with expensive acceptors (e.g. *N*-acetyl-D-lactosamine). Application of *Trypanosoma cruzi* trans-sialidase in 3′-sialyllactose synthesis from the irreversible sialyl donor pNP-αNeu5Ac gave conversion yields of 49%[35] and 87%[36], respectively. Fetuin (80% yield)[37] and cGMP (64% yield)[38] were also used as donor substrates. However, the enzyme´s origin from a pathogenic organism responsible for Chagas disease, causing up to 18 Mio infections and 50,000 deaths per year[39], and constituting an important virulence factor[40] is a significant drawback for its use in industrial production of food-grade sialyllactose, even if the recombinant enzyme is used.[29,33] Lactose is a very poor substrate for available mammalian sialyltransferases.[41-44]

Sialic acid attached to galactose via α2,3- and α2,6-linkage is also found in complex glycan structures[45], where sialylation represents the final step of a crucial post-translational modification of proteins. The lack of the sialic acid negatively influences half-life and efficacy of many therapeutics proteins.[45,46] Wild-type PdST and its variants were tested for activity on complex protein *N*-glycans and a model glycoprotein asialofetuin (ASF). The free glycans were prepared by treatment of ASF by PNGase F and purification via ultrafiltration spin columns. As can be seen in Figure 4a both wild type enzyme and double mutant were able to transfer the sialic acid from CMP-Neu5Ac onto the glycans. The products of the wild type were completely desialylated by a specific α2,3-neuraminidase, while the products of the double mutant remained unaffected during the same treatment, proving that the wild-type enzyme catalyzes α2,3-sialyltransfer and the double mutant α2,6-sialyltransfer with the glycan acceptor substrate (Figure 4b). Additionally, we performed sialylation of the glycoprotein ASF [see Figure S3 in the Supporting Information (SI)]. The reaction conditions were kept identical but the free glycans were replaced by equivalent amount of ASF. The amount of sialylated glycans dropped to a half in comparison to experiments with the free glycans. ~25% of glycans from ASF were sialylated with both enzymes. The regioselectivity of the double mutant remained almost unaffected (~90%). However, the complexity and size of the acceptor structure clearly influenced the selectivity in the wild-type enzyme, which showed decrease in regioselectivity by ~40 %. Regioselective α2,6-sialylation by *P. damsela* ST was reported by Yamamoto et al. for individual pyridylaminated biantennary carbohydrates, resembling simple glycans of glycoproteins,[14] but not for complex protein *N*-glycans. Sialylation of different glycoproteins, including ASF, was demonstrated before using α2,6-STs from *P. leiognathi*[24] and *P. damsela*[47], lacking the subsequent determination of regioselectivity.

In conclusion, we report here complete switch from α2,3- to α2,6-regioselecivity in family GT-80 ST PdST based on rational redesign of the active site. Wild-type PdST together with the tailor-made P7H-M117A double

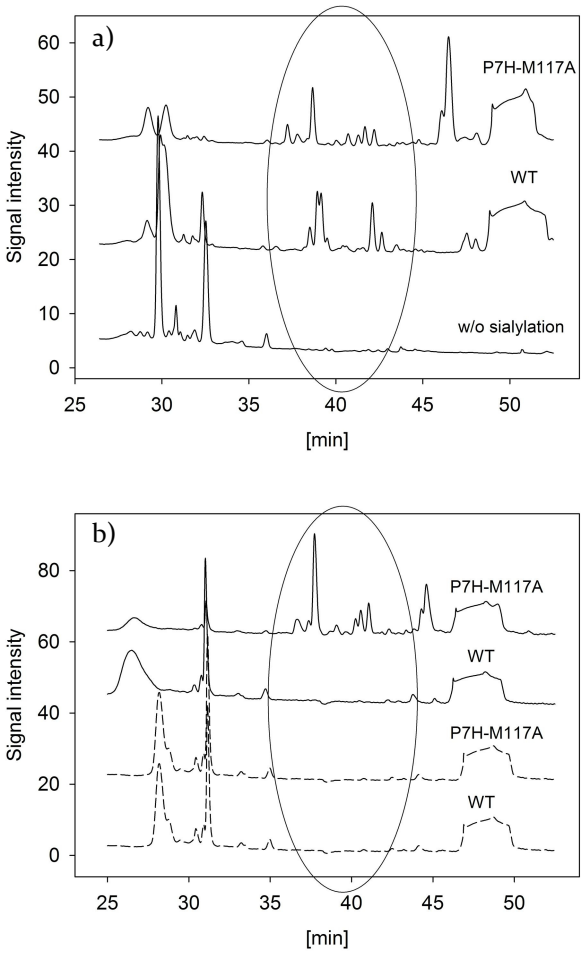

Figure 4. HPAEC-PAD analysis of wild-type and P7H-M117A PdST catalyzed sialyltransferase reaction with free glycans as acceptor substrate. (a) Sialylation of free glycans by wild-type and P7H-M117A PdST and (b) determination of regioselectivity by treatment with a specific α2,3-neuraminidase (solid line) and an unspecific neuraminidase (dashed line), which catalyzes the hydrolysis of α2,3- and α2,6- linked Neu5Ac residues. See the Supporting Information (SI) for details.

mutant represent the very first example of an extremely powerful sialyltransferase toolbox, comprising two variants of a single enzyme toggling between strict α2,3- and α2,6-regioselectivity. Their application in the high-yield production (≥ 70%.) of 3′- and 6′-sialyllactose is described. We have demonstrated that regioselectivity is fully retained in modification of a complex protein *N*-glycan substrate. A high expression level in *E. coli* enables the application of these PdST enzymes in the large scale production of sialyloligosaccharides as shown previously by Antoine et al.[48] and Drouillard et al.[49].

ASSOCIATED CONTENT

Supporting Information

General experimental methods, sialyltransferase assays, HPLC analysis, HPAEC-PAD analysis, sequence alignment, and synthesis experiment using P7H. This material is available free of charge via the Internet at http://pubs.acs.org.

AUTHOR INFORMATION

Corresponding Author

bernd.nidetzky@tugraz.at

Notes

The authors declare no competing financial interests.

ACKNOWLEDGMENT

This work was supported by the Federal Ministry of Economy, Family and Youth (BMWFJ), the Federal Ministry of Traffic, Innovation and Technology (BMVIT), the Styrian Business Promotion Agency, SFG, the Standortagentur Tirol and ZIT-Technology Agency of the City of Vienna through the COMET-Funding Programme managed by the Austrian Research Promotion Agency FFG.

REFERENCES

(1) Bode, L. *Glycobiology* **2012**, *22*, 1147.

(2) Ninonuevo, M. R.; Park, Y.; Yin, H.; Zhang, J.; Ward, R. E.; Clowers, B. H.; German, J. B.; Freeman, S. L.; Killeen, K.; Grimm, R.; Lebrilla, C. B. *J. Agric. Food Chem.* **2006**, *54*, 7471.

(3) Kunz, C.; Rudloff, S.; Baier, W.; Klein, N.; Strobel, S. *Annu. Rev. Nutr.* **2000**, *20*, 699.

(4) Wang, B. *Annu. Rev. Nutr.* **2009**, *29*, 177.

(5) Marotta, M.; Ryan, J. T.; Hickey, R. M. *J. Funct. Foods* **2014**, *6*, 367.

(6) Zivkovic, A. M.; Barile, D. *Adv. Nutr. Int. Rev. J.* **2011**, *2*, 284.

(7) Hickey, R. In *Dairy-derived ingredients. Food and nutraceutical uses*; Corredig, M., Ed.; Woodhead Publishing Ltd: 2009, p 308.

(8) Hickey, R. M. *Int. Dairy J.* **2012**, *22*, 141.

(9) Choi, Y. H.; Kim, J. H.; Park, J. H.; Lee, N.; Kim, D.-H.; Jang, K.-S.; Park, I.-H.; Kim, B.-G. *Glycobiology* **2014**, *24*, 159.

(10) Guo, Y.; Jers, C.; Meyer, A. S.; Arnous, A.; Li, H.; Kirpekar, F.; Mikkelsen, J. D. *J. Biotechnol.* **2014**, *170*, 60.

(11) Evans, D. G.; Evans, D. J.; Moulds, J. J.; Graham, D. Y. *Infect. Immun.* **1988**, *56*, 2896.

(12) Mine, T.; Katayama, S.; Kajiwara, H.; Tsunashima, M.; Tsukamoto, H.; Takakura, Y.; Yamamoto, T. *Glycobiology* **2010**, *20*, 158.

(13) Tsukamoto, H.; Takakura, Y.; Mine, T.; Yamamoto, T. *J. Biochem.* **2008**, *143*, 187.

(14) Yamamoto, T.; Nakashizuka, M.; Kodama, H.; Kajihara, Y.; Terada, I. *J. Biochem.* **1996**, *120*, 104.

(15) Scudder, P. R.; Chantler, E. N. *Biochim. Biophys. Acta* **1981**, *660*, 136.

(16) Comb, D. G.; Watson, D. R.; Roseman, S. *J. Biol. Chem.* **1966**, *241*, 5637.

(17) Kurosawa, N.; Hamamoto, T.; Inoue, M.; Tsuji, S. *Biochim. Biophys. Acta* **1995**, *1244*, 216.

(18) Sadler, J. E.; Rearick, J. I.; Paulson, J. C.; Hill, R. L. *J. Biol. Chem.* **1979**, *254*, 4434.

(19) Chiu, C. P. C.; Lairson, L. L.; Gilbert, M.; Wakarchuk, W. W.; Withers, S. G.; Strynadka, N. C. J. *Biochemistry* **2007**, *46*, 7196.

(20) Chiu, C. P. C.; Watts, A. G.; Lairson, L. L.; Gilbert, M.; Lim, D.; Wakarchuk, W. W.; Withers, S. G.; Strynadka, N. C. J. *Nat. Struct. Mol. Biol.* **2004**, *11*, 163.

(21) Schmölzer, K.; Ribitsch, D.; Czabany, T.; Luley-Goedl, C.; Kokot, D.; Lyskowski, A.; Zitzenbacher, S.; Schwab, H.; Nidetzky, B. *Glycobiology* **2013**, *23*, 1293.

(22) Sugiarto, G.; Lau, K.; Qu, J.; Li, Y.; Lim, S.; Mu, S.; Ames, J. B.; Fisher, A. J.; Chen, X. *ACS Chem. Biol.* **2012**, *7*, 1232.

(23) Yu, H.; Chokhawala, H.; Karpel, R.; Yu, H.; Wu, B.; Zhang, J.; Zhang, Y.; Jia, Q.; Chen, X. *J. Am. Chem. Soc.* **2005**, *127*, 17618.

(24) Yamamoto, T.; Hamada, Y.; Ichikawa, M.; Kajiwara, H.; Mine, T.; Tsukamoto, H.; Takakura, Y. *Glycobiology* **2007**, *17*, 1167.

(25) Ni, L.; Chokhawala, H. A.; Cao, H.; Henning, R.; Ng, L.; Huang, S.; Yu, H.; Chen, X.; Fisher, A. J. *Biochemistry* **2007**, *46*, 6288.

(26) Kakuta, Y.; Okino, N.; Kajiwara, H.; Ichikawa, M.; Takakura, Y.; Ito, M.; Yamamoto, T. *Glycobiology* **2008**, *18*, 66.

(27) Yu, H.; Huang, S.; Chokhawala, H.; Sun, M.; Zheng, H.; Chen, X. *Angew. Chem. Int. Ed.* **2006**, *45*, 3938.

(28) Mcjarrow, P.; Garman, J.; Harvey, S.; Van, A. A.; Patent WO 2003049547 A2, June 19, 2003.

(29) Jers, C.; Michalak, M.; Larsen, D. M.; Kepp, K. P.; Li, H.; Guo, Y.; Kirpekar, F.; Meyer, A. S.; Mikkelsen, J. D. *PLoS ONE* **2014**, *9*, e83902.

(30) Zeuner, B.; Riisager, A.; Mikkelsen, J.; Meyer, A. *Biotechnol Lett* **2014**, *36*, 1315.

(31) Tanaka, H.; Ito, F.; Iwasaki, T. *Biosci. Biotech. Biochem.* **1995**, *59*, 638.

(32) Watson, J. N.; Indurugalla, D.; Cheng, L. L.; Narine, A. A.; Bennet, A. J. *Biochemistry* **2006**, *45*, 13264.

(33) Michalak, M.; Larsen, D. M.; Jers, C.; Almeida, J. R. M.; Willer, M.; Li, H.; Kirpekar, F.; Kjærulff, L.; Gotfredsen, C. H.; Nordvang, R. T.; Meyer, A. S.; Mikkelsen, J. D. *Process Biochem.* **2014**, *49*, 265.

(34) Zeuner, B.; Luo, J.; Nyffenegger, C.; Aumala, V.; Mikkelsen, J. D.; Meyer, A. S. *Enzyme Microb. Technol.* **2014**, *55*, 85.

(35) Neubacher, B.; Schmidt, D.; Ziegelmuller, P.; Thiem, J. *Org. Biomol. Chem.* **2005**, *3*, 1551.

(36) Singh, S.; Scigelova, M.; Hallberg, M. L.; Howarth, O. W.; Schenkman, S.; Crout, D. H. G. *Chem. Commun.* **2000**, 1013.
(37) Lee, S.-G.; Shin, D.-H.; Kim, B.-G. *Enzyme Microb. Technol.* **2002**, *31*, 742.
(38) Holck, J.; Larsen, D. M.; Michalak, M.; Li, H.; Kjærulff, L.; Kirpekar, F.; Gotfredsen, C. H.; Forssten, S.; Ouwehand, A. C.; Mikkelsen, J. D.; Meyer, A. S. *New Biotechnol.* **2014**, *31*, 156.
(39) Prata, A. *Lancet Infect. Dis.* **2001**, *1*, 92.
(40) Pereira, M. E.; Zhang, K.; Gong, Y.; Herrera, E. M.; Ming, M. *Infect. Immun.* **1996**, *64*, 3884.
(41) Bartholomew, B. A.; Jourdian, G. W.; Roseman, S. *J. Biol. Chem.* **1973**, *248*, 5751.
(42) Hirano, Y.; Suzuki, T.; Matsumoto, T.; Ishihara, Y.; Takaki, Y.; Kono, M.; Dohmae, N.; Tsuji, S. *J. Biochem.* **2012**, *151*, 197.
(43) Paulson, J. C.; Rearick, J. I.; Hill, R. L. *J. Biol. Chem.* **1977**, *252*, 2363.
(44) Weinstein, J.; de Souza-e-Silva, U.; Paulson, J. C. *J. Biol. Chem.* **1982**, *257*, 13845.
(45) Byrne, B.; Donohoe, G. G.; O'Kennedy, R. *Drug Discov. Today* **2007**, *12*, 319.
(46) Ghaderi, D.; Zhang, M.; Hurtado-Ziola, N.; Varki, A. *Biotechnol. Genet. Eng. Rev.* **2012**, *28*, 147.
(47) Yamamoto, T.; Nagae, H.; Kajihara, Y.; Terada, I. *Biosci. Biotechnol. Biochem.* **1998**, *62*, 210.
(48) Antoine, T.; Priem, B.; Heyraud, A.; Greffe, L.; Gilbert, M.; Wakarchuk, W. W.; Lam, J. S.; Samain, E. *ChemBioChem* **2003**, *4*, 406.
(49) Drouillard, S.; Mine, T.; Kajiwara, H.; Yamamoto, T.; Samain, E. *Carbohydr. Res.* **2010**, *345*, 1394.

Table of Contents Artwork

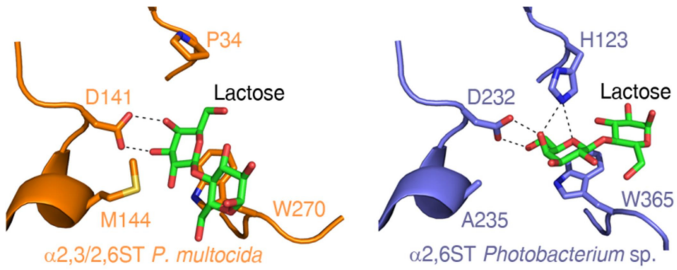

Supporting Information for

Complete Switch from α2,3- to α2,6-Regioselectivity in *Pasteurella dagmatis* β-D-Galactoside Sialyltransferase by Active-Site Redesign

Katharina Schmölzer[†], Tibor Czabany[‡], Christiane Luley-Goedl[†], Doris Ribitsch[†], Helmut Schwab[†,§], Bernd Nidetzky[†,‡,*]

[†]Austrian Centre of Industrial Biotechnology, Petersgasse 14, 8010 Graz, Austria

[‡]Institute of Biotechnology and Biochemical Engineering, Graz University of Technology, Petersgasse 12/I, 8010 Graz, Austria

[§]Institute of Molecular Biotechnology, Graz University of Technology, Petersgasse 14, 8010 Graz, Austria

Table of contents

Materials and methods	S3
Chemicals	S3
Site-directed mutagenesis	S3
Protein expression and purification	S4
Preparation of free glycans	S5
Neuraminidase treatment	S5
Sialyltransferase assay using lactose as acceptor substrate	S5
Sialyltransferase assay using free glycans	S6

Sialyltransferase assay using glycoprotein S6

HPLC analysis of CMP and CMP-Neu5Ac S6

Sialyllactose analysis S7

Glycan analysis S7

Table S1. Partial sequence alignment displaying differences among α2,3- and α2,6-STs in GT family 80. S9

Figure S1. Gradual change from α2,3- to α2,6-regioselective sialyltransfer from CMP-Neu5Ac to lactose, resulting from substitution of Pro^{7} by His and from additional substitution of Met^{117} by Ala in PdST. S10

Figure S2. Time course of enzymatic synthesis of sialyllactose using 0.1 μM of the P7H variant of PdST. S11

Figure S3. HPAEC-PAD analysis of (a) P7H-M117A and (b) wild-type PdST catalyzed sialyltransferase reaction with the model glycoprotein ASF as acceptor substrate. S12

References for Supporting Information S13

Materials and methods

Chemicals

PNGase F, α2,3-neuraminidase and neuraminidase were from New England Biolabs (Ipswich, Massachusetts, USA). All other materials are described elsewhere.[1]

Site-directed mutagenesis

Mutations to replace Pro^{7} by His (P7H) and Met^{117} by Ala (P7H-M117A) were introduced by two-stage PCR[2] where a pET23a(+) expression vector encoding ∇3PdST (variant of wild-type PdST elongated by three amino acids at the N-terminus)[1] was used as a template. A pair of complementary oligonucleotide primers, each introducing the desired site-directed substitution at the protein level, was used. The mismatched bases are underlined.

P7H forward:

5´-ATACATATGAAAACAATCACAATCTATTTAGATCATGCTTCATTACCCACATTA

AACCAATTAATGCAC-3´

P7H reverse:

5´-GTGCATTAATTGGTTTAATGTGGGTAATGAAGCATGATCTAAATAGATTGTGA

TTGTTTTCATATGTAT-3´

M117A forward:

5´-CTTTATGATGATGGCACAGCGGAATATGTTGATTTAG-3´

M117A reverse:

5´-CTAAATCAACATATTCCGCTGTGCCATCATCATAAAG-3´

The PCR was performed in a Gene Amp® PCR 2200 thermocycler (Applied Biosystems, USA). The PCR was carried out in 50 µL using 0.3 µM forward and reverse primer, 0.2 mM dNTP-mix, 3.6 U Pfu DNA Polymerase (Promega, USA) and 1x reaction buffer provided by the supplier. The two-stage protocol involved in the first step two separate PCR reactions with the forward and reverse primers. These reactions consisted of a preheating step at 95°C for 60 s followed by 4 reaction cycles (95°C, 50 s; 55°C, 50 s; 70°C, 10 min). After this first step both PCR reactions were mixed together in a 1:1 ratio followed by second standard mutagenesis PCR reaction using the same temperature program (95°C, 50 s; 55°C, 50 s; 70°C, 10 min) for 18 cycles. The amplification product was subjected to parental template digest by *Dpn*I (Fermentas, Germany) in accordance to the manufacturer's instructions and transformed into electro-competent *E. coli* BL21_Gold(DE3) cells. All inserts were sequenced as custom service by Agowa (Germany). Wizard® Plus SV Minipreps Kit from Promega (USA) was used to prepare plasmid DNA. DNA analysis was performed with Vector NTI Suite 10 (Invitrogen, USA).

Protein expression and purification

Protein expression in *E. coli* and preparation of the cell lysate were done as previously described.[1] Target proteins were purified via their C-terminal His-tag using an ÄKTAprime plus system (GE Healthcare, Germany). The cleared cell lysate was loaded onto two HisTrap HP FF 5 mL columns (GE Healthcare, Germany) at a flow rate of 2 mL/min. The columns had been equilibrated with binding buffer (30 mM potassium phosphate, 300 mM NaCl, 15 mM imidazol, 10% glycerol, pH 7.4). After a washing step of 10 column volumes, the enzyme was eluted with a linear gradient of 15 - 300 mM imidazol within 10 column volumes. Fractions of 3 mL were collected

and analyzed by SDS-PAGE. Sialyltransferase containing fractions were pooled and dialyzed overnight against 20 mM Tris/HCl, 150 mM NaCl, pH 7.5. SDS PAGE was used to confirm purity of enzyme preparations. Purified enzymes were aliquoted and stored at -70°C.

Preparation of free glycans

After heat denaturation free glycans were prepared by a PNGase F (500U) digest of 500 µg of asialofetuine in 160 µL of 1x PNGase buffer for 16 hours at 37°C. Subsequently, glycans were separated from proteins by ultracentrifugation (Vivaspin 500, cutoff 10 kDa, Sartorius Stedim Biotech GmbH, Germany) and stored at -20°C.

Neuraminidase treatment

When appropriate the products of sialyltransferase reaction were treated by commercial α2,3-neuraminidase or unspecific neuraminidase. The procedure followed the instructions provided by supplier.

Sialyltransferase assay using lactose as acceptor substrate

Sialyltransferase activity was assayed in a total volume of 20 µL using 50 mM sodium phosphate buffer, pH 8.0. Reaction mixture contained 1 mM CMP-Neu5Ac, 1 mM lactose, 1 µM enzyme, and 1 mg/mL BSA. Enzymatic conversion was carried out at 25°C and agitation rate of 400 rpm using a Thermomixer comfort (Eppendorf, Germany). All assays were performed in duplicate. Reactions were stopped after 30 min by adding 40 µL of ice-cold acetonitrile. Mixtures were incubated on ice for 10 min and centrifuged at 4°C, 13,000 rpm for 10 min to remove precipitated protein. For

time course experiments 0.1 µM enzyme was used, under otherwise identical conditions, and reactions were stopped after 0, 15, 30, 60, 90 and 180 min.

Sialyltransferase assay using free glycans

Free glycans released from 1.5 mg of asialofetuine were mixed with 0.5 mg of CMP-Neu5Ac and sodium acetate solution (pH 7.4) in the final volume of 180 µL. The reaction was started by addition of 10 µg of enzyme and incubated at room temperature for 60 min. The reaction was stopped by heating the sample at 80°C for 10 min and centrifuged at 4°C, 13,000 rpm for 10 min to remove precipitated protein. The glycans were analyzed by High-Performance Anion-Exchange (HPAE) chromatography.

Sialyltransferase assay using glycoprotein

1.5 mg of asialofetuine was mixed with 0.5 mg of CMP-Neu5Ac and sodium acetate solution (pH 7.4) in the final volume of 180 µL. The reaction was started by addition of 10 µg of enzyme and incubated at room temperature for 60 min. The reaction was stopped by heating the sample at 80°C for 10 min. Prior to analysis glycans were released from glycoprotein by PNGase digest as described above. Glycans were analyzed by HPAE chromatography.

HPLC analysis of CMP and CMP-Neu5Ac

For CMP-and CMP-Neu5Ac analysis 5 µL supernatant (see Sialyltransferase activity assay using lactose as acceptor substrate) were injected after appropriate dilution in HPLC analysis using a Chromolith® HighResolution RP-18 (100 x 4.6 mm; Merck Chemicals, Germany) column in reversed phase ion-pairing mode on an Agilent

Technologies 1200 Series system. The column was equilibrated with 20 mM phosphate buffer, pH 6.8 containing 2 mM tetrabutylammonium at a flow rate of 2 mL/min. A temperature control unit maintained 30°C throughout the analysis. Samples were eluted with a linear gradient from 0 – 2% acetonitrile in 3 min followed by 2 – 25% acetonitrile in 7 min and detected by UV at 254 nm.

Sialyllactose analysis

The sialyltransferase assay products (3´- and/or 6´-sialyllactose) were identified by HPAE chromatography on a Dionex BioLC system equipped with a CarboPac® PA200 column (3 x 250 mm; Thermo Fisher Scientific Inc., Dionex) and a CarboPac® guard column. After appropriate dilution of the supernatant (see Sialyltransferase activity assay using lactose as acceptor substrate) 25 µL were injected and eluted using an isocratic concentration of 60 mM NaOH with 35 mM sodium acetate at a flow rate of 0.4 mL/min at 25°C. An ED50 electrochemical detector with a carbohydrate certified gold working electrode was used for pulsed amperometric detection (PAD) in the carbohydrate waveform (as recommended by the supplier).
One unit (1 U) was defined as the amount of enzyme that could transfer 1 µmol of sialic acid per min to lactose under the conditions described above.

Glycan analysis

The assay products (3´- and/or 6´-sialylglycans) were identified by HPAE chromatography on a Dionex BioLC system equipped with a CarboPac® PA200 column (3 x 250 mm; Thermo Fisher Scientific Inc., Dionex) and a CarboPac® guard column. After appropriate dilution 25 µL were injected and eluted using the following

gradient: 0-20 min linear gradient from 50 to 100 mM NaOH, 20-80 min linear gradient from 0 to 200 mM sodium acetate in the presence of 100 mM NaOH. This gradient was followed by 10 min of column wash with 450 mM sodium acetate/20 mM NaOH and 10 min of column was with 200 mM NaOH. Afterwards, the column was equilibrated in 50 mM NaOH for 10 minutes. An ED50 electrochemical detector with a carbohydrate certified gold working electrode was used for PAD in the carbohydrate waveform (as recommended from the supplier).

Table S1. Partial sequence alignment displaying differences among α2,3- and α2,6-STs in GT family 80.

	Sialyltransferase	Acceptor	Accession number		
P. dagmatis	α2/3	β	AFY98851	TIYLDP^{7} ASLPT	YDDGTM^{117}EYVDL
P. multocida	α2,3/α2,6	β	AAY89061	TLYLDP^{34} ASLPA	YDDGSM^{144}EYVDL
P. phosphoreum	α2,3	α/β	BAF63530	EVYVDR^{47} ATLPT	YDDGSA^{151}EYVRL
Vibrio sp.	α2,3	α/β	BAF91160	EIYVDR^{41} ATLPT	YDDGSA^{145}EYVRI
Photobacterium sp. JT-ISH-224	α2,3	α/β	BAF92025	EVYVDR^{47} ATLPT	YDDGSA^{151}EYVRL
H. ducreyi	α2,3	-	AAP95068	EIYLDY^{13} ATIPS	YDDGSE^{128}GIVTQ
Photobacterium sp. JT-ISH-224	α2,6	β	BAF92026	EVYVDH^{123}ASLPT	YDDGSA^{235}EYVNL
P. damselae	α2,6	β	BAA25316	EVYIDH^{120}ASLPS	YDDGSS^{232}EYVSL
P. leiognathi JT-SHIZ-145	α2,6	β	BAF91416	EVYVDH^{120}ASLPS	YDDGSA^{232}EYVSL
P. leiognathi JT-SHIZ-119	α2,6	β	BAI49484	EVYVDH^{120}ASLPS	YDDGSA^{232}EYVNL

P. dagmatis, *Pasteurella dagmatis* β-galactoside α2,3-sialyltransferase (PdST); *P. multocida*, *Pasteurella multocida* β-galactoside α2,3/α2,6-sialyltransferase (PmST1); *P. phosphoreum*, *Photobacterium phosphoreum* α/β-galactoside α2,3-sialyltransferase; *Vibrio* sp., *Vibrio* sp. α/β-galactoside α2,3-sialyltransferase; *Photobacterium* sp., *Photobacterium* sp. α/β-galactoside α2,3-sialyltransferase; *H. ducreyi*, *Haemophilus ducreyi* α2,3-sialyltransferase; *Photobacterium* sp., *Photobacterium* sp. β-galactoside α2,6-sialyltransferase; *P. damselae*, *Photobacterium damselae* β-galactoside α2,6-sialyltransferase; *P. leiognathi, Photobacterium leiognathi* β-galactoside α2,6-sialyltransferase. Sequence alignment was performed with ClustalW using a blosum scoring matrix and an open gap penalty of 10. Potentially critical amino acids for reaction specificity are indicated by an arrow

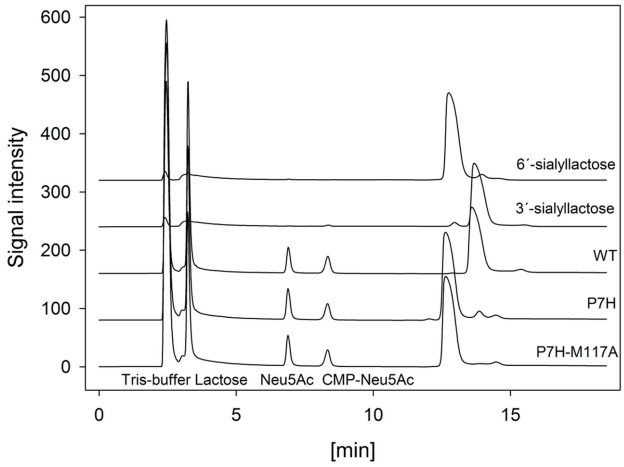

Figure S1. Gradual change from α2,3- to α2,6-regioselective sialyltransfer from CMP-Neu5Ac to lactose, resulting from substitution of Pro^{7} by His and from additional substitution of Met^{117} by Ala in PdST. Traces of HPAEC-PAD analysis of samples from different enzymatic reactions are superimposed along with traces of authentic 3'- and 6'-sialyllactose standards. The concentration of sialyllactose in each sample was approximately 0.7 mM.

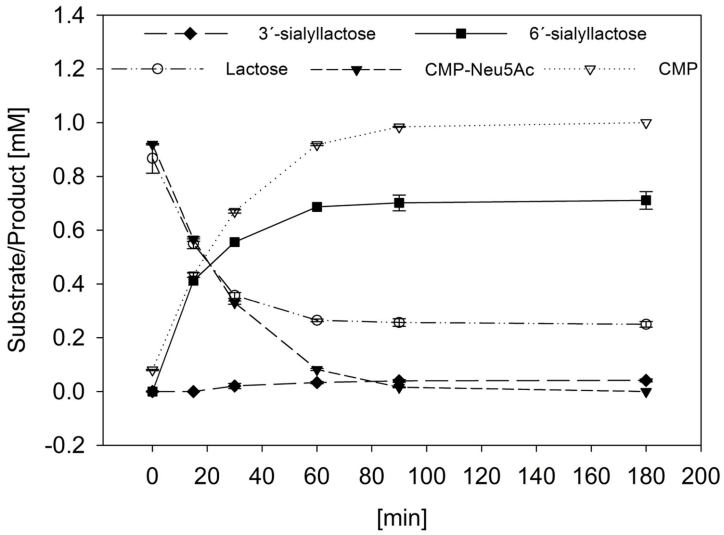

Figure S2. Time course of enzymatic synthesis of sialyllactose using 0.1 µM of the P7H variant of PdST at pH 8.0.

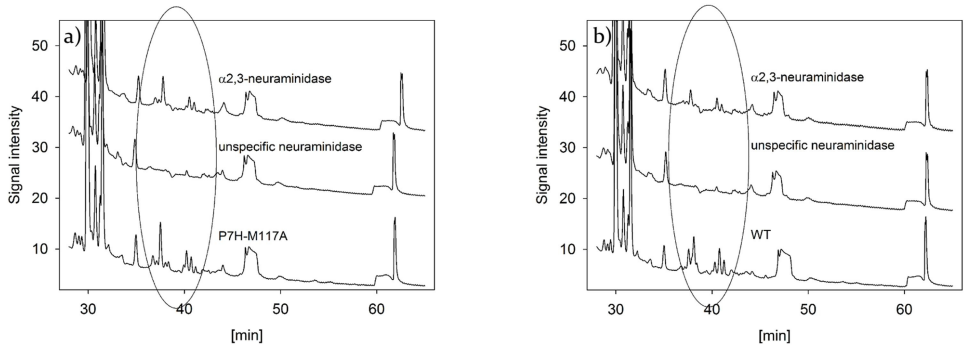

Figure S3. HPAEC-PAD analysis of (a) P7H-M117A and (b) wild-type PdST catalyzed sialyltransferase reaction with the model glycoprotein ASF as acceptor substrate. Determination of regioselectivity by treatment with a specific α2,3-neuraminidase and an unspecific neuraminidase, which catalyzes the hydrolysis of α2,3- and α2,6- linked Neu5Ac residues.

References for Supporting Information

(1) Schmölzer, K.; Ribitsch, D.; Czabany, T.; Luley-Goedl, C.; Kokot, D.; Lyskowski, A.; Zitzenbacher, S.; Schwab, H.; Nidetzky, B. *Glycobiology* **2013**, *23*, 1293.

(2) Wang, W.; Malcolm, B. A. *BioTechniques* **1999**, *26*, 680.

Two variants of human β-galactoside α2,6 sialyltransferase I with distinct properties

Christiane Luley-Goedl[1], Katharina Schmölzer[1], Marco Thomann[2], Sebastian Malik[2], Michael Greif[2], Doris Ribitsch[1], Harald Sobek[2], Alfred Engel[2], Rainer Müller[2], Helmut Schwab[3] and Bernd Nidetzky[4]

[1]Austrian Center of Industrial Biotechnology, Petersgasse 14, 8010 Graz, Austria

[2]Roche Diagnostics GmbH, Nonnenwald 2, 82377 Penzberg, Germany

[3]Institute of Molecular Biotechnology, Graz University of Technology, Petersgasse 14, 8010 Graz, Austria

[4]Institute of Biotechnology and Biochemical Engineering, Graz University of Technology, Petersgasse 12/I, 8010 Graz, Austria

Corresponding author: bernd.nidetzky@tugraz.at, Phone: +43 316 873-8400; FAX: +43 316 873-8434

In preparation.

Abstract

We report on the distinct properties of two N-terminally truncated variants of human ST6-Gal-I, namely Δ89ST6Gal-I and Δ108ST6Gal-I, which were successfully expressed in HEK cells. The different properties of these enzymes result most probably from the deletion of residue Arg^{108} in the Δ108ST6Gal-I variant, which was identified by Kuhn et al. [11] as an essential residue in the substrate binding area. The K_m for *N*-acetyl-D-lactosamine is 10-fold increased for Δ108ST6Gal-I (84 mM) as compared to Δ89ST6Gal-I (8.3 mM). The enzyme Δ89ST6Gal-I exhibits both sialyltransferase and sialidase activity on a monoclonal antibody and is therefore a suitable tool for the terminal modification of *N*-glycans.

Introduction

Human β-galactoside α2,6 sialyltransferase I (ST6Gal-I, E.C 2.4.99.1; data base entry P15907) catalyzes the transfer of *N*-acetylneuramic acid (Neu5Ac) residues to the C6 hydroxyl group of a terminal galactose residue of type II disaccharides (Galβ1-4GlcNAc). The sequence of the enzyme consists of 406 amino acids [1]. Human ST6Gal-I belongs to the GT29 family comprising eukaryotic and viral STs. Like other vertebrate STs, human ST6Gal-I is localized in the Golgi apparatus and shows the characteristic architecture consisting of 4 different domains. There is a short N-terminal cytoplasmic tail (aa 1-9), a transmembrane domain (aa 10-26), a stem region (aa 27-62) and a C-terminal catalytic domain facing the luminal side of the Golgi apparatus. In the catalytic domain of all eukaryotic STs several conserved peptide sequences were identified referred to as sialylmotifs L (large), S (small), motif 3 and VS (very small) [2]. The motifs have different functions in the protein: the L-motif participates in the binding of the sugar donor CMP-Neu5Ac, the S-motif is involved in the binding of the donor and acceptor substrates and finally, the VS-motif participates in the catalytic reaction. The fold of the enzyme is predicted to belong to the GT-A fold [3].

The fine structures of *N*-glycans are important determinants for the activities of glycoproteins, e.g. antibodies. However, naturally occurring and recombinant glycoproteins display a heterogeneity in the structure of their *N*-glycans. Therefore, glycosylation remodeling through trimming and extending the sugar chains by glycosidases and glycosyltransferases is an attractive approach. In the glycan structure of glycoproteins the sialic acid moiety is usually found in the terminal position of the oligosaccharide. Being in an exposed position sialic acid plays an important role in the biology of glycoproteins and is a potential target for glycan remodeling. E.g., the terminal α2,6-sialylated Fc glycoform, a component of the intravenous immunoglobulin (IVIG) was identified as

the active species for the anti-inflammatory activity of IVIG. Human ST6Gal-I was used as tool for the *in vitro* sialylation of IVIG [4,5].

Here, we report on the cloning, expression, purification and characterization of two N-terminally truncated variants, namely Δ89ST6Gal-I and Δ108ST6Gal-I (lacking aa 1-89 and 1-108, respectively). The enzyme Δ89ST6Gal-I exhibits both sialyltransferase and sialidase activity on a monoclonal antibody and is therefore a suitable tool for the terminal modification of *N*-glycans.

Results and Discussion

Biochemical characterization of recombinant human ST6Gal-I variants

The truncated variants of recombinant human ST6Gal-I were purified from HEK culture supernatant by an ultrafiltration step followed by two chromatographic steps. Analytical size exclusion chromatography showed that the final enzyme preparation had a purity of 98%. The Δ89ST6Gal-I and the Δ108ST6Gal-I enzymes migrated as single bands on SDS-PAGE with an apparent molecular weight of 38 and 35 kDa, respectively (Figure 1).

Mass spectrometry analysis of the purified enzymes revealed that the construct of Epo-AP-Δ89ST6Gal-I was expressed without the N-terminal amino acids AP. This surprising finding indicated an unusual cleavage of the expressed protein by the Epo signal peptidase. However, for the construct Epo-APPR-Δ108ST6Gal-I the N-terminal sequence was confirmed as APPR indicating the expected cleavage. For the recombinant human Δ108ST6Gal-I from HEK cells a specific activity of >600 RFU/mg was determined. The variant Δ89ST6Gal-I showed an increased specific activity of >1100 RFU/mg. In the presence of the inhibitor CTP (0.47 mM) the enzymatic activity was reduced to 5% of the original enzymatic activity (data not shown).

The primary amino acid sequence of Δ89ST6Gal-I reveals six cysteine residues. Using 13.6 µM of purified enzyme a theoretical number of 81.6 µM of free sulfhydryl groups was calculated. However, in the absence or presence of guanidine hydrochloride (4 M) a concentration of only 3.4 or 4.1 µM of free sulfhydryl groups was determined according to Ellman et al. [6] corresponding to about 4 or 5% of the theoretically accessible SH-groups. The enzyme was tryptically digested and peptide fragments were analyzed by mass spectrometry to determine the number and the location of disulfide bonds. All six cysteine residues were found to be involved in disulfide linkages (Table 1) in accordance to the recent publication of rat ST6Gal-I [7]. Carboxymethylation of the tryptic peptides by iodoacetic acid identified free Cys364 to a negligible level of 0.006%.

Sialyltransferase activity

The recombinant Δ89ST6Gal-I was used in sialylation experiments with a recombinant monoclonal antibody IgG4 as model target. The content of G2, G2+1SA and G2+2SA (Scheme 1) was determined by mass spectrometry. After 2 h of incubation a high content (88%) of the fully sialylated form G2+2SA was obtained (Figure 2A, left panel). The data also showed that with extended incubation time the content of G2+2SA decreased while the content of G2 and G2+1SA increased again. After an incubation of 48 h, a G2+1SA content of 71% was obtained.

Cytidine triphosphate (CTP) is a potent inhibitor of sialyltransferases [8]. To demonstrate that this hydrolytic activity is an intrinsic activity of Δ89ST6Gal-I, inhibition experiments were performed. In the first phase of the experiment the sialylation of IgG4 by Δ89ST6Gal-I was performed to achieve a high content of G2+2SA. After 7 h of incubation the G2+2SA content was 94%. At this time CTP was added to the reaction mixture in a final concentration of 0.67 mM. At different times the content of G2, G2+1SA and G2+2SA was determined by mass spectrometry. Compared to inhibitor-free conditions shown in Figure 2A the degradation of G2+2SA was significantly reduced in the presence of CTP (Figure 2B). After 72 h of incubation there were still 73% of G2+2SA present. The inhibition of the hydrolytic activity by the specific sialyltransferase inhibitor CTP strongly indicates that both activities are located in the same active center of human ST6Gal-I. Different kinetics and specificities (mono- and di-sialylation) were observed for Δ108ST6Gal-I (Figure 2A, right panel). After 8 h of incubation a high content (~70%) of the mono-sialylated form G2+1SA was obtained, and no G2+1SA degradation was observed during the examined time period of 72 h. The maximum yield of G2+2SA was well below 10%.

Regioselectivity of sialyltransfer

Regioselectivity of the sialylation of IgG4 by Δ89ST6Gal-I and Δ108ST6Gal-I was analyzed using high-performance anion exchange chromatography with pulsed amperometric detection (HPAE-PAD) and results are shown in Figure 3. Linkage analysis was performed by addition of α2,3-neuraminidase to either the G2+1SA or the G2+2SA product. The products remained unaffected by this treatment and release of G2 was not observed, proving that both enzyme variants catalyze α2,6-sialyltransfer (Figure 3B). In addition, the sialyltransfer product towards sialyl-*N*-acetyl-lactosamine was clearly identified as 6´-sialyl-*N*-acetyl-lactosamine (data not shown).

Basic characterization of activities and structural interpretation

Further characterization of Δ89ST6Gal-I and Δ108ST6Gal-I constructs is summarized in Table 2. The K_m for *N*-acetyl-D-lactosamine is 10-fold increased for Δ108ST6Gal-I (84 mM), while the k_{cat} was 6.7-fold decreased (1.3 s^{-1}) as compared to Δ89ST6Gal-I. This can be explained by the deletion of residue Arg^{108} in the Δ108ST6Gal-I variant. Kuhn et al. [11] showed, that Arg^{108} is the first residue contacting a glycan substrate (Figure 4) and deletion perturbs the structure of this substrate binding area, which leads as a consequence to the increased K_m value for *N*-acetyl-D-lactosamine. The K_m for asialofetuin was not altered much with 0.12 mM for Δ89ST6Gal-I and 0.10 mM for Δ108ST6Gal-I. However, substrate inhibition with a K_i of 0.25 mM was observed for the Δ108ST6Gal-I variant. The catalytic efficiency of Δ89ST6Gal-I increased 70-fold when *N*-acetyl-D-lactosamine was replaced by asialofetuin as acceptor substrate. Extremely low sialidase activity was only detected for 6´-sialyl-*N*-acetyl-lactosamine and not for 3´-sialyl-*N*-acetyl-lactosamine. The sialidase activity increased slightly (1.5-fold) when pH was decreased from 6.5 to 4.5 (data not shown). Both variants showed almost no CMP-Neu5Ac hydrolase activity.

Material and methods

Cloning strategy for transient gene expression

Two N-terminally truncated fragments of human ST6Gal-I were cloned. Instead of the natural leader sequence and the N-terminal protein sequence, the ST6Gal-I coding region harbors an Erythropoetin (Epo) signal sequence followed by an AP or APPR linker sequence in order to ensure correct processing of the polypeptides by the secretion machinery of the host cell line. Codon-optimized cDNAs were synthesized for Epo-AP-Δ89ST6Gal-I and Epo-APPR-Δ108ST6Gal-I. In addition, the expression cassettes feature *Sal*I and *Bam*HI sites for cloning into the multiple cloning site of the predigested pM1MT vector fragment (Roche Applied Science). Expression of the ST6Gal-I coding sequences is therefore under control of a human cytomegalovirus (CMV) immediate-early enhancer/promoter region, followed by an intron A for regulated expression and a BGH polyadenylation signal.

Fermentation of human embryonic kidney (HEK) cells

Transient gene expression (TGE) by transfection of plasmid DNA is a rapid strategy to produce proteins in mammalian cell culture. For high-level expression of recombinant human proteins a TGE platform based on a suspension-adapted HEK 293 cell line was used. Cells were cultured in

shaker flasks at 37°C under serum-free medium conditions. The cells were transfected at approximately $2x10^6$ vc/mL with the expression plasmids (0.5 to 1.0 mg/L cell culture) and complexed by the 293-Free transfection reagent (Merck) according to the manufacturer's guidelines. 3 h post-transfection, valproic acid, a HDAC inhibitor, was added in a final concentration of 4 mM in order to boost the expression [9]. Each day, the culture was supplemented with 6% (v/v) of a soybean peptone hydrolysate-based feed. The culture supernatant was collected at day 7 post-transfection by centrifugation.

Purification of recombinant human ST6Gal-I variants from HEK supernatant

The recombinant ST6Gal-I variants were purified using a three-step purification protocol. In a first step, 0.1 L of culture supernatant was ultrafiltrated (0.2 µm) and the solution was dialyzed against buffer A (20 mM potassium phosphate, pH 6.5). Second, the dialysate was loaded onto a S-Sepharose FF column (1.6 cm x 2 cm, GE Healthcare) equilibrated with buffer A. After washing with 100 mL buffer A, the enzyme was eluted with a linear gradient of 10 mL buffer A and 10 mL buffer A containing 200 mM NaCl, followed by a wash step using 48 mL buffer A containing 200 mM NaCl. Fractions (4 mL) were analyzed by analytical SDS-PAGE. Fractions containing the enzyme were pooled and dialyzed against buffer B (50 mM MES, pH 6.0). Third, the dialyzed pool was loaded onto a Heparin Sepharose FF column (0.5 cm x 5 cm, GE Healthcare) equilibrated with buffer B and eluted using buffer B containing 200 mM NaCl. Fractions (1 mL) containing the enzyme were pooled and dialyzed against buffer B. The purity of the enzymes was checked by analytical size exclusion chromatography on a Superdex 75 column (10/30, GE Healthcare) equilibrated with buffer B containing 500 mM NaCl. Protein concentrations were determined at 280 nm.

Sialyltransferase assay

HPLC-based activity assay. Sialyltransferase activity was assayed in a total volume of 20 µL using 50 mM MES buffer, pH 6.5. Reaction mixture contained 0.75 mM CMP-Neu5Ac, acceptor (10 mM *N*-acetyl-D-lactosamine or 17 mg/mL asialofetuin), enzyme (0.1 µM of Δ89ST6Gal-I or 1.0 µM of Δ108ST6Gal-I) and 0.1% TritonX-100. Enzymatic conversion was carried out at 37°C and agitation rate of 400 rpm using a Thermomixer comfort (Eppendorf). All assays were performed in duplicate. Reactions were stopped at certain time points by addition of 40 µL of ice-cold acetonitrile. Samples were incubated on ice for 30 min and centrifuged to remove precipitated protein. 5 µL of the supernatant were injected to HPLC analysis using a Chromolith® Performance RP-18 (100 x 4.6

mm; Merck Chemicals) column in reversed phase ion-pairing mode on an Agilent Technologies 1200 Series system. The column was equilibrated with 20 mM phosphate buffer, pH 6.8 containing 2 mM tetrabutylammonium at a flow rate of 2 mL/min. A temperature control unit maintained 30°C throughout the analysis. Samples were eluted with 0% acetonitrile in 4 min followed by a linear gradient from 0 – 25% acetonitrile in 2 min and detected by UV at 254 nm. CMP-Neu5Ac and CMP were analyzed. One unit (1 U) was defined as the amount of enzyme that could transfer 1 µmol of sialic acid per min to acceptor under the conditions described above.

Fluorescence-based assay. Sialyltransferase activity was assayed in a total volume of 20 µL using 50 mM MES buffer, pH 6.5. Reaction mixture contained 0.05 mM CMP-9-fluoresceinyl-NeuAc (CMP-9F-Neu5Ac) [10], 2.5 mg/mL asialofetuin, enzyme (0.1 µM of Δ89ST6Gal-I or 1.0 µM of Δ108ST6Gal-I) and 0.1% TritonX-100. Enzymatic conversion was carried out at 37°C and agitation rate of 400 rpm. Reaction was stopped after 30 min by addition of 10 µL of the inhibitor CTP (10 mM). The reaction mixture was loaded onto a PD10 desalting column equilibrated with 0.1 M Tris/HCl, pH 8.5. Samples were eluted from the column using the equilibration buffer. The fraction size was 0.5 mL. The concentration of formed fluorescent fetuin was determined using a fluorescence spectrophotometer. Excitation wavelength was 490 nm and emission was measured at 520 nm. Enzymatic activity was expressed as RFU (relative fluorescence unit). 10,000 RFU/µg is equivalent to a specific activity of 0.0839 nmol/µg·min.

Sialidase assay

Sialidase activity was assayed in a total volume of 20 µL using 50 mM MES buffer, pH 6.5. The reaction mixture contained 1.5 mM 3'- or 6'-sialyl-*N*-acetyl-lactosamine, 1 µM enzyme and 0.1% TritonX-100. Enzymatic conversion was carried out at 37°C and agitation rate of 400 rpm. All assays were performed in duplicate. Reactions were stopped after 10 h of incubation by addition of 40 µL of ice-cold acetonitrile. Samples were incubated on ice for 30 min, centrifuged to remove precipitated protein and diluted to a final volume of 200 µL with H_2O. 25 µL were injected to HPAE chromatography and analyzed as described for "Determination of product regioselectivity".

Hydrolase activity

Hydrolase activity was assayed in a total volume of 20 µL using 50 mM MES buffer, pH 6.5. The reaction mixture contained 0.75 mM CMP-Neu5Ac, 1 µM enzyme and 0.1% TritonX-100. Enzymatic conversion was carried out at 37°C and agitation rate of 400 rpm. All assays were

performed in duplicate. Reactions were stopped after 5 h of incubation by addition of 40 µL of ice-cold acetonitrile and further processed and analyzed as described for the HPLC-based sialyltransferase activity assay.

SDS-PAGE and protein determination

Analytical SDS-PAGE was carried out using NuPAGE gels (4-12%, Invitrogen). Samples (36 µL) were diluted with 12 µL NuPAGE LDS sample buffer (Invitrogen) and incubated for 2 min at 85°C. Aliquots (5 µg protein) were loaded on the gel. The gels were stained using SimplyBlue SafeStain (Invitrogen). An extinction coefficient ε_{280} (10 mg/mL) of 1.931 and 1.871 was used for protein concentration determination of Δ89ST6Gal-I and Δ108ST6Gal-I, respectively.

Analysis of sulfhydryl groups

5,5´-Dithiobis(2-nitrobenzoic) acid (DTNB) was used for quantitative determination of free sulfhydryl groups [6]. Purified Δ89ST6Gal-I (13.6 µM) was used in this assay. The reaction was carried out in 0.1 M potassium phosphate buffer, pH 8.0 in the absence or presence of guanidine hydrochloride (4 M). The reaction was monitored at 412 nm. L-cysteine hydrochloride was used as a standard. For peptide mapping an aliquot (21 µL, 350 µg) was denatured by adding 8 M guanidine hydrochloride (279 µL). The sample was incubated for 1 h at 50°C. Carboxymethylation of free cysteine residues was done by adding iodoacetic acid (10 µL, 330 mg/mL). After incubation in the dark at room temperature for 30 min the samples were applied to a NAP5 column (GE-Healthcare) equilibrated with 0.1 M Tris/HCl, pH 7.0. To the eluted fraction (500 µL) trypsin (10 µL, 0.25 mg/mL) was added and the sample was incubated at 37°C overnight. The digestion was stopped by addition of 20 µL TFA solution (10%). The peptides were separated and analyzed by LCMS using an UPLC (C18 column) coupled to a mass spectrometer (Orbitrap, Thermo Fisher). Peptides were identified using Massmap software.

N-terminal sequencing by Edman degradation

The N-terminal sequences of expressed variants of human ST6Gal-I were analyzed by Edman degradation using reagents and devices obtained from Life Technologies. Preparation of the samples was done as described in the instruction manual of the ProSorb Sample Preparation cartridges and the ProBlott Mini PK/10 membranes. For sequencing the Procise Protein Sequencing Platform was used.

Sialylation of monoclonal antibody

A highly galactosylated humanized monoclonal antibody (IgG4) was used in sialylation experiments. The reaction mixture contained IgG4 (300 µg in 54 µL 35 mM sodium actetate/Tris buffer pH 7.0), the donor substrate CMP-Neu5Ac (150 µg in 50 µL water) and the ST6Gal-I variant (30 µg in 26 µL 20 mM potassium phosphate, 0.1 M NaCl, pH 6.5). The samples were incubated at 37°C up to 72 h. At certain time points the transfer reaction was stopped by addition of 100 µL denaturing buffer (6 M guanidine hydrochloride) and 30 µL TCEP (0.1 mM, diluted in denaturing buffer) and incubation at 37°C for 1 h. The samples were buffered in electrospray-medium (20% ACN, 1% FA) using pre-equilibrated illustraTM Nap5-Columns (GE Healthcare). Samples were analyzed by electrospray ionization mass spectrometry and the content of G2, G2+1SA and G2+2SA *N*-glycans was determined. A Micromass Q-Tof Ultima and a Synapt G2 HDMS device (Waters UK) with a MassLynx V 4.1 software were used.

Determination of product regioselectivity by HPAE chromatography

3´- and/or 6´-sialyl-*N*-acetyl-lactosamine and 3´- and/or 6´-sialyl glycan were separated and identified by HPAE chromatography on a Dionex BioLC system equipped with a CarboPac® PA200 column (3 x 250 mm; Thermo Fisher Scientific Inc.) and a CarboPac® guard column. 25 µL of the sample were injected and eluted at a flow rate of 0.4 mL/min and 25°C using adapted conditions. For the separation of 3´- and/or 6´-sialyl-*N*-acetyl-lactosamine an isocratic concentration of 35 mM sodium acetate in 60 mM NaOH was used. For the separation of 3´- and/or 6´-sialyl glycan the following protocol was used: 0-20 min linear gradient from 50 to 100 mM NaOH, 20-80 min linear gradient from 0 to 200 mM sodium acetate in 100 mM NaOH. Afterwards, the column was washed with 450 mM sodium acetate in 20 mM NaOH for 10 min followed by 200 mM NaOH for 10 min and re-equilibrated with 50 mM NaOH for 10 min before further analysis. An ED50 electrochemical detector with a carbohydrate certified gold working electrode was used for pulsed amperometric detection (PAD) in the carbohydrate waveform (as recommended by the supplier). Samples of sialyl glycan, treated with specific α2,3-neuramidase, were also analyzed according to the protocol described above.

Scheme and figure legends

Scheme 1: Schematic drawing of *N*-glycan patterns used in this study. Blue square, *N*-acetyl glucosamine moiety; cyan circle, mannose moiety; yellow circle, galactose moiety; pink rhombus, sialic acid moiety.

Figure 1: SDS-PAGE of purified recombinant human ST6Gal-I variants. Lane 1, 4: molecular weight marker; lane 2: Δ108ST6Gal-I; lane 3: Δ89ST6Gal-I.

Figure 2: Time course of sialylation of IgG. (A) Analysis of *N*-glycan pattern from reaction catalyzed by Δ89ST6Gal-I (left panel) and Δ108ST6Gal-I (right panel). (B) Analysis of *N*-glycan pattern from reaction catalyzed by Δ89ST6Gal-I when CTP (0.67 mM) was added after 7 h. Color code: black, G2; gray, G2+1SA; dark gray, G2+2SA.

Figure 3: Determination of product regioselectivity. (A) Proof-of-principle with commercially available ST6Gal-I and ST3Gal-I. (B) Analysis of *N*-glycans synthesized by Δ89ST6Gal-I and Δ108ST6Gal-I.

Figure 4: Close-up view of the acceptor binding site of Δ89ST6Gal-I [11].

Scheme 1

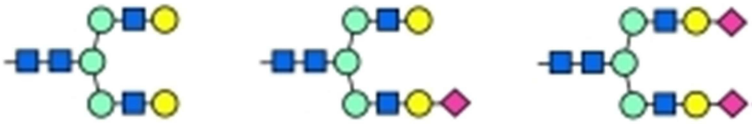

G2 G2+1SA G2+2SA

Figure 1

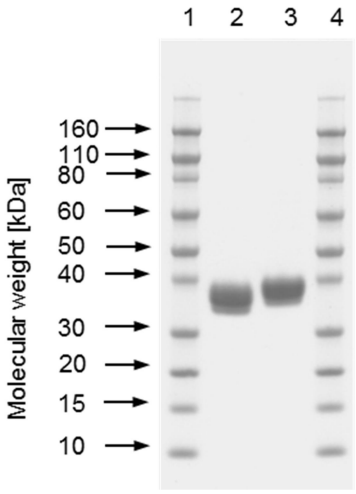

Figure 2

(A)

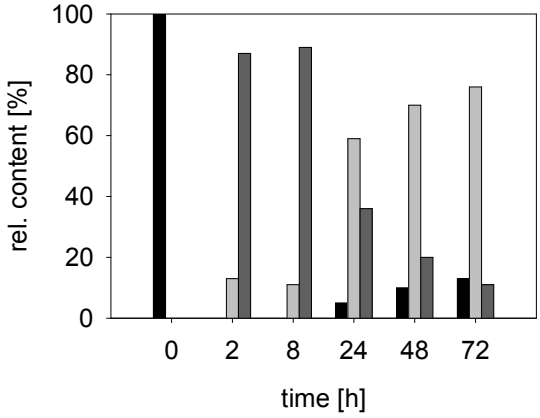
100
80
60
40
20
0
rel. content [%]
0
2
8
24
48
72
time [h]

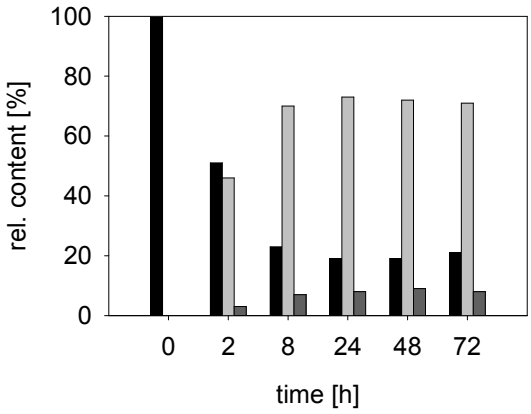
100
80
60
40
20
0
rel. content [%]
0
2
8
24
48
72
time [h]

(B)

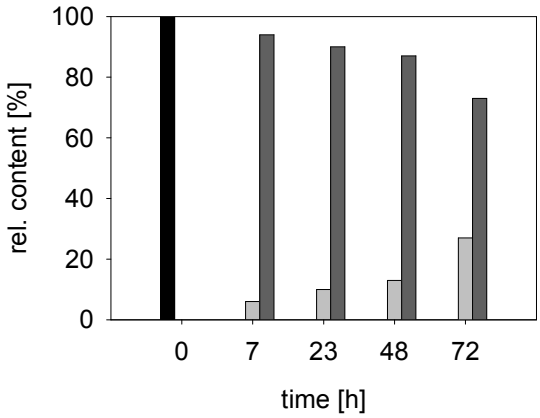
100
80
60
40
20
0
rel. content [%]
0
7
23
48
72
time [h]

Figure 3

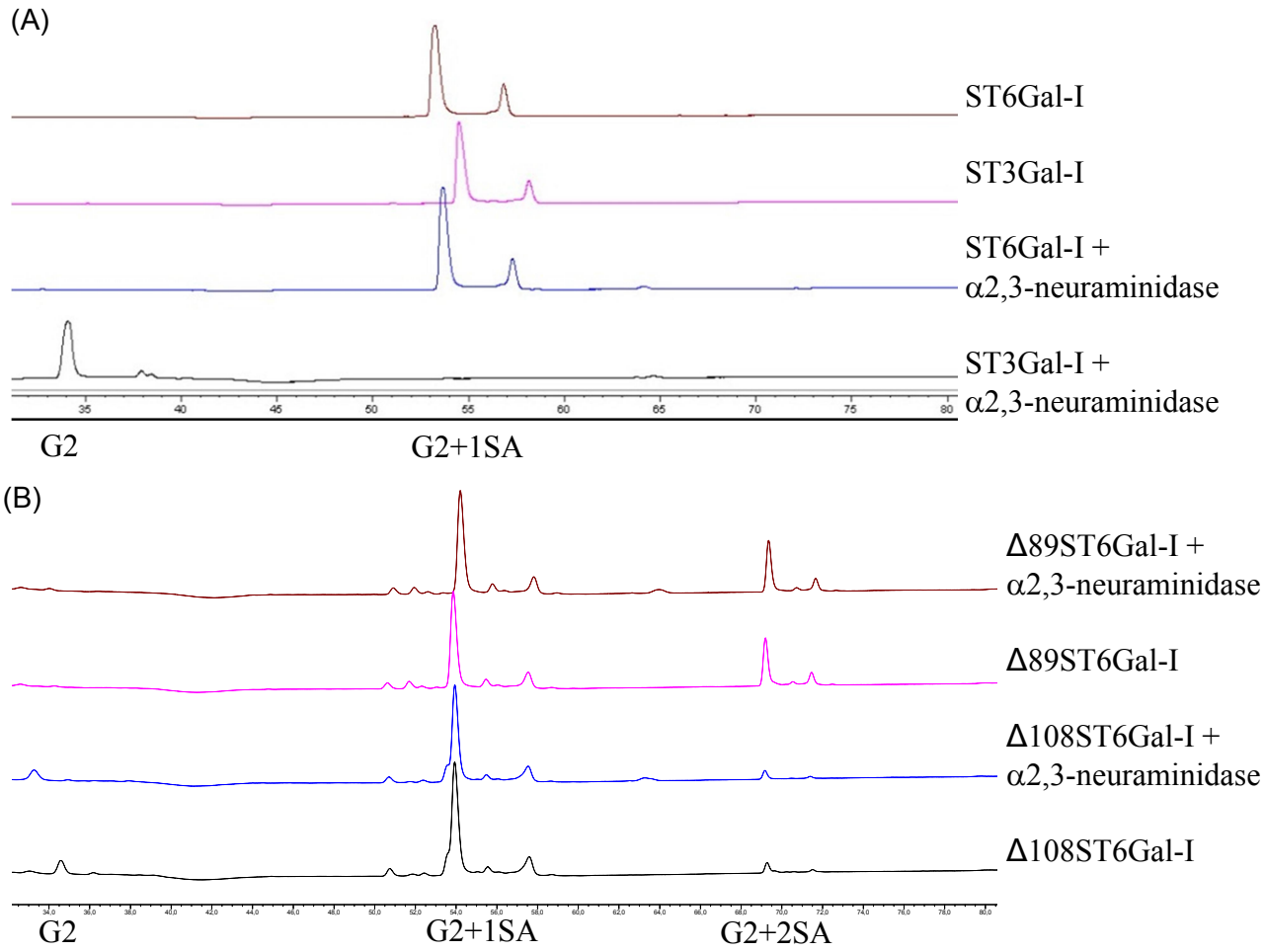
(A)
ST6Gal-I
ST3Gal-I
ST6Gal-I +
α2,3-neuraminidase
ST3Gal-I +
α2,3-neuraminidase
G2
G2+1SA
(B)
Δ89ST6Gal-I +
α2,3-neuraminidase
Δ89ST6Gal-I
Δ108ST6Gal-I +
α2,3-neuraminidase
Δ108ST6Gal-I
G2
G2+1SA
G2+2SA

Figure 4

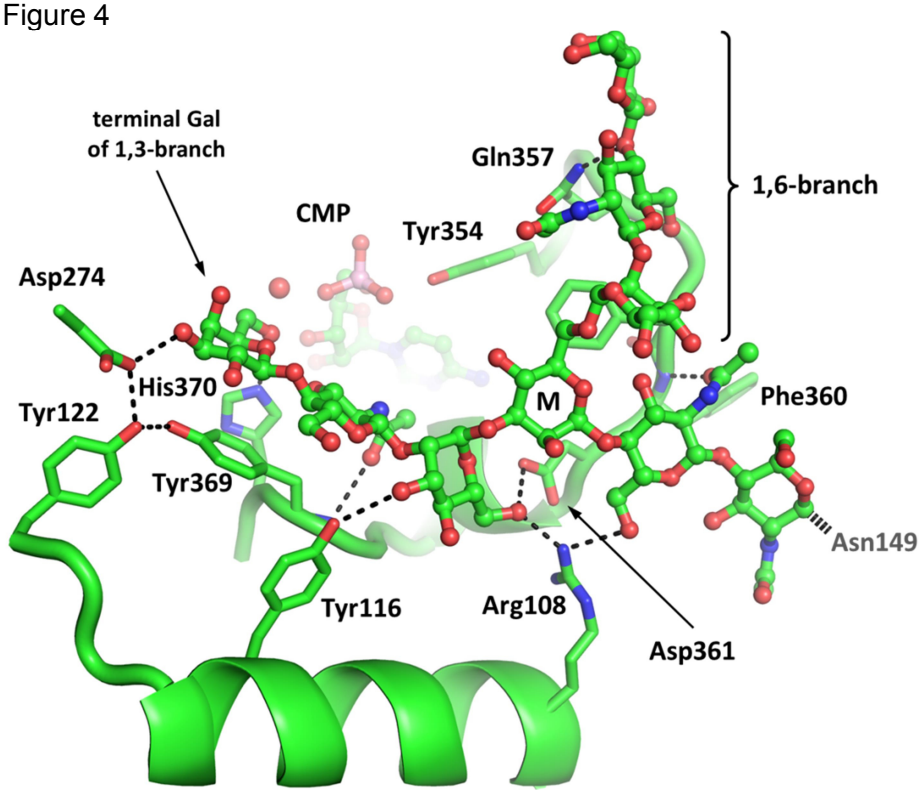
terminal Gal
of 1,3-branch
Gln357
1,6-branch
CMP
Tyr354
Asp274
His370
Tyr122
M
Phe360
Tyr369
Asn149
Tyr116
Arg108
Asp361

Table 1. Identification of peptides involved in disulfide bond formation.

	Sequence Peptide 1 // Peptide 2	mi-Mass [amu]	Delta [ppm]	Rel. Counts [%]
Cys141 – Cys406	**C**HLR // TIH**C**	997.46	0.00	4.2
Cys184 – Cys335	**C**AVVSSAGLSK // LHPNQPFYILKPQMPWELWDILQE ISPEEIQPNPPSSGMLGIIIMMTL**C**DQVDI YEFLPSK	8140.06	4.57	20.3
Cys353 – Cys364	TDV**C**YYYQK // FFDSA**C**TMGAYHPLLYEK	3271.43	0.86	74.4

Table 2. Kinetic parameters of Δ89ST6Gal-I and Δ108ST6Gal-I enzyme variants.

		Δ89ST6Gal-I	Δ108ST6Gal-I
SIALYLTRANSFERASE			
N-acetyl-D-lactosamine	K_m [mM]	8.3 ± 2.0	84 ± 16
	k_{cat} [s^{-1}]	8.7	1.3
	k_{cat}/K_m [$s^{-1}\cdot mM^{-1}$]	1.05	0.02
Asialofetuin	K_m [mM]	0.12 ± 0.02	0.10 ± 0.01
	K_i [mM]	n.a.	0.25
	k_{cat} [s^{-1}]	8.4	0.3
	k_{cat}/K_m [$s^{-1}\cdot mM^{-1}$]	70	3
HYDROLASE			
CMP-Neu5Ac	[U/mg]	0.04	0.03
SIALIDASE			
6'-SLA	[U/mg]	$7.1\cdot10^{-5}$	$1.2\cdot10^{-5}$

n.a., not applicable

References

[1] Grundmann, U., Nerlich, C., Rein, T. and Zettlmeissl, G. (1990). Complete cDNA sequence encoding human b-galactoside a2,6-sialyltransferase. Nucleic Acids Res. 18, 667.

[2] Datta, A.K. (2009). Comparative sequence analysis in the sialyltransferase protein family: Analysis of motifs. Curr. Drug Targets 10, 483-498.

[3] Audry, M., Jeanneau, C., Imberty, A., Harduin-Lepers, A., Delannoy, P. and Breton, C. (2011). Current trends in the structure-activity relationships of sialyltransferases. Glycobiology 21, 716-26.

[4] Anthony, R.M., Nimmerjahn, F., Ashline, D.J., Reinhold, V.N., Paulson, J.C. and Ravetch, J.V. (2008). Recapitulation of IVIG anti-inflammatory activity with a recombinant IgG Fc. Science 320, 373-6.

[5] Barb, A.W., Brady, E.K. and Prestegard, J.H. (2009). Branch-specific sialylation of IgG-Fc glycans by ST6Gal-I. Biochemistry 48, 9705-7.

[6] Ellman, G.L. (1959). Tissue sulfhydryl groups. Arch. Biochem. Biophys. 82, 70-77.

[7] Meng, L. et al. (2013). Enzymatic Basis for *N*-Glycan Sialylation: Structure of rat a2,6-sialyltransferase (ST6Gal1) reveals conserved and unique features for glycan sialylation. J. Biol. Chem. 288, 34680-34698.

[8] Scudder, P.R. and Chantler, E.N. (1981). Glycosyltransferases of the human cervical epithelium II. Characterization of a CMP-*N*-acetylneuraminate: Galactosyl-glycoprotein sialyltransferase. Biochimica et Biophysica Acta (BBA) - Enzymology 660, 136-141.

[9] Backliwal, G., Hildinger, M., Chenuet, S., Wulhfard, S., De Jesus, M. and Wurm, F.M. (2008). Rational vector design and multi-pathway modulation of HEK 293E cells yield recombinant antibody titers exceeding 1 g/l by transient transfection under serum-free conditions. Nucleic Acids Res. 36, e96.

[10] Brossmer, R. and Gross, H.J. (1994). Fluorescent and photoactivatable sialic acids. Methods Enzymol. 247, 177-93.

[11] Kuhn, B., Benz, J., Greif, M., Engel, A.M., Sobek, H. and Rudolph, M.G. (2013). The structure of human a-2,6-sialyltransferase reveals the binding mode of complex glycans. Acta Crystallogr., Sect. D - Biol. Crystallogr. 69, 1826-1838.

High-quality production of human α-2,6-sialyltransferase in *Pichia pastoris* requires control over N-terminal truncations by host-inherent protease activities

Doris Ribitsch[1, *] (doris.ribitsch@acib.at)

Sabine Zitzenbacher[1] (sabine.zitzenbacheracib.at)

Peter Augustin[1] (peter.augustin@tugraz.at)

Katharina Schmölzer[1] (katharina.schmoelzer@acib.at)

Tibor Czabany[1] (tibor.czabany@tugraz.at)

Christiane Luley-Goedl[1] (christiane.luley@acib.at)

Marco Thomann[5] (marco.thomann@roche.com)

Christine Jung[5] (christine.jung@roche.com)

Harald Sobek[4] (harald.sobek@roche.com)

Rainer Müller[4] (rainer.mueller.rm3@roche.com)

Bernd Nidetzky[1,3] (bernd.nidetzky@tugraz.at)

Helmut Schwab[1,2] (helmut.schwab@tugraz.at)

***Corresponding Author: doris.ribitsch@acib.at**

Submitted to Microbial Cell Factories
MS ID: 5860187381304371

Abstract

Background

α-2,6-sialyltransferase catalyzes the terminal step of complex *N*-glycan biosynthesis on human glycoproteins, attaching sialic acid to outermost galactosyl residues on otherwise fully assembled branched glycan structures. This "capping" of *N*-glycans with sialic acids is critical for therapeutic efficacy of specific pharmaceutical glycoproteins, making the degree of sialylation an important parameter of glycoprotein quality control. Expression of recombinant glycoproteins in mammalian cell culture usually delivers heterogeneous *N*-glycan structures, with an only minor degree of sialylation. *In-vitro* chemo-enzymatic glycoengineering of the *N*-glycans provides an elegant solution to increase the degree of sialylation for analytical purposes but also possibly for modification of therapeutic proteins.

Results

Human α-2,6-sialyltransferase (ST6Gal-I) was produced as secretory protein in *Pichia pastoris* KM71H. Codon-optimized ST6Gal-I genes featuring complete deletion of both the N-terminal cytoplasmic tail and the transmembrane domain, and also partial truncation of the stem region up to residue 108 were expressed under control of the AOX1 promoter using constructs harboring the α factor signal peptide plus a His or FLAG-Tag at the N-terminus. FLAG-tagged proteins proved much more resistant to proteolysis during production than the corresponding His-tagged proteins, whose degradation was shown by Western blot analysis to be very fast. Because volumetric transferase activity measured on small-molecule and native glycoprotein acceptor substrates did not correlate to ST6Gal-I protein secreted to *P.pastoris* supernatant, recombinant enzymes were purified and characterized in their action on non-sialylated protein-linked and released *N*-glycans, and the respective N-terminal sequences

were determined by automated Edman degradation. Irrespective of deletion construct used (Δ27, Δ48, Δ62, Δ89), isolated proteins showed N-terminal processing to a highly similar degree, with prominent truncations at residue 108, 111, 112, and 114, whereby only Δ108ST6Gal-I appeared to have retained activity. Proteolysis-resistant FLAG-tagged Δ108ST6Gal-I was therefore produced and obtained with a yield of 4.5 mg protein/L medium. The protein was isolated and shown by MS to be intact. Purified enzyme exhibited useful activity (0.18 U/mg) for sialylation of different substrates.

Conclusions

Functional expression of human ST6Gal-I as secretory protein in *P.pastoris* necessitates that N-terminal truncations promoted by host-inherent proteases be tightly controlled. N-terminal FLAG-Tag contributes extra stability to the N-terminal region as compared to N-terminal His-Tag. Proteolytic degradation proceeds up to residues 108 – 114 and of the resulting short-form variants (Δ108 – Δ114), only the Δ108 enzyme seems to be active. FLAG-Δ108ST6Gal-I transfers sialic acids to monoclonal antibody substrate with high specificity, and because it is stably produced in *P.pastoris*, it is identified here as an interesting glycoengineering catalyst.

Keywords

Therapeutic glycoproteins; *in-vitro* glycosylation; human sialyltransferase; ST6Gal-I; *N*-glycan remodeling; proteolysis in *Pichia pastoris*

Background

Therapeutic glycoproteins have gained enormous importance in the treatment of serious diseases [1, 2, 3, 4]. Clinically used glycoproteins became one of the fastest growing markets in the pharmaceutical industry, accounting for 77 high-value drugs out of 642 pharmaceuticals approved by the European Medicines Agency [4]. One of the most critical quality attributes of these drugs is the N-linked glycosylation which is known to have a dramatic impact on the therapeutic efficacy, serum half-life and immunogenicity [5, 6].

Glycosylation is the most complex and widespread posttranslational modification of proteins [7]. The sophisticated glycosylation machinery needed for the biosynthesis of therapeutically acceptable glycoprofiles is most likely provided in mammalian cells [8]. Hence, recombinant therapeutic glycoproteins are mainly produced in Chinese hamster ovary (CHO) cell lines but also in cell lines from baby hamster kidney (BHK-21) and murine tissues [9]. The *N*-glycans of proteins produced in these cells closely resemble the human glycan structure but still differ in crucial points [10, 11, 12]. In humans, the terminal monosaccharides of *N*-glycans are partially capped with the sialic acid derivative N-acetylneuramic acid (Neu5Ac) which strongly affects the solubility, stability and immunogenic properties of the respective glycoproteins. Glycoproteins expressed in CHO cells are also incompletely capped at the terminal monosaccharides [13].

To overcome these problems, the *in-vitro* glycosylation of therapeutic proteins by glycosyltransferases (GTs, EC 2.4.) has attracted the interest of the pharmaceutical industry since it offers the opportunity to control the glycosylation of therapeutic proteins to a desired, homogenous and bioactive glycoform [14, 15]. *In-vitro* sialylation offers the possibility to complete sialylation of therapeutic glycoproteins for analytical purposes, e.g. for analyzing the effect of sialylation on receptor binding, but also to modify the drug substance itself. Human sialyltransferases are a functional family of at least 20 glycosyltransferases which are

subdivided into ST3Gal-, ST6Gal-, ST6GalNAc- and ST8Sia- families [16,17], depending on the acceptor they act on (Gal: galactose, GalNAc: *N*-acetylgalactosamine, Sia: sialic acid) and the linkage they form (α2,3-, α2,6-, α2,8-linkage). The ST6 family includes two subfamilies, ST6Gal-I and ST6Gal-II, both mediating the transfer of sialic acid in α–2,6-linkeage from the donor substrate CMP-sialic acid to the terminal galactose but with slight differences in their acceptor specificities [18]. Human ST6Gal-I (β-galactoside α-2,6-sialyltransferase 1, E.C 2.4.99.1) belongs to the CAZy family GT29. Like all mammalian Golgi-resident GTs, ST6Gal-I features a type II transmembrane architecture consisting of an N-cytoplasmic tail, a single transmembrane domain and a large C-terminal catalytic domain facing the luminal side of the Golgi apparatus [19]. The catalytic domain of human ST6Gal-I adopts the predicted global GT-A fold, a seven-stranded central sheet flanked by α-helices, and is stabilized by three disulfide bindings [20]. The domain contains two NxS/T motifs for potential N-glycosylation which is supposed to contribute to the protein stabilization but is not absolutely required for *in-vivo* activity [21].

Much effort has already been expended to express human ST6Gal-I as full-length glycoprotein but without achieving acceptable activities. For instance, ST6Gal-I activity in stably transfected CHO cells was restricted to a crude membrane fraction [22]. ST6Gal-I expressed in *Saccharomyces cerevisiae* was retained in the endoplasmatic rediculum [23] and secretory expression in *Pichia pastoris* resulted in only 10 mU/L culture supernatant [24]. Obviously, the strong hydrophobic character of the transmembrane domain has clearly restrained the translocation, folding and solubility of the enzyme. Consequently, human ST6Gal-I was N-terminally truncated by the hydrophobic structural domains. As a result, transiently expression of truncated ST6Gal-I in HEK293 cells resulted in a considerably improved production rate [20]. In COS cells, truncated ST6Gal-I was secreted with a rate of 10 nm/1106 cells/h [25]. Expression experiments of ST6Gal-I in CHO cells has shown, that

N-terminal truncation of the first 89 amino acids - including the short N-terminal cytoplasmic tail, the transmembrane domain and the stem region - was tolerated even though the acceptor preference got lost, whereas further truncation to residue 100 completely abolished enzymatic activity [26]. The results led to the conclusion that the conserved motif QVWxKDS (aa 94-100 in human ST6Gal-I), which has been found within all sialyltransferase subfamilies, is crucial for activity.

In this work we report on the identification of a minimized catalytic domain of human β-galactoside α-2,6-sialyltransferase 1 corresponding to Δ108ST6Gal-I and its soluble expression in *P.pastoris* for the use in *in-vitro* sialylation of therapeutic proteins. Expression of N-terminally truncated ST6Gal-I variants revealed that the enzyme is proteolytically degraded in *P.pastoris* KM71H. Precise analysis of the degradation products by MS unveiled Δ108ST6Gal-I as the main degradation product. Contrary to the expectations from literature, Δ108ST6Gal-I was found to be active and catalyzed the transfer of sialic acid to a humanized monoclonal antibody IgG1. Variant Δ108ST6Gal-I was successfully expressed in the methylotropic yeast *P.pastoris* in sufficient yields for a potential large scale application.

Results and Discussion

Protein design for soluble expression of ST6Gal-I

For soluble expression of human ST6Gal-I in *P.pastoris,* the N-terminal hydrophobic topology domains were progressively deleted due to the truncation sites which have been determined from sequence comparison and published truncation experiments [25, 26].

According to the literature, the cytoplasmic-, transmembrane- and stem- (CTS) region contributes to the Golgi retention [27]. Analysis of the CTS region by the SACS HMMTOP Algorithm [28] predicts amino acids 1-9 as the NH_2-terminal cytoplasmic tail (CT) followed by a single transmembrane domain (TMD) ranging from aa 10-27 (Fig.1). The stem region which tethers the catalytic domain is highly variable in length among the human STs and assumed to range from aa 28-60 in human ST6Gal-I. Consequently, the catalytic domain includes amino acids 61-466. Similar boundaries were obtained from isolation of a soluble ST6Gal-I from rat liver tissues lacking a 62 aa NH_2-terminal peptide which indicates aa 63-466 as the catalytic domain [29]. Altogether, four different variants were constructed by progressive truncation of the structural domains *i.e.* the short NH_2-terminal cytoplasmic tail and the transmembrane domain (Δ27ST6Gal-I), the stem region (partially and fully, yielding Δ48ST6Gal-I and Δ62ST6Gal-I) and parts of the catalytic domain (Δ89ST6Gal-I). The deletions were located in the hypervariable region outside the conserved domain of human ST6Gal-I [23]. The genes coding for the truncated variants were optimized for expression in *P.pastoris* and fused to an N-terminal 6xHisTag.

Production in *P.pastoris* KM71H

The N-terminally truncated ST6Gal-I variants were produced in *P.pastoris* KM71H as secretory protein. In order to monitor and analyze the expression levels of the ST6Gal-I

variants, samples were withdrawn from the cultures at the start of induction (0 h) and 24, 48, 72 and 96 h after addition of MeOH. From each culture, aliquots of fermentation supernatant were precipitated with TCA and analyzed by Western Blot (WB) using two HRP conjugated antibodies for immunodetection, the polyclonal anti-α2,6ST6 and the monoclonal anti-polyHis. The antibodies were selected since they recognized different sequence parts of the protein and enabled the detection of the N-terminus (monoclonal anti-polyHis) as well as the C-terminal sequence (anti-α2,6ST6) of the enzyme. Comparison of samples drawn after 96 h of induction revealed conspicuous protein signals (Fig.2, -PI). In general, strong signals were obtained from detection with anti-α2,6ST6 which indicated that the expression, procession and secretion of ST6Gal-I worked sufficiently in the selected transformants. However, the main protein bands of the variants occurred just below 40 kDa which was lower than the expected molecular weights for the glycosylated enzymes and even lower than the calculated masses for the deglycosylated forms of Δ27ST6Gal-I (44.7 kDa), Δ48ST6Gal-I (42.1 kDa) and Δ62ST6Gal-I (40.7 kDa). Additional protein bands which were observed at very low molecular weights strengthened the presumption that proteolytic degradation has taken place. Moreover, no signals appeared with anti-polyHis which led to the conclusion that the proteolytic degradation proceeded from the N-terminus of each enzyme variant. The degradation was also detected at shorter induction times (data not shown) and increased with proceeding time. In order to reduce proteolysis, the expression of variants was repeated with addition of protease inhibitors (Fig.2, +PI). Now, less degradation products were detected with anti-α2,6ST6 but like before, the main protein bands appeared around 40 kDa and no signals were observed with anti-polyHis. Apparently, the addition of protease inhibitors significantly reduced the degradation to smaller products below 20 kDa but could not prevent the first steps of proteolysis concerning the N-terminus of ST6Gal-I including the His-Tag.

8

After WB analysis, the fermentation supernatants of N-terminal truncated ST6Gal-I variants, expressed in the presence of protease inhibitors, were analyzed regarding their sialyltransferase activity by measuring the transfer of fluorescence-labeled sialic acid from CMP-9-fluoresceinyl-Neu5Ac (CMP-9F-Neu5Ac) to asialofetuin [30]. Measurements at 37 °C and pH 6.5 resulted in 34 mU/L for Δ27ST6Gal-I, 80 mU/L for Δ48ST6Gal-I and 115 mU/L for Δ62ST6Gal-I and Δ89ST6Gal-I, respectively. Interestingly, the activities did not correlate with the expression levels of the main protein bands in Figure 2 (+PI) which might indicate that most of the immuno-detected enzyme variants were degraded to less active or inactive products and only small amounts of active protein were existent. In general, the volumetric enzyme activities increased with progressive truncation of ST6Gal-I.

Functional characterization of ST6Gal-I variants and identification of Δ108ST6Gal-I

Expression analysis of differently truncated ST6Gal-I variants clearly demonstrated that the enzyme was degraded to specific cleavage products accompanied by a loss of activity. For identification of the main cleavage site and its impact on activity, the dominating protein band at approximately 40 kDa of each ST6Gal-I variant (except of the lowest active Δ27ST6Gal-I) was purified from the fermentation supernatant (supplementary file 1) and subjected to an extensive characterization. First, the specific activity for the sialic acid transfer from CMP-9F-Neu5Ac to asialofetuin was measured and calculated as RFU/µg. Afterwards, the sialylation capacity towards a highly galactosylated humanized monoclonal antibody IgG1 was assayed in respect of the intended *in-vitro* glycosylation of antibodies; therefore, the transfer reaction samples were analyzed by electrospray ionization mass spectrometry to determine formation of G2+1SA and G2+2SA *N*-glycans with 1 and 2 sialic acid groups attached, respectively. In a last step, the N-terminal sequence of a purified sample of each

variant was determined by Edman degradation. After deglycosylation, the amino acid sequences of the different ST6Gal-I variants were deduced from MS analysis.

From each variant, several batches were characterized. The most significant results are summarized in Table 1.

Interestingly, activity of purified Δ48ST6Gal-I towards asialofetuin was not detectable but the variant formed 7 % G2+1SA when assayed towards IgG1. Variant Δ62ST6Gal-I showed a low batch-to-batch reproducibility which was reflected by fluctuating transfer activities (Table 1). Specific activities ranging from 70 to 689 RFU/µg were obtained for asialofetuin and a similar performance was observed towards IgG1. While batches with lower activities on asialofetuin (70 to 208 RFU/µg) also displayed low capability to sialylate the terminal galactosyl moieties of IgG1 (22 to 51 %), batches of Δ62ST6Gal-I which were highly active on asialofetuin (664 and 689 RFU/µg) were able to mask much more of total galactosyl moieties available. Formation of G2+1SA was favored (63 -82 %), however, disialylation (G2+2SA) was also observed at a reasonable extent of 15 – 34 % (based on initial G2+0SA concentration). After purification, variant Δ89ST6Gal-I showed no transfer activity towards asialofetuin or IgG1 anymore. Hence Δ89ST6Gal-I was not further investigated.

Mass analysis of the different constructs confirmed the presumption from WB analysis of the fermentation supernatants with anti-polyHis that in each case the N-terminal sequence of ST6Gal-I has been fully degraded to products corresponding to Δ108 – Δ114 truncations. In general, the transfer activities correlated well with the N-terminal truncations. The low active Δ48ST6Gal-I was found to be solely present as Δ114 product starting with NH_2-NYLS. Batches of Δ62ST6Gal-I performing best on asialofetuin and IgG1 were strictly existent as Δ108 variants starting with NH_2-LQKIWKNYLS whereas batches with lower activities on acceptor proteins contained mixtures of truncated products ranging from Δ111 (NH_2-IWKNYLS) to Δ114 (NH_2-NYLS). Apparently, the presence of the Δ108ST6Gal-I construct

correlated well with the observed transfer activities. Interestingly, Δ108ST6Gal-I was still very active even though significant parts of the predicted catalytic domain were missing. This is contradicting to previous studies [25, 26] reporting that the conserved sequence QVWxKDS covering residues 94-100 is crucial for activity. Proceeding degradation from Δ108 to Δ114 drastically reduced and almost abolished enzyme activity as demonstrated for Δ48ST6Gal-I which ended up in 100 % of Δ114. Since only low amounts of Δ111 and Δ112 were found we assumed that the degradation from Δ108 to Δ114 proceeds very fast. The results strongly support that not only the stem region but also carboxyl-terminal sequence parts of the predicted catalytic domain are highly sensitive to proteolytic processing events like they occur also in nature. Glycosyltransferases are type II membrane proteins and retained in the Golgi apparatus. However, some of the enzymes are cleaved by endogenous proteases and secreted out of the cell [31]. These proteolytic cleavage events frequently occur in the stem region and release a catalytically active fragment of the glycosyltransferases [31]. Hence, glycosyltransferases have been initially isolated from various body fluids [32]. Soluble ST6Gal-I has been purified first from goat, bovine, and human colostrum [33] and from rat liver missing 63 aa from the N-terminus of the enzyme [29]. Recently, it has been demonstrated that the β-amyloid-converting enzyme 1 (BACE1) is responsible for cleavage and secretion of human ST6Gal-I into the plasma [34]. BACE1 is a membrane-bound aspartic acid protease that cleaves the amyloid precursor protein to produce the neurotoxic amyloid β-peptide, which is a crucial initiation process of the pathogenesis of Alzheimer's disease. Investigation of this proteolysis by incubation of rat ST6Gal-I (88 % similarity to human ST6Gal-I) with BACE1 revealed that the enzyme was first cleaved between Leu^{37} and Gln^{38} to generate the sequence Gln^{38}-Ala^{39}-$\underline{Lys}^{40}$-$\underline{Glu}^{41}$-Phe^{42} at the N-terminus. In a second step, peptide Gln^{38}-Ala^{39}-Lys^{40} was trimmed by luminal aminopeptidase(s) yielding Glu^{41} as the N-terminal amino acid of the soluble ST6Gal-I. It is assumed that the generation of soluble

ST6Gal-I by BACE1 is needed for the sialylation of soluble plasma glycoproteins to protect them from clearance by the hepatic asialoglycoprotein receptors [34]. This two-step process of proteolytic degradation bears certain resemblance to the degradation of human ST6Gal-I during expression in yeast concerning the way it proceeds. The cleavage started between Arg^{108} and Leu^{109} and proceeded to Asn^{115} in Leu^{109}-Gln^{110}-Lys^{111}-Ile^{112}-Trp^{113}-$\underline{Lys}^{114}$-$\underline{Asn}^{115}$-Tyr^{116}. In both cases the final cleavage takes place after a Lysine residue. The proteolytic sensitivity of the stem region is highly relevant for physiological processes but strongly affects the stability during expression in yeast.

Expression and characterization of FLAG-Δ108ST6Gal-I

In order to confirm the activity of the newly identified Δ108ST6Gal-I variant and to evaluate its potential for large scale application, the variant was cloned into pPICZαB and expressed in *P.pastoris* KM71H. Now, the hydrophilic FLAG-Tag peptide was N-terminally fused to the protein for protection against proteolysis yielding FLAG-Δ108ST6Gal-I. SDS-PAGE analysis of culture supernatants drawn at certain time points after induction (Fig.3, A) revealed that FLAG-Δ108ST6Gal-I was produced and secreted in unexpected high amounts and purity. Apparently, deletion of the first 108 aa of human ST6Gal-I enhanced the folding and solubility of the enzyme significantly and improved the secretion rates without overloading the secretory pathway of *P.pastoris.*

At all time points, two protein bands, running closely together at about 40 kDa, appeared at the SDS-PAGE. Immunodetection with anti-α2,6ST6 generated two signals (Fig.3, B). After stripping, the membrane was re-used for detection with anti-FLAG which recognized solely the upper protein band (Fig.3, C). The results indicated that variant FLAG-Δ108ST6Gal-I was not only present as the entire protein but also as an N-terminally truncated variant lacking the FLAG-Tag and presumably a few amino acids of the catalytic domain. The weaker signals

obtained with anti-FLAG might probably be caused by the re-usage of the membrane after stripping and do not reflect original protein concentrations. In contrast to the Δ27-Δ89ST6Gal-I variants, no further proteolysis to smaller degradation products did occur, which provides evidence for an improved stability of FLAG-Δ108ST6Gal-I. Due to the highly similar surface charges the two protein bands could not be completely separated by ion exchange chromatography. Hence, a FLAG-Δ108ST6Gal-I variant comprising a certain percentage of truncated and therefore less active or inactive protein was used for further characterization.

So far, only little information has been published on specific activities of ST6Gal-I. This might be attributed to the poor availability of the enzyme. ST6Gal-I isolated from human liver revealed a transfer activity of 1.2 U/mg using CMP-9F-Neu5Ac and asialofetuin as donor and acceptor substrate, respectively [30]. Specific activities of $6 \cdot 10^{-5}$ U/mg [23] and $3 \cdot 10^{-4}$ U/mg [35] were obtained for the sialyltransfer from CMP-[^{14}C]-Neu5Ac towards asialofetuin for the human full-length ST6Gal-I expressed in *Saccharomyces cerevisiae* before and after up-scale (150-L bioreactor). Expression of a human ST6Gal-I construct, lacking the transmembrane domain, in insect cells yielded an enzyme preparation with 1.6 U/mg towards asialofetuin when assayed with the radio-labeled sugar donor [36]. In this work, the specific activity of FLAG-Δ108ST6Gal-I was not only determined towards high- but also towards low-molecular weight acceptors (Table 2). Using an HPLC-based assay, specific activities of 0.05 and 0.18 U/mg were obtained for asialofetuin and lactosamine, respectively. These values are intermediate to the specific activities reported above. However, comparison with data from literature has to be treated with caution, due to the different assay conditions used and the great variation in enzyme length and glycosylation pattern. But not only transferase activity is an important parameter for enzyme usability in biocatalysis. In general, the main obstacle for application of glycosyltransferases is the presence of different hydrolytic side reactions [37].

Therefore, we also had a look on sialidase activity and donor sugar hydrolysis. While α2,6-sialidase activity was not observed within the detection limit of 10^{-5}·U/mg, CMP-Neu5Ac was hydrolyzed with a specific activity of 0.03 U/mg (Table 2). This hydrolase activity of human Δ108ST6Gal-I is substantial, however, it is still 100-fold lower compared to bacterial sialyltransferases [38, 39]. *In-situ* generation of sugar nucleotides could partially compensate for the loss in efficiency of bacterial counterparts [40, 41]. Few relevant protein engineering strategies are reported which rely on a more detailed understanding of the underlying molecular mechanism [38]. However this is beyond the scope of this work.

Minimizing of the catalytic domain to a Δ108 construct and N-terminal fusion of a FLAG-Tag could remarkably improve the stability of ST6Gal-I during enzyme production (Fig.4). Nevertheless, proteolytic degradation did still occur to a certain degree during expression in shake flasks. It is known that temperature, pH and medium composition strongly influence the proteolytic activity of *P.pastoris* [42]. Hence, FLAG-Δ108ST6Gal-I was produced in a 5-L fed-batch bioreactor which offered the opportunity to tightly control the process conditions for potential reduction of proteolysis during the long expression phase. Expression of FLAG-Δ108ST6Gal-I was performed at 20 °C and pH 5.2 for 48 h. The culture supernatant was purified *via* anion exchange chromatography. Typically, 4.5 mg of purified protein were obtained from 1 L fermentation supernatant.

Analysis of the N-terminus by Edman degradation confirmed that 85 % of the deglycosylated enzyme was present as the entire protein and only low amounts of enzyme were degraded to Δ114 (10 %) and Δ115 (5 %). In comparison, only 50 % of Δ108 but also 50 % of Δ114 was detected in shake-flask experiments (data not listed). However, the specific activity (33 RFU/µg) was not significantly increased compared to a value of 20 RFU/µg obtained from shake-flask expression. Summing up, no substantial reduction in proteolysis during expression could be achieved under the fed-batch conditions used. Moreover, FLAG-

Δ108ST6Gal-I did only form 14 % of the G2+1SA *N*-glycan when assayed towards IgG1 and no G2+2SA *N*-glycan product was obtained at all. This is an interesting finding because variant Δ62ST6Gal-I, which was fully degraded to Δ108 (Table 1), showed 60-80 % G2+1SA and 15-30 % G2+2SA formation. It can be speculated that the N-terminal FLAG-Tag has a negative effect on enzyme activity although it is beneficial during enzyme expression. A study on acceptor substrate specificity revealed a similar observation [25]. The transfer efficiency was decreased up to 6-fold for truncated enzymatic forms (Δ28-Δ80) carrying an N-terminal Flag-Tag compared to the full-length enzyme. Ronin and co-workers [30] postulated that parts of the stem-region might participate in formation of the acceptor binding pocket. A recent crystal structure of human ST6Gal-I in complex with a high-molecular substrate [20], shows important interactions of residues 108-122 with the glycan acceptor. These residues are located on a helix which is involved in formation of the binding pocket. These observations support the hypothesis that linkage of a negatively charged FLAG-Tag is disordering secondary structure formation and thereby reducing the enzyme's activity. Nevertheless, for the first time we were able to prove activity of a Δ108ST6Gal-I construct, while a deletion of 100 aa led to complete inactivation of human ST6Gal-I when transiently expressed in CHO cells [25].

Conclusions

Precise analysis of degradation products, which were obtained during expression of N-terminally truncated human ST6Gal-I variants in *P.pastoris* KM71H, led to the identification of a minimal catalytic domain corresponding to Δ108ST6Gal-I. So far, it has been reported in literature that the deletion of more than 100 amino acids completely abolished enzyme activities. In this work we have demonstrated that N-terminal truncation of 108 amino acids not only maintained the activity but also increased the solubility of ST6Gal-I significantly.

Additionally, expression of the N-terminal Flag-tagged Δ108ST6Gal-I clearly indicated an improved stability of the enzyme against proteolysis. FLAG-Δ108ST6Gal-I catalyzed the transfer of sialic acid to the galactosyl residues of a humanized antibody which verified the potential for *in-vitro* glycosylation of therapeutic proteins.

16

Materials and Methods

Chemicals, Strains and Vectors

E. coli XL-1 Blue, *P.pastoris* KM71H and vector pPICZαB were purchased from Invitrogen (Austria). Asialofetuin, CMP-Neu5Ac, CMP-9F-Neu5Ac and cOmplete protease inhibitor tablets were obtained from Roche (Germany). Anti-α2,6-Sialytransferase© Rabbit IgG Antibody solution was purchased from IBL (Japan, #1898), monoclonal anti-polyHis from Sigma-Aldrich (Germany).

General recombinant DNA techniques

Phusion DNA Polymerase (Finnzyme) and dNTP´s from MBI Fermentas (Germany) were used for PCR. The PCR was performed in a Gene Amp® PCR 2200 thermocycler (Applied Biosystems, USA). Digestion of DNA was performed with restriction endonucleases from New England Biolabs (USA). Wizard ® Plus SV Minipreps DNA Purification System (Promega, Germany) was utilized to prepare plasmid DNA. PCR products and DNA fragments were purified by the Wizard ® SV Gel and PCR Clean-up System (Promega, Germany).

Construction and transformation of the recombinant plasmids

The gene coding for the human ST6Gal-I lacking the transmembran anchor (Δ27ST6) was codon optimized for *P.pastoris* and synthesized by the GeneArt® Gene Synthesis Service (Life Technologies, Germany). The synthesized DNA fragment was digested with *Xho*I and *Not*I and cloned into pPICZαB behind the α-factor yielding pPICZαB_Δ27ST6 (Fig.4). The DNA fragment included the *Xho*I restriction site, the *P.pastoris* Kex2 protease cleavage site, an ALE-6xHisTag coding peptide, the *Nde*I restriction site, the optimized gene, the stop

codon and the *Not*I restriction site. The respective truncated versions Δ27ST6Gal-I, Δ48ST6Gal-I, Δ62ST6Gal-I, Δ89ST6Gal-I and Δ108ST6Gal-I of the gene encoding human ST6Gal-I were amplified by PCR from pPICZαB_Δ27ST6 using the primers listed in Table 4. The following conditions were employed for PCR amplification (30 cycles): 98 °C for 30 s, 98 °C for 10 s, 62 °C for 25 s, 72 °C for 40 s and 72 °C for 7 min with Phusion® DNA polymerase. The PCR mixtures were purified, digested with *Nde*I/ *Not*I, ligated into pPICZαB_Δ27ST6 restricted with *Nde*I/ *Not*I and transformed into *E.coli* XL-1 Blue. Identity of the cloned genes was confirmed by DNA sequencing.

Introduction of the N-terminal FLAG-Tag (Fig.4) was performed by PCR using plasmid pPICZαB_Δ108ST6 as template and the primer pair 5'-TATCTCTCGAGAAAA-GAGATTACAAGGATGACGACGATAAGTTGCAGAAGATTTGGAAGAACTACTTGC-CATGAACAAG-3' for amplification. The reaction was performed with Phusion® DNA polymerase accordingly to the manufacturer`s instructions.

Transformation and selection for multi-integration events

About 1 µg of each plasmid was linearized with *Sac*I and transformed into 80 µL of freshly prepared competent cells of KM71H by electroporation at 1500 V, 25 µF and 600 Ω using a Gene Pulser (BioRad). Transformed cells were plated out on agar plates supplemented with 100 µg/mL Zeocin and incubated at 30 °C. Transformants were cultivated in microtiter plates and screened for multiple plasmid integration events on agar plates using Zeocin concentrations from 100 – 2,000 µg/mL. Selected clones were stored in MTP at -80 °C.

Expression of ST6Gal-I

Expression in Deep Well plates

Transformants were cultivated in deepwell plates (96-well format) in a Multitron II stackable incubation system (Infors, Bottmingen, Switzerland). Briefly, following a 12 h long incubation in 600 µL BYPD medium (1 % yeast extract, 2 % peptone, 2 % glucose, 200 mM potassium phosphate buffer pH 7) at 320 rpm, 28 °C and 80 % air humidity, cells were induced by addition of BBM (1 % glycerol, 1.34% yeast nitrogen base, $4x10^{-5}$ % biotin, 1 % (v/v) methanol, 200 mM potassium phosphate buffer pH 7). Following induction cycle was performed: 12 h 0.5 % MeOH – 12 h 1 % MeOH – 12 h 0.5 % MeOH – 12 h 1 % MeOH. After 48 h of induction, cells were harvested by centrifugation (4 °C, 2000 rpm, and 20 min). Culture supernatants and cell pellets were used for analysis of activity and expression levels.

Expression in shake flasks

Transformants were used to inoculate a 1-L baffled shake flask containing 200 mL BMGY broth (1 % yeast extract, 2 % peptone, 1 % glycerol, $4x10^{-5}$ % biotin, 100 mM potassium phosphat buffer pH 6). The cultures were incubated at 28 °C, 250 rpm for approximately 16-18 h until an OD_{600} of 2-6 was reached. The cells were harvested by centrifugation at 3,000 x g for 5 min and the cell pellet was resuspended in 1/10 of the original volume (20 mL). The culture was placed in a 100-mL baffled shake flask. Expression was induced by the addition of methanol to a final concentration of 0.5 %. Samples were collected after 48, 72, 96 and 120 h of induction and stored at -20 °C.

5-L Fermentation

After transformation of the human Δ108ST6Gal-I gene into *P.pastoris* KM71H, cells were grown in a defined glycerol medium at 30 °C and pH 5.2 until an OD_{578} of 200 was reached. The temperature was reduced to 20 °C and expression was induced by feeding the cells with methanol. At a final OD_{578} of 400 the culture medium was cooled to 4 °C and the cells were

separated by centrifugation. The supernatants containing Δ108ST6Gal-I were stored at -20 °C.

Purification of ST6Gal-I

From shake flasks

A two-step work-up procedure was used. In a first step, the culture supernatant was centrifuged (10 min at 3,000 rpm), filtrated (0.2 µm) and dialyzed against 20 mM potassium phosphate, pH 7.0. The dialysate was loaded onto a HisTrap HP FF 5-mL column (GE Healthcare, Germany) at a flow rate of 2 mL/min. After a washing step of 10 column volumes, the enzyme was eluted with a linear gradient of 0-500 mM imidazol within 10 column volumes. Fractions of 2-mL were collected and analyzed by SDS-PAGE. Sialyltransferase containing fractions were pooled and buffer was exchanged to 50 mM MES, pH 6.5.

From 5-L fermentation

A similar work-up procedure, as described above, was used. In a first step, two liters of supernatant were centrifuged (15 min at 8,500 rpm), filtrated (0.2 µm), dialyzed against 20 mM potassium phosphate, pH 6.5 (buffer A) and concentrated. The dialysate was loaded onto an S-Sepharose FF column (5.0 x 5.1 cm), equilibrated with buffer A. After washing with 600 mL buffer A, the enzyme was eluted with a linear gradient of 0-200 mM NaCl within 200 mL. Fractions (50 mL) were analyzed by SDS-PAGE.

SDS-PAGE and Immunoblotting

Analytical SDS gel electrophoresis was carried out using NuPAGE gels (4-12 %, Invitrogen). Samples (36 µL) were diluted with 12 µL NuPAGE LDS sample buffer (Invitrogen) and

incubated for 2 min at 85 °C. Aliquots, typically containing 5 µg of protein were loaded on the gel. The gels were stained using SimplyBlue SafeStain (Invitrogen).

For Dot Blot analysis, 5 µL of the culture supernatant from deepwell cultivation were loaded onto a Biodyne® A nylon 6.6 membrane (pore size 0.45 µm, Pall Corporation, Germany) and tried for 1 h at 60 °C. For Western Blot analyses, protein samples were separated by SDS-PAGE and blotted onto PVDF Transfer membranes (Amersham Hybond-P, GE Healthcare). Dot Blots and Western Blots were treated similarly for receptor detection: the membranes were washed twice with 20 mL TBS for 7 min at room temperature with shaking and blocked for 1 h at room temperature in TBS buffer (10 mM Tris HCl, pH 7.5 and 150 mM NaCl) containing 3 % (w/v) BSA. After 2x washing with TBS-Tween/Triton buffer (20 mM Tris HCl pH 7.5, 500 mM NaCl, 0.05 % (v/v) Tween 20, 0.2 % (v/v) Triton X-100) and 1x washing with TBS buffer (for each time at room temperature, 7 min with shaking), the membranes were incubated with the Anti-α2,6-Sialytransferase© Rabbit IgG Antibody solution (2 µg/mL dilution in blocking buffer of antibody) at room temperature for 1 h. The membranes were washed twice for 7 min with TBS-Tween/Triton buffer at room temperature and incubated with 7.5 mL of SuperSignal West Pico Substrate Working Solution for 3 min. Detection was performed using the G:Box F3 (Syngene).

Mass spectrometry

The molecular masses of variants of human ST6Gal-I expressed in *P.pastoris* were analyzed by mass spectroscopy. Therefore, the deglycosylated forms of human ST6Gal-I were prepared and analyzed using Micromass Q-Tof Ultima and Synapt G2 HDMS devices (Waters UK) and the MassLynx V 4.1 software. For deglycosylation, samples were denatured and reduced; 45 µL denaturing buffer (6 M guanidine hydrochloride) and 13 µL TCEP (0.1 mM, diluted in denaturing buffer) were added to 100 µg sialyltransferase. An appropriate volume of ultrapure water was added to reach an overall concentration of about 4 M of guanidine hydrochloride.

After incubation of the sample for 1 h at 37 °C the buffer was changed using a Bio-SpinR 6 Tris column (BioRad), which was pre-equilibrated with ultrapure water. The whole sample was applied onto the column and eluted by centrifugation. To the resulting eluate, 5.5 µL of a 0.1 U/µL solution of PNGase F was added and the mixture was incubated at 37 °C overnight. Afterwards the samples were adjusted to 30 % ACN and 1 % FA and analyzed by electrospray ionization mass spectrometry.

N-terminal sequencing by Edman degradation

The N-terminal sequences of expressed variants of human ST6Gal-I were analyzed by Edman degradation using reagents and devices obtained from Life Technologies. Preparation of the samples was done as described in the instruction manual of the ProSorb Sample Preparation cartridges and the ProBlott Mini PK/10 membranes. For sequencing the Procise Protein Sequencing Platform was used.

Activity assays

Fluorescence-based assay

Enzymatic activity was determined by measuring the transfer of fluorescence-labeled sialic acid to asialofetuin according to the literature [20]. Enzymatic activity was expressed as RFU/µg (relative fluorescence unit). 10,000 RFU/µg correspond to a specific activity of 0.084 U/mg.

HPLC-based assay

The reaction mixture consisted of 0.75 mM CMP-Neu5Ac, 10 mM lactosamine or 0.35 mM asialofetuin and 1 µM purified enzyme solution in 20 µL of 50 mM MES, pH 6.5 containing 0.1 % Triton X-100. The enzymatic reaction was carried out at 37 °C and 300 rpm. All assays were performed in duplicate. The enzymatic reaction was stopped after a certain time of

incubation by quenching on ice and addition of 40 µL of ice-cold acetonitrile. The reaction mixture was centrifuged at 4 °C, 13,000 rpm for 3 min to remove precipitated protein. After appropriate dilution, 10 µL were injected to HPLC analysis using a Chromolith® Performance RP-18 (100 x 4.6 mm; Merck Chemicals, Germany) column in reversed phase ion-pairing mode on an Agilent Technologies 1200 Series system. The column was equilibrated with 20 mM phosphate buffer, pH 6.8 containing 2 mM tetrabutylammonium at a flow rate of 2 mL/min. A temperature control unit maintained 30 °C throughout the analysis. Samples were eluted with a linear gradient from 0-2 % acetonitrile in 3 min followed by 2-25 % acetonitrile in 7 min and detected by UV at 254 nm. The increase of CMP and the decrease of CMP-Neu5Ac were recorded. One unit (1 U) was defined as the amount of enzyme that could transfer 1 µmol of sialic acid per min to lactosamine under the conditions described above.

Hydrolase and Sialidase assay

The reaction mixture for determination of CMP-Neu5Ac hydrolase activity consisted of 0.75 mM of CMP-Neu5Ac and 1 µM of purified enzyme in 20 µL of 50 mM MES, pH 6.5 containing 0.1 % Triton X-100. Reactions were allowed to proceed for 0.5, 10, 15, 30 and 60 min at 37 °C and 300 rpm. The reaction products were analyzed by HPLC as described above. The reaction mixture for determination of α2,6-sialidase activity consisted of 1.5 mM of 6'-sialyllactosamine, 0 or 1.0 mM CMP and 1 µM of purified enzyme in 20 µL of 50 mM MES, pH 6.5 containing 0.1 % Triton X-100. Reactions were allowed to proceed for up to 22 h at 37 °C and 300 rpm. The reaction products were analyzed by HPAE chromatography on a Dionex BioLC system equipped with a CarboPac® PA200 column (3 x 250 mm; Thermo Fisher Scientific Inc., Dionex) and a CarboPac® guard column. 25 µL of sample were injected and eluted using an isocratic concentration of 100 mM NaOH with 40 mM sodium acetate and a flow rate of 0.5 mL/min at 30°C. An ED50 electrochemical detector with a carbohydrate

certified gold working electrode was used for pulsed amperometric detection (PAD) in the carbohydrate waveform (as recommended from the supplier). Increase of sialic acid and decrease of 6'-sialyllactosamine was recorded.

Sialylation of monoclonal antibody

A highly galactosylated humanized monoclonal antibody IgG1 was used in sialylation experiments. The reaction mixture contained IgG1 (300 µg in 54 µL 35 mM sodium acetate/Tris buffer pH 7.0), the donor substrate CMP-Neu5Ac (150 µg in 50 µL water) and sialyltransferase (30 µg in 26 µL 20 mM potassium phosphate, 0.1 M NaCl, pH 6.5). The samples were incubated at 37 °C for a defined time. To stop the reaction 100 µL denaturing buffer (6 M guanidine hydrochloride) and 30 µL TCEP (0.1 mM, diluted in denaturing buffer) were added to the samples and the samples were incubated at 37 °C for 1 h. The samples were buffered in electrospray-medium (20 % ACN, 1 % FA) using pre-equilibrated illustraTM Nap5-Columns (GE-Healthcare). Samples were analyzed by electrospray ionization mass spectrometry and the content of G2+0SA, G2+1SA and G2+2SA N-glycans was determined. A Micromass Q-Tof Ultima and a Synapt G2 HDMS device (Waters UK) and the MassLynx V 4.1 software were used.

Abbreviations

RFU: Relative Fluorescence Unit; BYPD: Buffered Yeast extract Peptone Dextrose; BMGY: Buffered Glycerol-complex Medium; TBS: Tris Buffered Saline; FA: Formic Acid; HPAE chromatography: High-Performance Anion-Exchange Chromatography; TCEP: Tris(2-CarboxyEthyl)Phosphine

Competing interests

The authors declare no commercial or financial conflict of interest.

Author`s contribution

DR, TC, MT and HaS designed experiments; SZ and PA performed molecular biological experiments and enzyme expression; KS and CLG measured volumetric and specific enzyme activities; MT carried out MS analysis; BN, HeS, HaS, CJ and RM conceived the study and supervised the research; DR and CLG drafted the manuscript and MK wrote the paper; all authors have read the final version of the manuscript and given their approval.

Authors`information

[1]ACIB - Austrian Centre of Industrial Biotechnology, Petersgasse 14, A-8010 Graz, Austria; [2]Institute of Molecular Biotechnology, Graz University of Technology, Petersgasse 14, A-8010 Graz, Austria; [3]Institute of Biotechnology and Biochemical Engineering, Graz University of Technology, Petersgasse 12, A-8010 Graz, Austria; [4]Roche Diagnostics GmbH, Nonnenwald , D-82377 Penzberg, Germany; [5]Roche Diagnostics GmbH, Pharma Biotech Development, Nonnenwald , D-82377 Penzberg, Germany

Acknowledgements

This work has been supported by the Federal Ministry of Economy, Family and Youth (BMWFJ), the Federal Ministry of Traffic, Innovation and Technology (bmvit), the Styrian Business Promotion Agency SFG, the Standortagentur Tirol and ZIT - Technology Agency of the City of Vienna through the COMET-Funding Program managed by the Austrian Research Promotion Agency FFG.

References

1. Walsh G: **Biopharmaceutical benchmarks.** *Nature Biotechnology* 2010, **28(9)**:917-924.
2. Bertozzi CR, Freeze HH, Varki A, Esko JD: **Glycans in biotechnology and the pharmaceutical industry.** *Essentials of Glycobiology* (2nd Edition) 2009, 719-732.
3. Modjtahedi H, Ali S, Essapen S: **Therapeutic application of monoclonal antibodies in cancer: advances and challenges**. *British Medical Bulletin* 2012, **104(1)**: 41-59.
4. Elvin JG, Couston RG, van der Walle CF: **Therapeutic antibodies: Market considerations, disease targets and bioprocessing**. *International Journal of Pharmaceutics* (Amsterdam, Netherlands) 2013, **440(1)**:83-98.
5. Jedrzejewsk PM, del Val IJ, Polizzi KM, Kontoravdi C: **Applying quality by design to glycoprotein therapeutics: experimental and computational efforts of process control.** *Pharmaceutical Bioprocessing* 2013, **1(1)**:51–69.
6. Kontermann RE: **Strategies for extended serum half-life of protein therapeutics**. *Current Opinion in Biotechnology* 2011, **22**:868-876.
7. Berger M, Kaup M, Blanchard V: **Protein Glycosylation and Its Impact on Biotechnology**. *Advances in Biochemical Enginineering/Biotechnology* 2012, **127**:165-185.
8. Walsh G, Jefferis R: **Post-translational modifications in the context of therapeutic proteins**. *Nature Biotechnology* 2006, **24(10)**:1241-1252.
9. Ghaderi D, Zhang M, Hurtado-Ziola N, Varki A: **Production platforms for biotherapeutic glycoproteins. Occurrence, impact, and challenges of non-human sialylation.** *Biotechnology and Genetic Engineering Reviews* 2012, **28**:147-176.

10. Bork K, Horstkorte R, Weidemann W: **Increasing the sialylation of therapeutic glycoproteins: the potential of the sialc acid biosynthetic pathway.** *Journal of Pharmaceutical Sciences* 2009, **98(10)**: 3499-3508.
11. Wang L, Lomino JV: **Emerging Technologies for Making Glycan-Defined Glycoproteins.** *ACS Chemical Biology* 2012, **7:**110-122.
12. Hossler P, Khattak SF, Li ZJ: **Optimal and consistent protein glycosylation in mammalian cell culture.** *Glycobiology* 2009, **19(9)**: 936-949.
13. Tanemura M, Miyoshi E, Nagano H, Eguchi H, Taniyama K, Kamiike W, Mori M, Doki Y: **Role of α-gal epitope/anti-Gal antibody reaction in immunotherapy and its clinical application in pancreatic cancer.** *Cancer Science* 2013, **104(3)**:282-290.
14. Raju TS, Briggs JB, Chamow SM, Winkler ME, and Jones AJS: **Glycoengineering of Therapeutic Glycoproteins: In Vitro Galactosylation and Sialylation of Glycoproteins with Terminal *N*-Acetylglucosamine and Galactose Residues.** *Biochemistry* 2001, **40(30)**:8868–8876.
15. Khmelnitsky YL: **Current strategies for in vitro protein glycosylation**. *Journal of Molecular Catalysis B: Enzymatic* 2004, **31**:73-81.
16. Harduin-Lepers A, Vallejo-Ruiz V, Krzewinski-Recchi MA, Samyn-Petit B, Julien S, Delannoy P: **The human sialyltransferase family** *Biochimie* 2001, 83:727−737.
17. Varki A: **Sialic acids in human health and disease** *Trends in Molecular Medicine* 2008, **14(8)**: 351–360.
18. Takashima S, Tsuji S, Tsujimoto M: **Characterization of the Second Type of Human β-Galactoside α 2,6-Sialyltransferase (ST6Gal II), which Sialylates Gal β1,4GlcNAc Structures on Oligosaccharides Preferentially: Genomic Analysis Of Human Sialyltransferase Genes.** *Journal of Biological Chemistry* 2002, **277:**45719-45728.

19. Audry M, Jeanneau C, Imberty A, Harduin-Lepers A, Delannoy P, Breton C: **Current trends in the structure-activity relationship of sialyltransferases.** *Glycobiology* 2011, **21(6)**:716-26.

20. Kuhn B, Benz J, Greif M, Engel AM, Sobek H and Rudolph MG: **The structure of human α-2,6-sialyltransferase reveals the binding mode of complex glycans.** *Acta Crystallographica Section D* 2013, **D69**, 1826–1838.

21. Chen C and Colley KJ: **Minimal structural and glycosylation requirements for ST6Gal I activity and trafficking.** *Glycobiology* 2000, **10(5)**: 531-583.

22. Zhang X, Lok, Serene HL, Kon OL: **Stable expression of human α-2,6-sialyltransferase in Chinese hamster ovary cells: functional consequences for human erythropoietin expression and bioactivity.** *Biochimica et Biophysica Acta* 1998, **1425(3)**: 441-452.

23. Krezdorn CH, Kleene RB, Watzele M, Svetoslav XI, Hokke CH, Kamerling JP And Berger EG: **Human β1,4 galactosyltransferase and α2,6 sialyltransferase expressed in *Saccharomyces cerevisiae* are retained as active enzymes in the endoplasmic reticulum** *European Journal of Biochemestry* 1994, **220**:809-817.

24. Chotigeat W, Chayanunnukul W, Phongdara A: **Expression of a mammalian α2,6-sialyltransferase gene in *Pichia pastoris***. *Journal of Biotechnology* 2000, **81(1)**:55-61.

25. Legaigneur P, El Battari A, Guillemot JC, Auge C, Malissard M, Berger EG, Ronin C: **Exploring the acceptor substrate recognition of the human beta-galactoside alpha 2,6-sialyltransferase.** *The Journal of Biological Chemistry* 2001, **276(24)**:21608-17.

26. Donadio S, Dubois C, Fichant G, Roybon L, Guillemot JC, Breton C, Ronin C: **Recognition of cell surface acceptors by two human alpha-2,6-sialyltransferases produced in CHO cells.** *Biochimie* 2003, **85(3-4)**:311-21.

27. Breton C, Imberty A: **Structure/function studies of glycosyltransferases.** *Current Opinion in Structural Biology*, 1999, **9(5):** 563–571.

28

28. Tusnady GE, Simon I.: **The HMMTOP transmembrane topology prediction server.** *Bioinformatics*, 2001, **17**:849-50.

29. Weinstein J, Lee EU. McEntee K, Lai PH, Paulson JC: **Primary structure of β-Galactosid α2,6-Sialyltransferase**. *The Journal of Biological Chemistry*, 1987, **262(36)**:17735-17743.

30. Gross HJ, Sticher U, and Brossmer R: **A Highly Sensitive Fluorometric Assay for Sialyltransferase Activity Using CMP-9-fluoresceinyl-NeuAc as Donor.** *Analytical Biochemistry* 1990, **186**: 127-134.

31. Colley KJ: **Golgi localization of glycosyltransferases: more questions than answers.** *Glycobiology* 1997, **7(1)**:1-13.

32. Varki A, Cummings R, Esko J: **Essentials of Glycobiology**. *Cold Spring Harbor (NY): Cold Spring Harbor Laboratory Press* 1999.

33. Paulson JC; Rearick JI, Hill RL**: Enzymatic properties of beta-D-galactoside alpha2 leads to 6 sialytransferase from bovine colostrum.** *The Journal of Biological Chemistry* 1977, **252**:2363-2371.

34. Sugimoto I, Futakawa S, Oka R, Ogawa K, Marth JD, Miyushi E, Taniguchi N, Hashimoto Y and Kitazume S**: β-Galactoside α2,6-sialyltransferase I cleavage by BACE1 enhances the sialylation of soluble glycoproteins.** *The Journal of Biological Chemistry* 2007, 282(48):34896-34903.

35. Borsig L, Ivanon SX, Herrmann GF, Kragl U, Wandrey C, and Berger EG: **Scaled-up expression of human α2,6-sialyltransferase in *Saccharomyces cerevisiae*.** *Biochemical and Biophysical Research Communications* 1995, **210**:14-20.

36. Kim HG, Yang SM, Lee YC, Do SI, Chung IS and Yang JM: **High-level expression of human glycosyltransferases in insect cells as biochemically active form.** *Biochemical and Biophysical Research Communications* 2003, 305:488–493.

37. Shaikh FA, Withers SG: **Teaching old enzymes new tricks: engineering and evolution of glycosidases and glycosyl transferases for improved glycoside synthesis**. *Biochemistry and Cell Biology* 2008, **86(2)**:169-177.

38. Schmoelzer K, Ribitsch D, Czabany T, Luley-Goedl C, Kokot D, Lyskowski A, Zitzenbacher S, Schwab H, Nidetzky B. **Characterization of a multifunctional α2,3-sialyltransferase from *Pasteurella dagmatis*.** *Glycobiology* 2013, **23(11):**1293-304.

39. Sugiarto G, Lau K, Qu J, Li Y, Lim S, Mu S, Ames JB, Fisher AJ, Chen X: **A Sialyltransferase Mutant with Decreased Donor Hydrolysis and Reduced Sialidase Activities for Directly Sialylating Lewis.** *ACS Chemical Biology* 2012, **7(7):** 1232–1240.

40. Yu H, Huang S, Chokhawala H, Sun M, Zheng H, Chen X: **Highly Efficient Chemoenzymatic Synthesis of Naturally Occurring and Non-Natural α-2,6-Linked Sialosides: A *P. damsela* α-2,6-Sialyltransferase with Extremely Flexible Donor–Substrate Specificity.** *Angewandte Chemie International Edition* 2006, **45(24):** 3938-3944.

41. Yu H, Chokhawala H, Karpel R, Yu H, Wu B, Zhang J, Zhang Y, Jia Q, Chen X: **A Multifunctional *Pasteurella multocida* Sialyltransferase: A Powerful Tool for the Synthesis of Sialoside Libraries** *Journal of the American Chemical Society* 2005, **127:** 17618-17619.

42. Potvin G, Ahmad A, Zhang Z: **Bioprocess engineering aspects of heterologous protein production in Pichia pastoris: A review.** *Biochemical Engineering Journal* 2012, **64**: 91– 105.

43. Sambrook J, Fritsch EF, Maniatis T: **Molecular cloning: a labatory manual**. *2nd edn. Cold Spring Harbor Laboratory Press*, Cold Spring Harbor, 1989.

Supporting information

Figure legends

Figure 1 Structural domains of human ST6Gal-I (data base entry P15907).

Italics: cytosolic domain (aa 1-9). *Bold*: transmembrane domain (aa 10-27). *Underlined*: stem-region (aa 28-62). *Bold and Italics*: potential N-glycosylation sites. N-termini of truncated variants are indicated by a grey arrow.

Figure 2. Expression of N-terminally truncated ST6Gal-I variants in *P.pastoris* KM71H in the absence (-PI) and presence (+PI) of protease inhibitors. WB analysis of fermentation supernatants (each 600 µL, precipitated with 20 % TCA). Immunodetection with HRP conjugated anti-α2,6ST6.

Figure 3. Expression analysis of human FLAG-Δ108ST6-WT in *P.pastoris*.

Analysis by A) SDS-PAGE and Western Blot using B) anti-α2,6ST6 and C) anti-FLAG for detection. *Lane 1*: Novex sharp protein standard; *lane 2-6*: fermentation supernatant (300 µL TCA precipitated) after 24, 48, 72, 96 and 120 h of induction in shake flasks.

Figure 4 Schematic representation of the pPICZαB-based *P.pastoris* expression vectors employed in this study. pAOX1: alcohol oxidase 1 gene promoter; α-factor: coding region for the signal sequence of *S. cerevisae* α-mating factor; 6xHis: coding sequence for 6 histidines; Flag: coding sequence for the Flag-Tag; Kex2: coding sequence for Kex2 protease cleavage sites; human ST6Gal-I: coding sequence for the truncated variants of human ST6Gal-I.

Supporting Information 1. SDS-PAGE of purified ST6Gal-I expressed in *P.pastoris* KM71H with protease inhibitors. *Lane 1*: Δ62ST6Gal-I; *lane 2*: Δ48ST6Gal-I; *lane 3*: Δ89ST6Gal-I; *lane 4*: Novex Sharp Protein Standard.

Supporting Information 2. TLC based activity assay. *Lane 1*, reaction catalyzed by purified FLAG-Δ108ST6 enzyme; *lane 2*, standard 6'-sialyl-N-acetyl-lactoseamine; *lane 3*, standard N-acetyl-lactoseamine. The reaction mixture (20 µL), containing 1 mM CMP-Neu5Ac, 2 mM N-acetyl-lactosamine, 0.8 µM enzyme, was incubated at 37 °C, 300 rpm for 24h. The reaction was stopped by addition of CTP in a final concentration of 2 mM. Samples were analyzed by TLC using silica plates (DC Alufolien, Kieselgel 60; Merck). 12 µL of the reaction mixture were loaded onto the plate. A mixture of n-butanol/acetic acid/H_2O in a ratio of 2:1:1 was used as mobile phase. The developed TLC plates were stained with thymol/H_2SO_4 (0.5 g thymol, 95 mL ethanol, 5 mL 97% sulfuric acid) at 120 °C.

Tables

Table 1. Analytic data of N-terminally truncated ST6Gal-I constructs.

Construct	Intensity of variant in ESMS [%]	MS Analysis	Truncation	IgG1		Asialofetuin
				G2+1SA [%]	G2+2SA [%]	Fetuin [RFU/µg]
Δ48ST6Gal-I	100	NYLS...	Δ114	7	0	n.d.
Δ62ST6Gal-I	75	NYLS...	Δ114	22	0	70
	25	WKNYLS...	Δ112			
Δ62ST6Gal-I	30	LQKIWKNYLS...	Δ108	29	0	208
	70	NYLS...	Δ114			
Δ62ST6Gal-I	50	LQKIWKNYLS...	Δ108	51	0	186
	20	NYLS...	Δ114			
	15	IWKNYLS...	Δ111			
	10	WKNYLS...	Δ112			
Δ62ST6Gal-I	100	LQKIWKNYLS...	Δ108	63	34	664
Δ62ST6Gal-I	100	LQKIWKNYLS...	Δ108	82	15	689

n.d. not detectable

Table 2. Multifunctionality of human FLAG-Δ108ST6Gal-I.

Enzyme activity	Donor	Acceptor	Specific activity [U/mg]
α2,6-Sialyltransferase	CMP-Neu5Ac	Lactosamine	0.18 ± 0.01
	CMP-Neu5Ac	Asialofetuin	0.05 ± 0.01
CMP-Neu5Ac hydrolase	CMP-Neu5Ac	-	0.03 ± 0.01
α2,6-Sialidase	6'-Sialyllactosamine	-	n.d.

n.d., not detectable

Table 3. Analytic data of human FLAG-Δ108ST6Gal-I expressed under fed-batch conditions.

Construct	Intensity of variant in ESMS [%]	MS Analysis	Truncation	IgG1		Asialofetuin
				G2+1SA [%]	G2+2SA [%]	Fetuin [RFU/µg]
FLAG-Δ108ST6Gal-I*	85	DYKDDDDKLQKIWKNYLS…	Δ108	14	0	33
	10	NYLS...	Δ114			
	5	YLS…	Δ115			

*The FLAG-Δ108ST6Gal-I construct was obtained from a 5-L fermentation.

Table 4: Primer sequences for truncation of human ST6Gal-I.

Primer name	**Nucleotide sequences**
Δ48_hST6Gal-I.FW	5'-CTGGAGATACT CATATG AAA TCC TTA GGC AAG TTA GCT ATG GGG T-3'
Δ62_hST6Gal-I.FW	5'-CTGGAGATACT CATATG GTT TCC TCA TCC TCC ACT CAA GAC C-3'
Δ89_hST6Gal-I.FW	5'-CTGGAGATACT CATATG GAA GCT TCT TTC CAG GTT TGG AAC AAG GAC -3'
Δ108_hST6Gal-I.FW	5'- ATCATCATATG TTG CAG AAG ATT TGG AAG AAC TAC TTG TCC ATG -3'
hST6Gal-I.REV	5'-CTGGAGATACT GCGGCCGCTCAACAGTG -3'

```
          10         20         30         40         50         60
MIHTNLKKKF  SCCVLVFLLF AVICVWKEKK KGSYYDSFKL QTKEFQVLKS LGKLAMGSDS

          70         80         90         100        110        120
QSVSSSSTQD  PHRGRQTLGS LRGLAKAKPE ASFQVWNKDS SSKNLIPRLQ KIWKNYLSMN

         130        140        150        160        170        180
KYKVSYKGPG  PGIKFSAEAL RCHLRDHVNV SMVEVTDFPF NTSEWEGYLP KESIRTKAGP

         190        200        210        220        230        240
WGRCAVVSSA  GSLKSSQLGR EIDDHDAVLR FNGAPTANFQ QDVGTKTTIR LMNSQLVTTE

         250        260        270        280        290        300
KRFLKDSLYN  EGILIVWDPS VYHSDIPKWY QNPDYNFFNN YKTYRKLHPN QPFYILKPQM

         310        320        330        340        350        360
PWELWDILQE  ISPEEIQPNP PSSGMLGIII MMTLCDQVDI YEFLPSKRKT DVCYYYQKFF

         370        380        390        400
DSACTMGAYH  PLLYEKNLVK HLNQGTDEDI YLLGKATLPG FRTIHC
```

Figure 1 Structural domains of human ST6Gal-I (data base entry P15907).

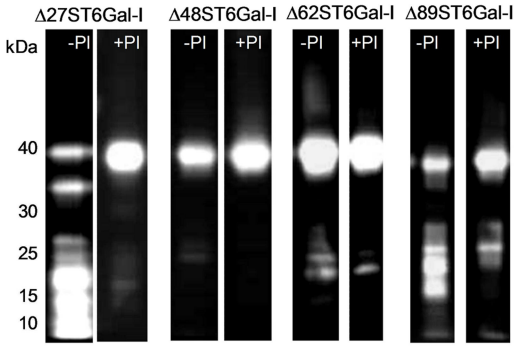

Figure 2. Expression of N-terminally truncated ST6Gal-I variants in *P.pastoris* KM71H in the absence (-PI) and presence (+PI) of protease inhibitors.

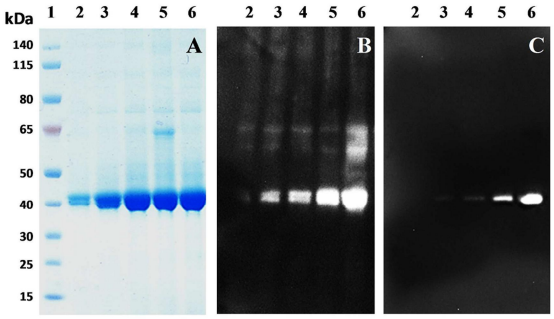

Figure 3. Expression analysis of human FLAG-Δ108ST6-WT in *P.pastoris*.

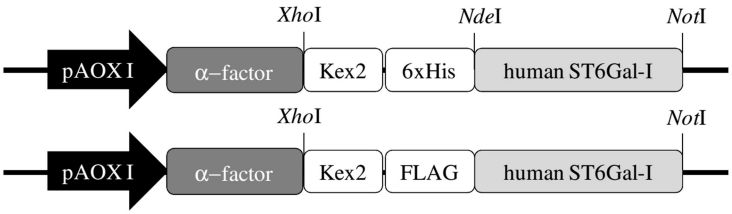

Figure 4 Schematic representation of the pPICZαB-based *P.pastoris* expression vectors employed in this study.

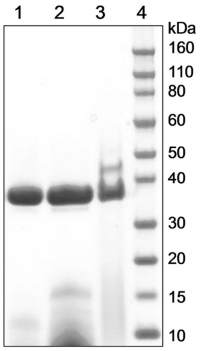

Supporting Information 1. SDS-PAGE of purified ST6Gal-I expressed in *P.pastoris* KM71H with protease inhibitors. *Lane 1*: Δ62ST6Gal-I; *lane 2*: Δ48ST6Gal-I; *lane 3*: Δ89ST6Gal-I; *lane 4*: Novex Sharp Protein Standard.

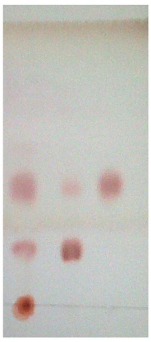

Supporting Information 2. TLC based activity assay.

Appendix

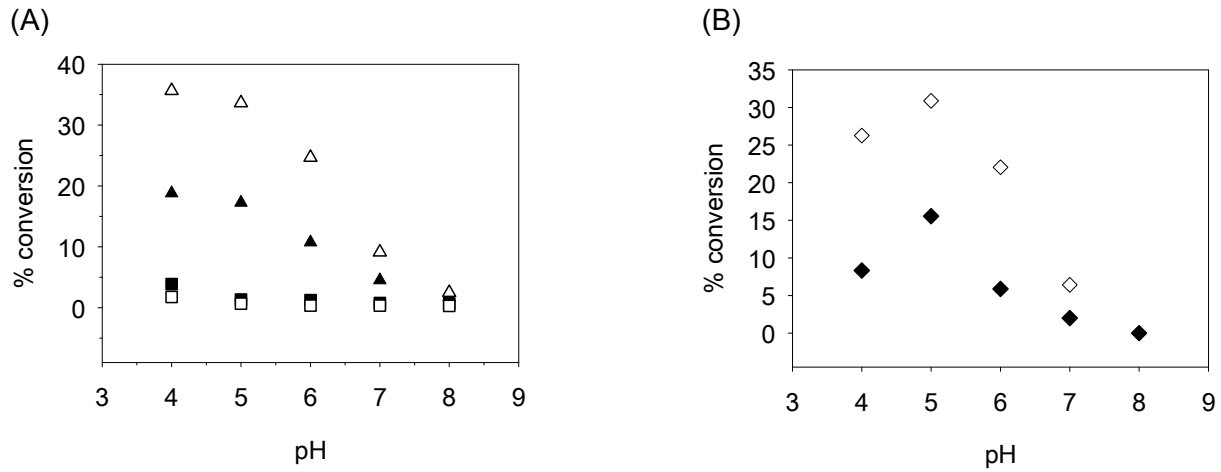

Fig. 1. pH profiles of α2,3-sialidase activity (A) and α2,3-trans-sialidase activity (B) catalyzed by wild-type PdST (closed symbols) and T116S mutant (open symbols). (A) The release of lactose from 3´-sialyllactose (triangle) and 6´-sialyllactose (square) was followed. (B) The formation of Neu5Acα2,3Gal-oNP (diamond) was followed.

Structures of wild-type PdST and of mutants thereof

Tea Pavkov-Keller[1], Andrzej Lyskowski[1]

[1]Austrian Centre of Industrial Biotechnology, Petersgasse 14, 8010 Graz, Austria

Methods

For the crystallization setups the proteins were concentrated using Amicon Ultra Centrifugal Filters (Ultracel-10K, Merck Millipore, USA) and the concentrations were determined using NanoDrop (ThermoSicentific, USA).

The crystallization experiments of wild-type PdST, T116S, P7H and P7H-M117A mutants were setup with vapour diffusion method by Oryx-8 robot (Douglas Instruments) using Index (Hampton Research) and JCSG+ (Molecular Dimensions) screens. Crystallizations were setup in the presence of CMP-Neu5Ac (2 mM final concentration) and lactose or oNP-βGal (5 mM final concentration). The total drop volume was 1 µL containing 50% of the protein and 50% of the reservoir solution. Protein concentrations used for crystallization setups were 3.3 mg/mL for wild-type PdST, 5 mg/mL for T116S, 5.2 mg/mL for P7H and 6.7 mg/mL for P7H-M117A (10 mM Tris/HCl pH 8.0, 50mM NaCl) mutant. Crystallization plates were kept in the incubator at 16°C. Crystals appeared after 3 days in several conditions. Small amount of glycerol was added to the drop and the crystals were pulled out of the drop with a nylon loop and immediately shock frozen in liquid nitrogen. Additionally, the same crystals were soaked with excess of lactose/oNP-βGal for 30 min - 1 h period before freezing in liquid nitrogen. Screening experiments were performed at our home source (Bruker) with copper rotating anode and with a Mar345 Image Plate Detector (Mar Research). Data collection on several crystals was performed at synchrotron sources DESY (PETRA III, Hamburg, Germany) and ESRF (Grenoble, France). The measurements were carried out at - 100K.

Data were processed, merged and scaled using the XDS programs [1]. The R_{free} column comprising a randomly selected 5% of the reflections was introduced. The structures were solved by the molecular-replacement method using the program Phaser [2]. The structure of Sialyltransferase Pm0188 from *Pasteurella multocida* was used as a template for solving the T116S structure. For all other structures the T116S structure or its N- and C-terminal domains were used as the initial phasing model. The refinement and manual model rebuilding were carried out with REFMAC5 [3] and Coot [4]. Refinement was concluded when no significant changes in R_{work} and R_{free} were observed. The validation of the final structures was performed with MolProbity [5].

Results

Crystals of wild-type PdST obtained in the Index screen condition D9 (0.1 M Tris pH 8.5, 25% w/v Polyethylene glycol 3350) belong to I121 space group with unit cell dimensions a=79.5 Å, b=56.5 Å, c=110.2 Å, α=γ=90° and β=110.1°. Data were collected to 2.5 Å. Crystals of P7H and P7H-M117A mutants from JCSG-plus screen conditions G7 (0.1 M succinic acid, 15% w/v PEG 3350, pH 7.0) and B9 (0.1 M citrate, 20%w/v PEG 6000, pH 5.0) diffracted to 2.2 and 2.3 Å. Crystals belong to C2 space group with the unit cell dimensions a=111.2 Å, b=56.9 Å, c=79.7 Å, α=γ=90° and β=111.3°. All four structures obtained from these data show the protein in the open conformation.

Structures of T116S, P7H and P7H-M117A mutants in closed conformation with bound CMP were solved from the crystals obtained by co-crystallization and soaking experiments with CMP-Neu5Ac and lactose or oNP-βGal. No extra electron density for lactose or oNP-βGal could be observed. Crystals of T116S mutant were obtained in JCSG+ screen (0.1 M Phosphate/citrate pH 4.2 and 40% w/v PEG 300). They belong to $C222_1$ space group with unit cell dimensions 75.6 Å, 140.5 Å, 80.7 Å, α=β=γ=90°. Data collected on P7H and P7H-M117A crystals grown in JCSG-plus screen conditions A9 (0.2 M ammonium chloride, 20% w/v PEG 3350), A2 (0.1 M sodium citrate, 20% w/v PEG 3000, pH 5.5), A5 (0.2 M magnesium formate, 20% w/v PEG3350) and A12 (0.2 M potassium nitrate, 20% w/v PEG 3350) show unit cell dimensions a=b=108.5 Å, c=62.4 Å, α=β=90° and γ=120° (space group $P6_5$).

The diffraction obtained for all measured crystals extends in the 1.7-2.5 Å range.

Table 1. Data collection and refinement statistics

	WT	**T116S+CMP**	**P7H**	**P7H+CMP**	**P7H-M117A**	**P7H-M117A+CMP**
Data collection						
Beamline	DESY P11	ESRF BM14	ESRF ID29	ESRF ID23-2	ESRF ID29	ESRF ID29
Space group	I121	$C222_1$	C2	$P6_5$	C2	$P6_5$
a, b, c (Å)	79.5, 56.5, 110.2	78.4, 143.7, 83.2	112.2, 57.1, 80.2	113.6, 113.6, 65.7	111.2, 56.9, 79.7	111.8, 111.8, 65.2
α, β, γ (°)	90, 110.1, 90	90, 90, 90	90, 111.4, 90	90, 90, 120	90, 111.3, 90	90, 90, 120
Resolution (Å)*	73.7-2.42 (2.51-2.42)	41.6-1.6 (1.69-1.6)	75-1.83 (1.9-1.83)	50-2.18 (2.26-2.18)	50-2.34 (2.52-2.34)	96-1.84 (1.84-1.92)
Rmerge*	0.18 (0.80)	0.04 (0.64)	0.06 (0.81)	0.09 (0.89)	0.13 (0.81)	0.06 (0.77)
I/δ*	11.3 (1.2)	29.7 (2.5)	11.9 (1.4)	9.5 (1.2)	10.9 (2.1)	18.8 (1.8)
Completeness (%)*	97.9 (96.4)	99.2 (94.8)	97.90 (87.3)	99.3 (97.7)	99.2 (99.4)	99.5 (99.6)
Multiplicity*	3.0 (2.9)	7.1 (5.2)	4.7 (3.6)	3.2 (3.0)	4.8 (4.9)	7.7 (7.8)
Refinement						
Resolution (Å)	73.7-2.42	41.6-1.60	75-2.18	50-2.18	50-2.34	96-1.84
R_{work}/R_{free}	0.21/0.27	0.21/0.24	0.21/0.25	0.20/0.26	0.22/0.28	0.19/0.24

* Values in parentheses refer to the outer resolution shell

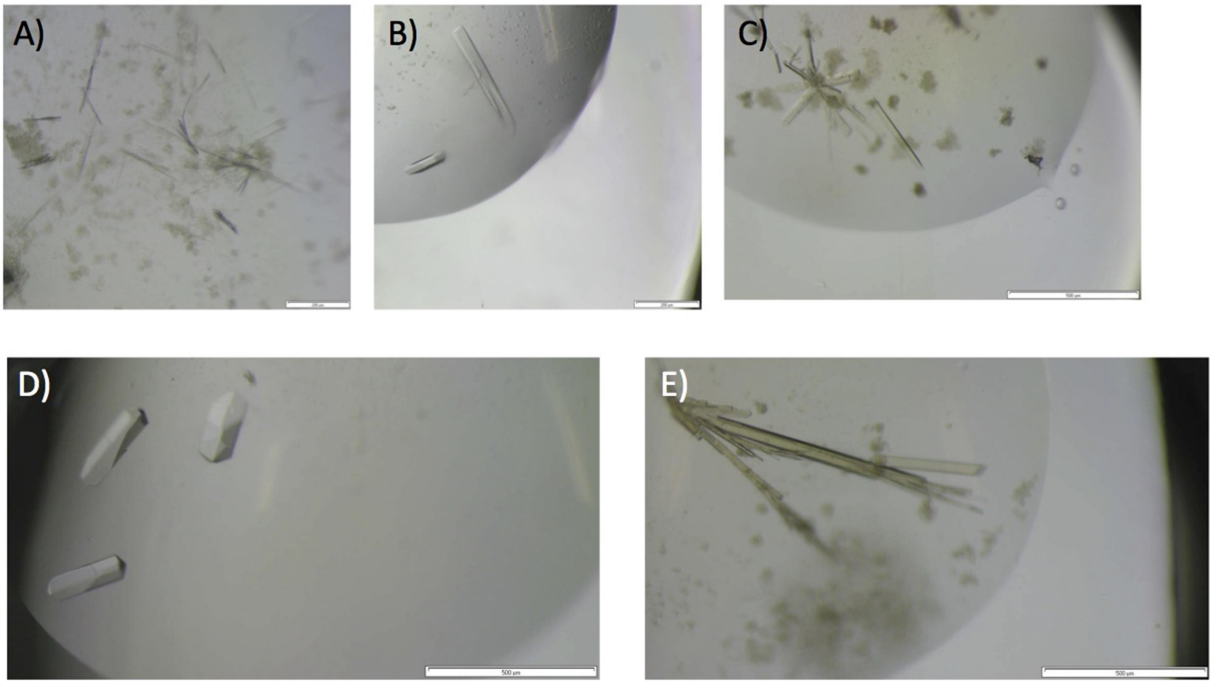

Fig. 2. Crystals of wild-type PdST obtained in Index D9 condition (A); P7H-M117A mutant obtained in JCSG+ A5 (B) and B9 (C) conditions; P7H mutant obtained in JCSG+ A9 (D) and G7 (E). Bar=200 µm (A and B) and 500 µm (C, D, E).

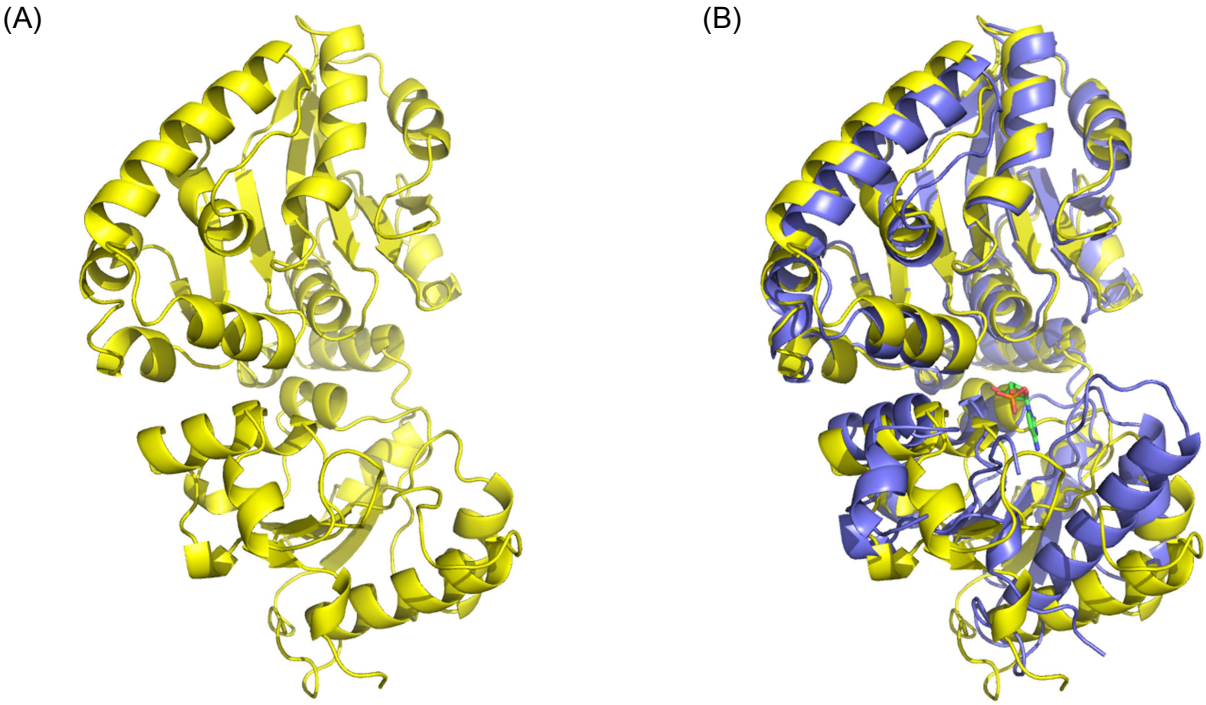

Fig. 3. PdST wild-type and T116S structures. (A) Apo PdST wild-type structure (yellow). (B) Overlay of CMP-bound PdST T116S structure (slate) with the apo PdST wild-type structure (yellow). CMP is drawn with green-colored carbon atoms.

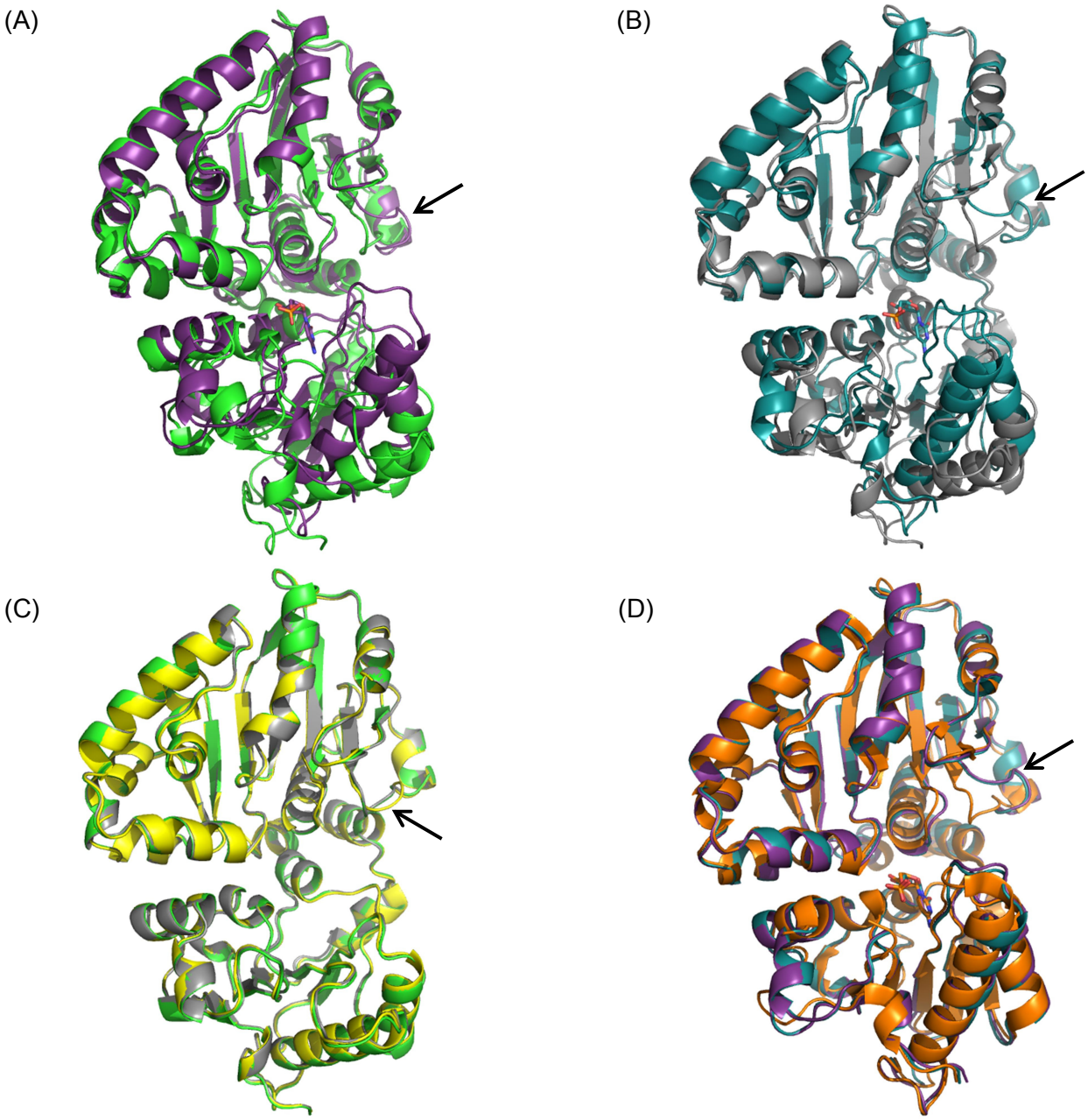

Fig. 4. (A) Overlay of apo (green) with CMP-bound (violet) structure of the PdST P7H mutant. CMP is drawn with violet-colored carbon atoms. (B) Overlay of apo (grey) with CMP-bound (teal) structure of the PdST P7H-M117A mutant. CMP is drawn with teal-colored carbon atoms. (C) Overlay of apo structures of wild-type (yellow), P7H (green) and P7H-M117A (grey) mutant of PdST. (D) Overlay of CMP-bound structures of PmST1 (orange, PDB code 2EX1), P7H (violet) and P7H-M117A (teal) mutant of PdST. Disordered loop in acceptor binding site in CMP-bound structures of P7H and P7H-M117A mutant of PdST is indicated by an arrow.

Characterization of PdST mutants

Methods

Site-directed mutagenesis

A pair of complementary oligonucleotide primers, each introducing the desired site-directed substitution at the protein level, was used. The mismatched bases are underlined.

H85N forward:

5´-GATCTCCATTTGAATATCGCAAACTCAATACAGTTATTCCACCC-3´

H85N reverse:

5´-GGGTGGAATAACTGTATTGAGTTTGCGATATTCAAATGGAGATC-3´

P285H forward:

5´-GGTGATCAATATAAAATCTATTTCAAAGGTCATCACAGAGGTGGAGATATCAA

TGATTATATTTTGAAG-3´

P285H reverse:

5´-CTTCAAAATATAATCATTGATATCTCCACCTCTGTGATGACCTTTGAAATAGAT

TTTATATTGATCACC-3´

Y361L forward:

5´-GAAGATGCGCTAAATGATCCTCTTGTACGTGTAATGTTACGTTTAG-3´

Y361L reverse:

5´-CTAAACGTAACATTACACGTACAAGAGGATCATTTAGCGCATCTTC-3´

The PCR was performed in a Gene Amp® PCR 2200 thermocycler (Applied Biosystems, USA). The PCR was carried out in 50 µL using 0.3 µM forward and reverse primer, 0.2 mM dNTP-mix, 3 U Pfu DNA Polymerase (Promega, USA) and 1x reaction buffer provided by the supplier. The two-stage protocol involved in the first step two separate PCR reactions with the forward and reverse primers. These reactions consisted of a preheating step at 95°C for 60 s followed by 4 reaction cycles (95°C, 60 s; 55°C, 50 s; 70°C, 10 min). After this first step both PCR reactions were mixed together in a 1:1 ratio followed by second standard mutagenesis PCR reaction using the same temperature program (95°C, 60 s; 55°C, 50 s; 70°C, 10 min) for 18 cycles. The amplification product was subjected to parental template digest by *Dpn*I (Fermentas, Germany) in accordance to the manufacturer's instructions and transformed into electro-competent *E. coli* BL21_Gold(DE3) cells. All inserts were sequenced as custom service by Agowa (Germany). Wizard® Plus SV Minipreps Kit from Promega (USA) was used to prepare plasmid DNA. DNA analysis was performed with Vector NTI Suite 10 (Invitrogen, USA).

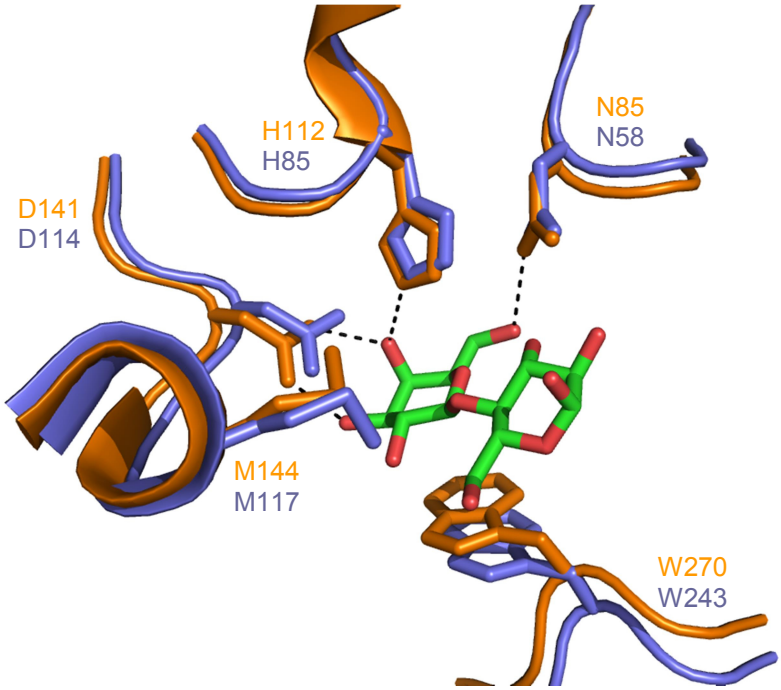

Fig. 5. Acceptor-binding site in an overlay of the experimental structure of PmST1 (orange, PDB code 2ILV) and the modeled structure of PdST (slate). Lactose is shown (colored by element). The homology model of PdST is in the closed conformation and was obtained using structure modeling with the program YASARA [6]. A H85N (His^{112} in PmST1) and a M117A (Met^{144} in PmST1) variant of PdST were created by site-directed mutagenesis.

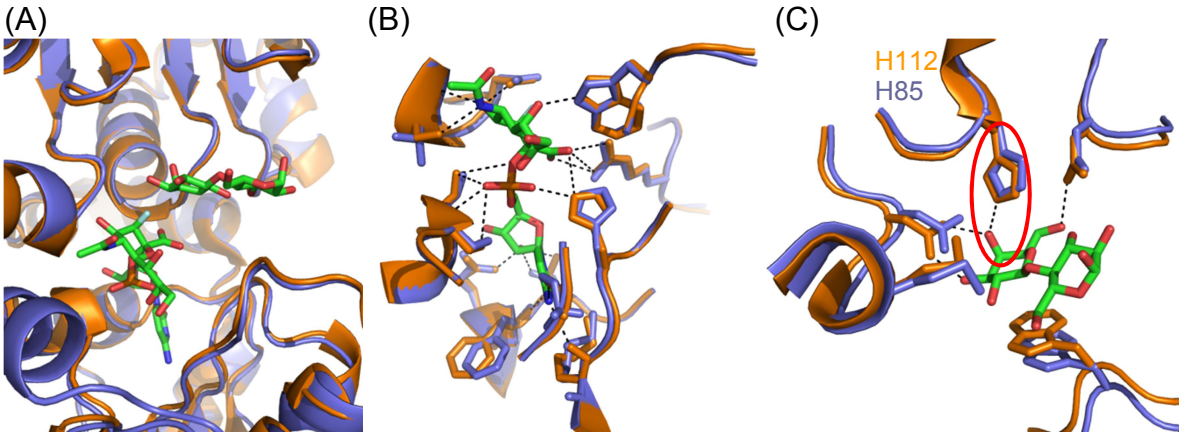

Fig. 6. (A) Overlay of the substrate-binding site in the experimental structure of PmST1 (orange, PDB code 2IHZ) and in the modeled structure of PdST (slate). CMP-3F(a)Neu5Ac and lactose are shown (colored by element). (B) Donor-binding site in an overlay of PdST (slate) and PmST1 (orange, PDB code 2IHJ). CMP-3F(a)Neu5Ac is shown (colored by element). (C) Acceptor-binding site in an overlay of the experimental structure of PmST1 (orange, PDB code 2ILV) and the modeled structure of PdST (slate). Lactose is shown (colored by element). The homology model of PdST is in the closed conformation and was obtained using structure modeling with the program YASARA [6]. Residues, interacting with the ligands, and corresponding interactions are shown [7]. Formed H-bond with the acceptor substrate by residue His^{85} is highlighted.

Table 2. Kinetic data for the α2,3-sialyltransferase activity of wild-type PdST and H85N mutant with oNP-βGal as acceptor substrate.

	WT	**H85N**
K_m [mM]	2.5 ± 0.3	-
V_{max} [mM/min]	$(8.1 \pm 0.3)\cdot10^{-1}$	-
V_{max}/K_m [min^{-1}]	-	$(4.1 \pm 0.1)\cdot10^{-3}$
k_{cat} [s^{-1}]	$1.3\cdot10^{1}$	-
k_{cat}/K_m [$s^{-1}\cdot mM^{-1}$]	5.4	$6.8\cdot10^{-2}$

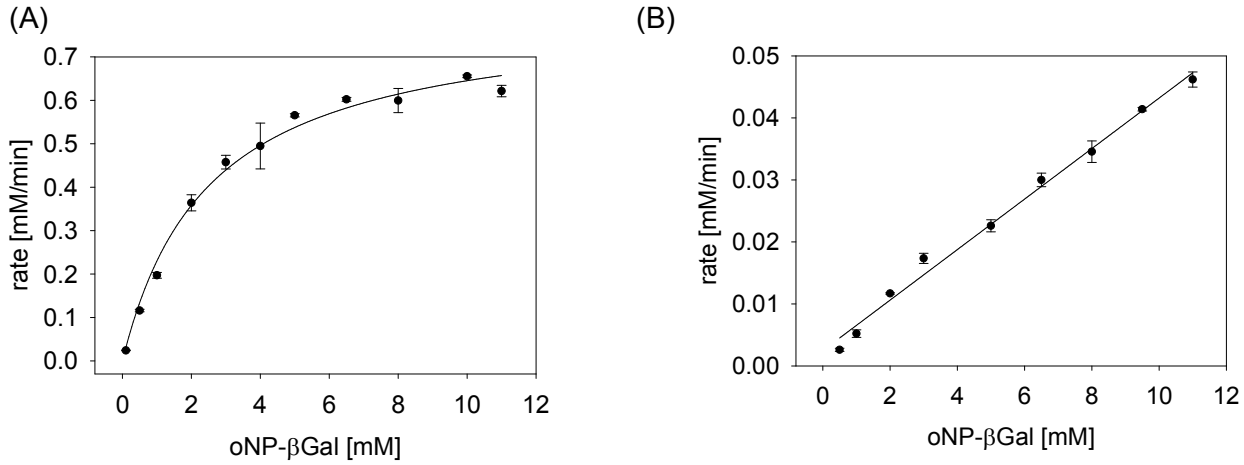

Fig. 7. Kinetic data determination for the α2,3-sialyltransferase activity of wild-type PdST (A) and H85N mutant (B) with oNP-βGal as acceptor substrate. The reaction mixture (20 µL), containing 10 mM CMP-Neu5Ac, 0.5 mM to 11 mM oNP-βGal, 1 µM enzyme, 1 mg/mL BSA in 50 mM sodium phosphate buffer, pH 8.0, was incubated at 25°C.

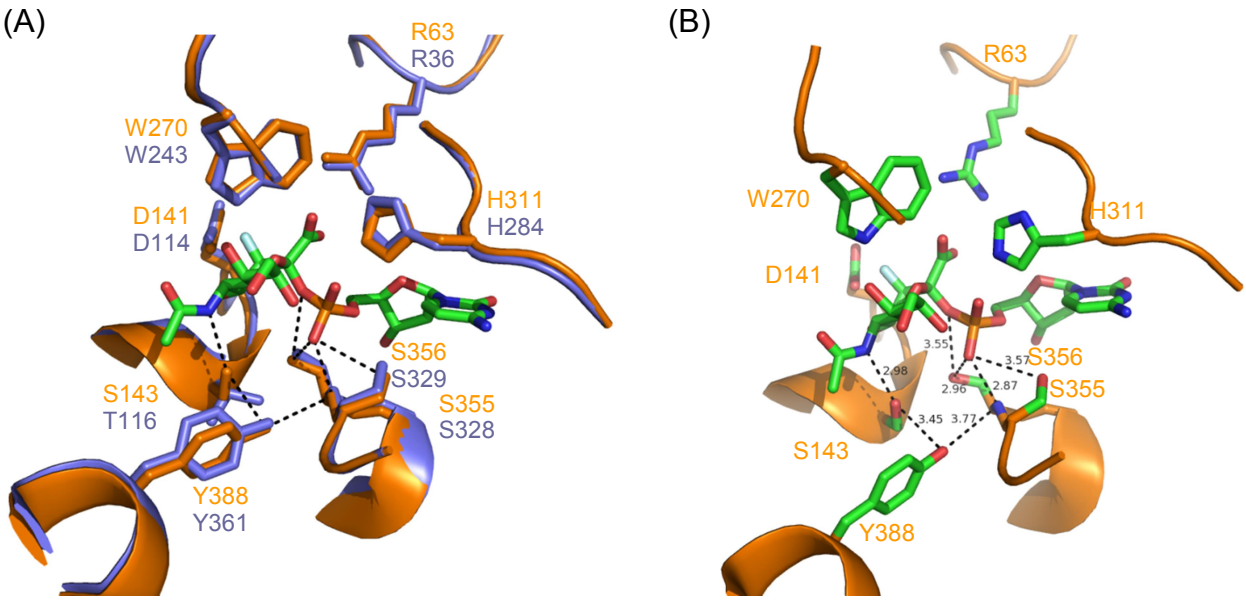

Fig. 8. (A) Donor-binding site in an overlay of the experimental structure of PmST1 (orange, PDB code 2IHJ) and the modeled structure of PdST (slate). CMP-3F(a)Neu5Ac is shown (colored by element). Residues, interacting with the substrates (CMP-Neu5Ac, lactose), and interactions with the sialic acid moiety and the phosphate group are shown [18]. (B) Corresponding distances in the PmST1 structure are shown (orange, PDB code 2IHJ). Tyr^{388} forms a hydrogen bond to Ser^{143}, which hydrogen bonds to the *N*-acetylgroup of Neu5Ac. Tyr^{388} is within 4Å to Ser^{355} and Ser^{356}, which form hydrogen bonds to the CMP-phosphate group. A Y361L (Tyr^{388} in PmST1) variant of PdST was created by site-directed mutagenesis.

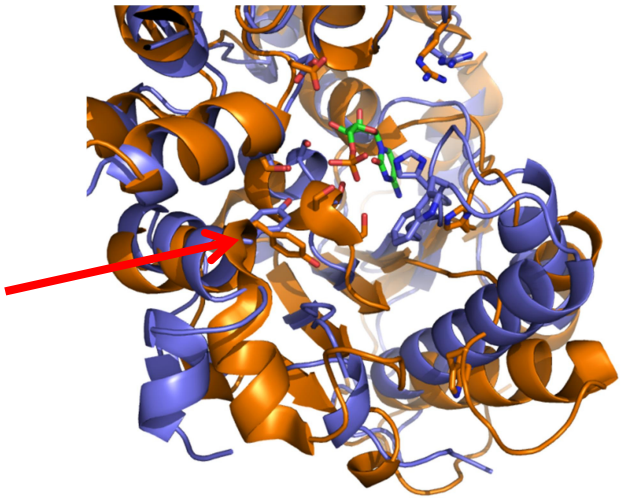

Fig. 9. Overlay of the experimental binary CMP-bound PdST T116S structure (slate) and the apo PmST1 structure (orange, PDB code 2EX0). CMP is shown (colored by element). Binding of CMP causes a large closure movement of the C-terminal nucleotide binding domain towards the N-terminal domain. Due to CMP-binding Tyr (Tyr^{388} in PmST1; Tyr^{361} in PdST) of the C-terminal domain forms a hydrogen bond to Ser/Thr (Ser^{143} in PmST1; Thr^{116} in PdST) of the N-terminal domain. It was reported for PmST1 that both Ser^{143} and Tyr^{388} form hydrogen bonds to a water molecule, which in turn hydrogen bonds to the terminal phosphate oxygen of CMP. These interactions may trigger the closure between the two domains [8].

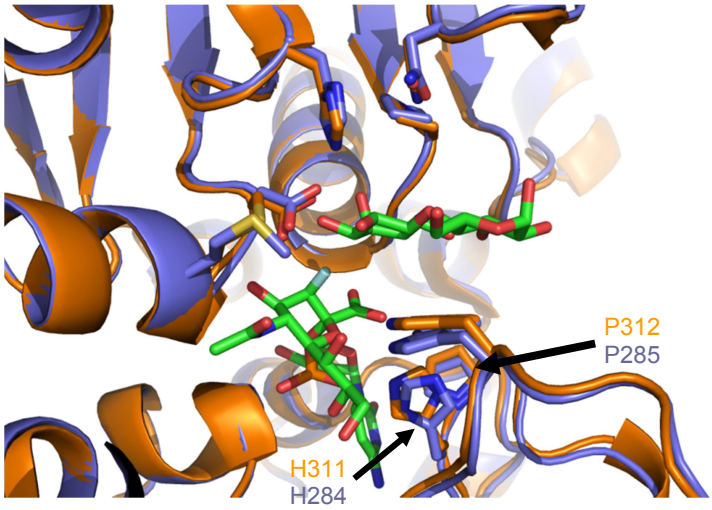

Fig. 10. Overlay of the experimental ternary structure of PmST1 (orange, PDB code 2IHZ) and the modeled structure of PdST (slate). CMP-3F(a)Neu5Ac and lactose are shown (colored by element). Pro^{285} (Pro^{312} in PmST1) is an important residue for correct positioning of the catalytic His (His^{284} in PdST; His^{311} in PmST1). The homology model of PdST is in the closed conformation and was obtained using structure modeling with the program YASARA [6]. A P285H (Pro^{312} in PmST1) variant of PdST was created by site-directed mutagenesis.

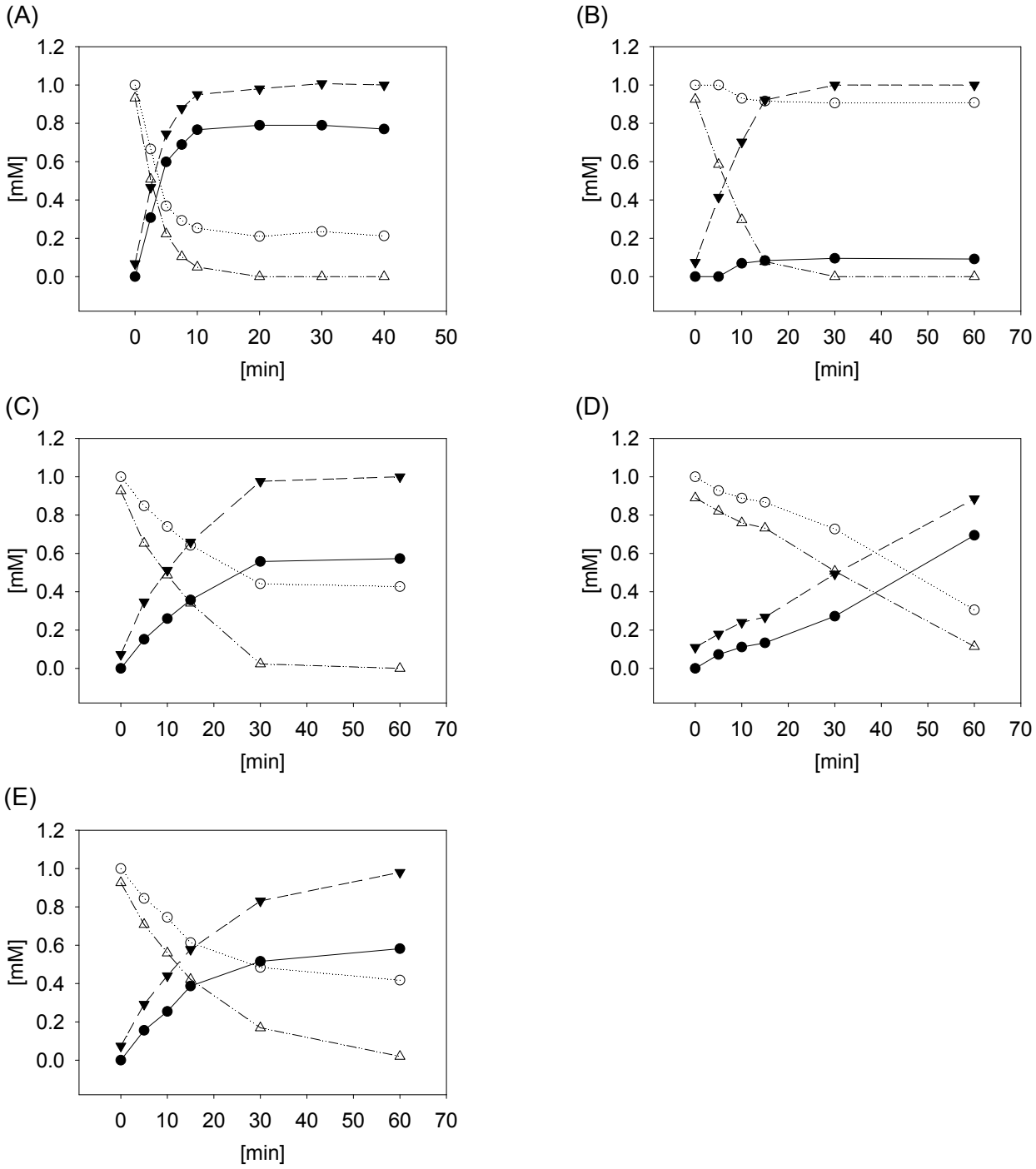

Fig. 11. Time course of the enzymatic synthesis of Neu5Acα2,3Gal-oNP using wild-type (A) [6], H85N (B), M117A (C), Y361L (D) and P285H (E) variants of PdST. oNP-βGal, open circle; Neu5Acα2,3Gal-oNP, filled circle; CMP-Neu5Ac, open triangle; CMP, closed reverse triangle. The reaction mixture (20 µL), containing 1 mM CMP-Neu5Ac, 1 mM oNP-βGal, 0.5 µM (wild-type) or 1 µM (PdST variants) enzyme, 1 mg/mL BSA in 50 mM sodium phosphate buffer, pH 8.0, was incubated at 25°C.

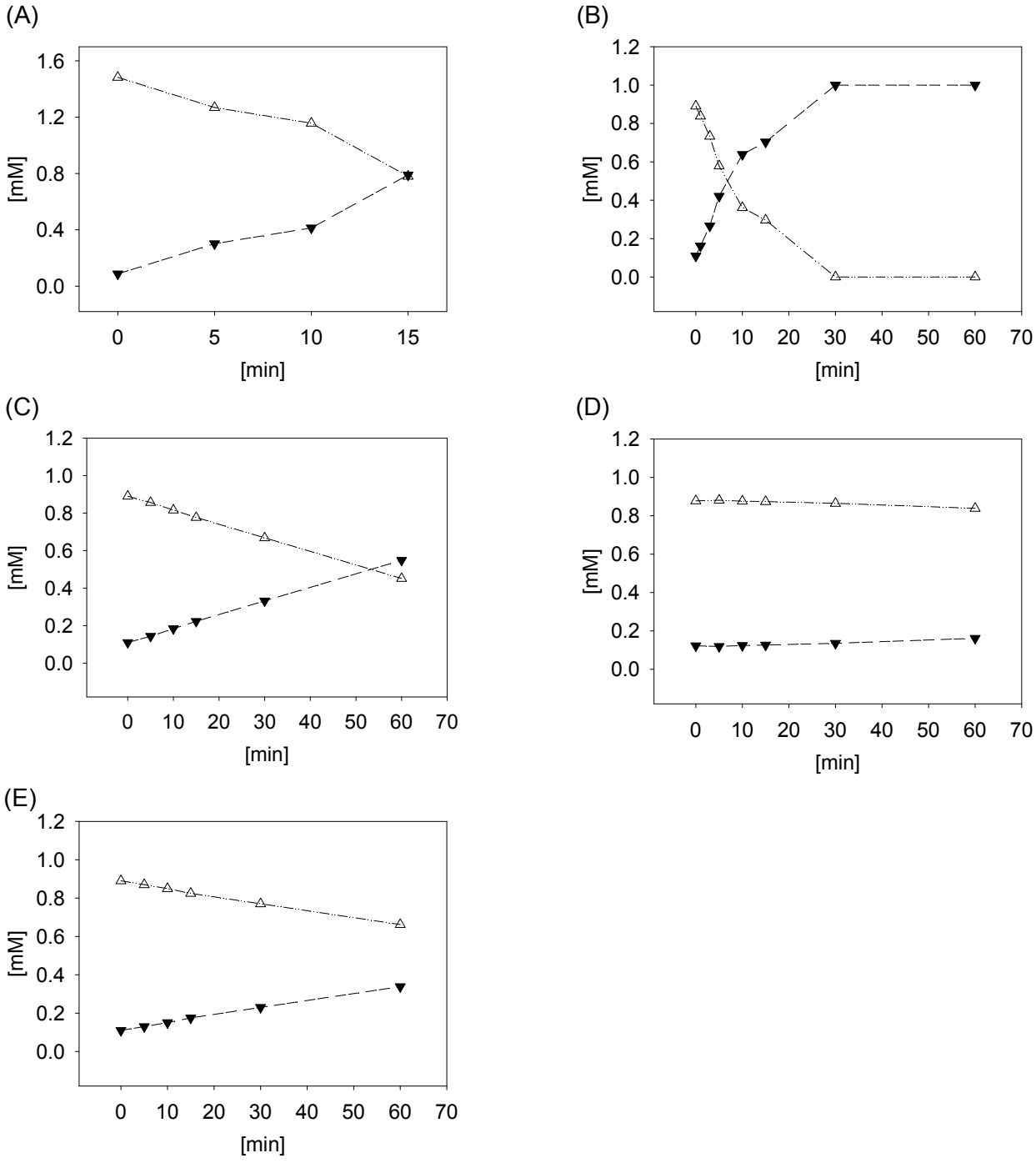

Fig. 12. Time course of the enzymatic hydrolysis of CMP-Neu5Ac using wild-type (A), H85N (B), M117A (C), Y361L (D) and P285H (E) variants of PdST. CMP-Neu5Ac, open triangle; CMP, closed reverse triangle. The reaction mixture (20 µL), containing 1.58 mM (wild-type) or 1 mM (PdST variants) CMP-Neu5Ac, 0.5 µM (wild-type) or 1 µM (PdST variants) enzyme, 1 mg/mL BSA in 50 mM sodium phosphate buffer, pH 8.0, was incubated at 25°C.

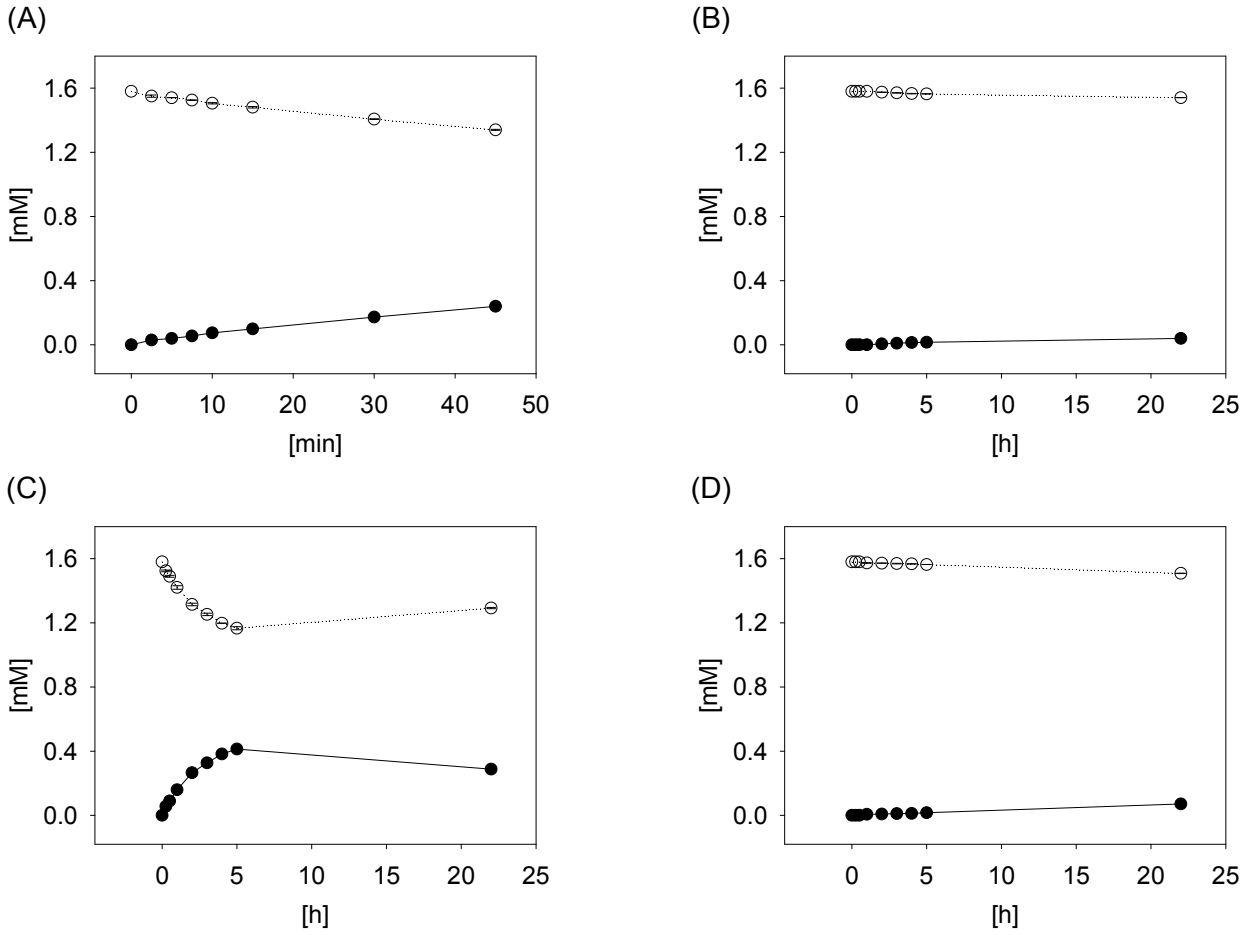

Fig. 13. Time course of the enzymatic trans-sialylation from 3´sialyllactose onto oNP-βGal using wild-type (A), H85N (B), M117A (C) and Y361L (D) variants of PdST. oNP-βGal, open circle; Neu5Acα2,3Gal-oNP, filled circle. The reaction mixture (20 µL), containing 1.58 mM 3´-sialyllactose, 1.58 mM oNP-βGal,, 1 µM (wild-type) or 5 µM (PdST variants) enzyme, 1 mg/mL BSA in 50 mM citric buffer, pH 5.5, was incubated at 25°C.

Table 3. Specific activities of wild-type and variants of PdST in different reactions catalyzed.

	Donor	Acceptor	pH	WT [U/mg]	H85N [U/mg]	M117A [U/mg]	Y361L [U/mg]	P285H [U/mg]
α2,3-Sialyltransferase activity	CMP-Neu5Ac	oNP-βGal	8.0	5.9	$1.4 \cdot 10^{-1}$	$6.4 \cdot 10^{-1}$	$2.4 \cdot 10^{-1}$	$6.6 \cdot 10^{-1}$
Hydrolase activity with acceptor	CMP-Neu5Ac	oNP-βGal	8.0	1.1	1.2	$5.2 \cdot 10^{-1}$	$3.4 \cdot 10^{-2}$	$2.6 \cdot 10^{-1}$
Hydrolase activity w/o acceptor	CMP-Neu5Ac	-	8.0	3.7	1.3	$1.5 \cdot 10^{-1}$	$1.5 \cdot 10^{-2}$	$8.1 \cdot 10^{-2}$
α2,3-Sialidase activity	3'-Sialyllactose	-	4.5	$5.0 \cdot 10^{-1}$	$7.3 \cdot 10^{-3}$	$6.0 \cdot 10^{-3}$	$4.6 \cdot 10^{-3}$	$7.6 \cdot 10^{-3}$
α2,3-Trans-sialidase activity	3'-Sialyllactose	oNP-βGal	5.5	$1.1 \cdot 10^{-1}$	$1.3 \cdot 10^{-4}$	$1.6 \cdot 10^{-2}$	$2.3 \cdot 10^{-4}$	n.d.

n.d., not detectable

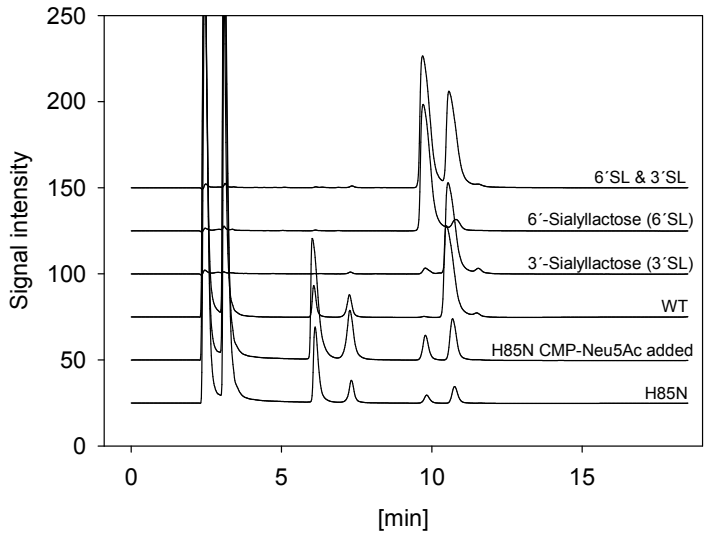

Fig. 14. HPAE-PAD analysis for regioselectivity comparison of wild-type PdST and H85N variant catalyzed sialylation of lactose as acceptor substrate at pH 8. The reaction mixture (20 µL), containing 1 mM CMP-Neu5Ac, 1mM lactose, 1 µM enzyme, 1 mg/mL BSA in 50 mM sodium phosphate buffer, pH 8.0, was incubated for 30 min at 25°C.To increase the conversion with the H85N mutant 1 mM CMP-Neu5Ac was added 3 times every 30 min to the reaction. In contrast to the wild-type enzyme, which produced only tiny amounts of 6´-sialyllactose (0.6% of total sialyllactose), with the H85N mutant 35% of produced sialyllactose was 6´-sialyllactose.

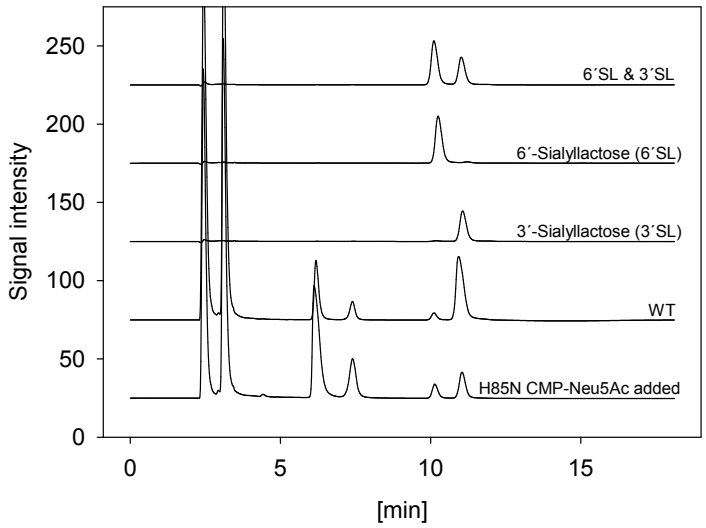

Fig. 15. HPAE-PAD analysis for regioselectivity comparison of wild-type PdST and H85N variant catalyzed sialylation of lactose as acceptor substrate at pH 4.5. The reaction mixture (20 µL), containing 1 mM CMP-Neu5Ac, 1mM lactose, 1 µM enzyme, 1 mg/mL BSA in 50 mM citric buffer, pH 4.5, was incubated for 30 min at 25°C. To increase the conversion with the H85N mutant 1 mM CMP-Neu5Ac was added 3 times every 30 min to the reaction. At pH 4.5 with wild-type PdST the ratio of 6´-sialyllactose (6.4% of total sialyllactose) to 3´-sialyllactose was increased (1:15) as compared to pH 8. Regioselectivity of the H85N mutant was not changed due to lowering the pH.

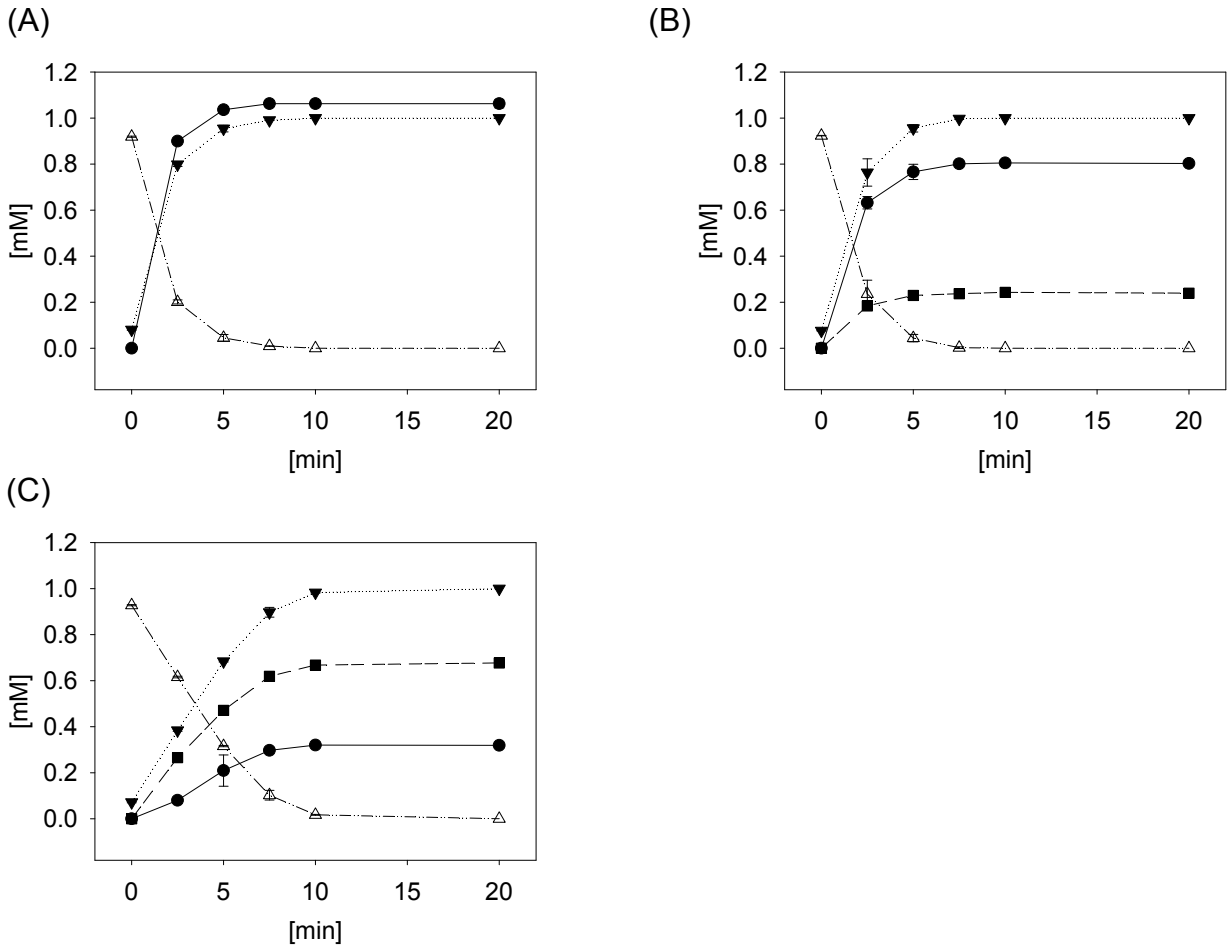

Fig. 16. Time course of the enzymatic synthesis of Neu5Acα2,3Gal-oNP (3´-sialyl-oNP-βGal) and Neu5Acα2,6Gal-oNP (6´-sialyl-oNP-βGal) using wild-type (A), P7H (B) and P7H-M117A (C) variant of PdST. Neu5Acα2,3Gal-oNP, filled circle; Neu5Acα2,6Gal-oNP, filled square; CMP-Neu5Ac, open triangle; CMP, closed reverse triangle. The reaction mixture (20 µL), containing 1 mM CMP-Neu5Ac, 10 mM oNP-βGal, 1 µM enzyme, 1 mg/mL BSA in 50 mM sodium phosphate buffer, pH 8.0, was incubated at 25°C.

Table 4. Specific activities for sialyltransfer from CMP-Neu5Ac onto oNP-βGal by wild-type and variants of PdST.[a]

	3´-sialyl-oNP-βGal		**6´-sialyl-oNP-βGal**	
	[U/mg]	[%][b]	[U/mg]	[%][b]
WT	7.6	100	0	0
P7H	5.4	80	1.6	20
P7H-M117A	$6.8 \cdot 10^{-1}$	30	2.3	70

[a]Sialyltransferase activity was assayed in a total volume of 20 µL using 50 mM sodium phosphate buffer, pH 8.0. Reaction mixture contained 1 mM CMP-Neu5Ac, 10 mM acceptor (oNP-βGal), 1 µM enzyme and 1 mg/mL BSA. Enzymatic conversion was carried out at 25°C and agitation rate of 400 rpm using a Thermomixer comfort (Eppendorf, Germany).
[b]Yields were calculated based on CMP-Neu5Ac.

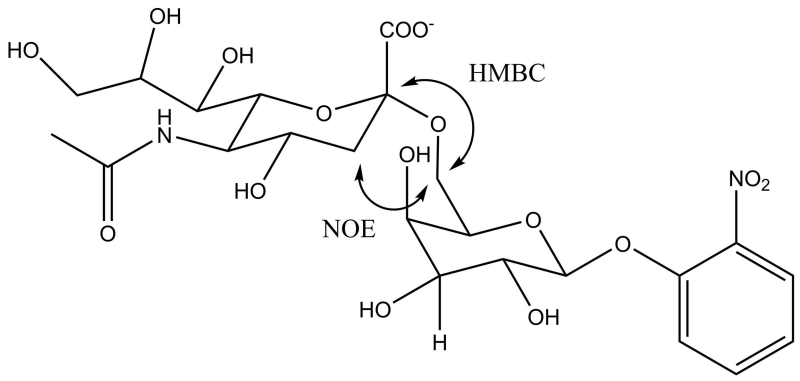

Fig. 17. NMR-Experiments performed for the identification of 6´-sialyl-oNP-βGal. ^{1}H NMR (500 MHz) and ^{13}C NMR (125 MHz) spectra were recorded on a Varian INOVA 500 MHz spectrometer equipped with a 5 mm Indirect Detection probe. A reaction mixture containing 6´-sialyl-oNP-βGal, CMP-Neu5Ac and Neu5Ac was dissolved in D_2O and ^{1}H spectra were recorded with presaturation of the residual water signal. The HMBC spectrum was measured with 128 scans per increment and adiabatic carbon 180° pulses. A NOESY1D spectrum was acquired with DPFGSE excitation of the axial proton at the CH_2 of Neu5Ac (the mixing time was 500 ms) to reveal an NOE to the proton at C-6 of galactose. In addition an HMBC correlation could be found between the proton at C-6 of galactose and the quaternary carbon-1 of Neu5Ac supporting the substitution pattern of galactose. The author gratefully acknowledges Dr. Hansjörg Weber from the Graz University of Technology for the NMR analysis.

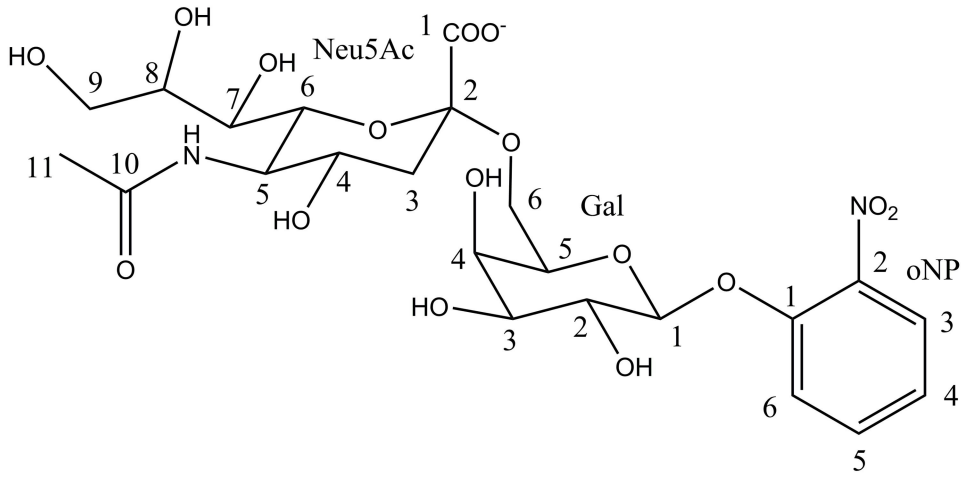

Table 5: Assignment of ^{1}H and ^{13}C chemical shifts and coupling constants

	Neu5Ac			Gal			oNP		
	^{1}H	J (Hz)	^{13}C	^{1}H	J (Hz)	^{13}C	^{1}H	J (Hz)	^{13}C
1			173.8	5.10	d, 7.6	102.2			149.9
2			100.8	3.76		71.7			139.8
3ax	1.59	dd, 12.2	40.1	3.68		71.8	7.90	d, 8.1	125.8
3eq	2.67	dd, 12.2, 4.7							
4	3.62		69.2	3.90		69.6	7.18	t, 8.1	123.4
5	3.79		52.1	3.89		74.5	7.65	t, 8.1	135.7
6	3.56		74.3	3.75		63.1	7.42	d, 8.1	117.8
6				3.65					
7	3.53		69.5						
8	3.85		72.3						
9	3.57		63.4						
10			175.4						
11	1.96		22.3						

The chemical shifts of ^{1}H and ^{13}C NMR signals are expressed relative to internal HOD = 4.75 ppm (303 K) and external 1,4-dioxane = 69.1 ppm (303 K) respectively.

The author gratefully acknowledges Dr. Hansjörg Weber from the Graz University of Technology for the NMR analysis.

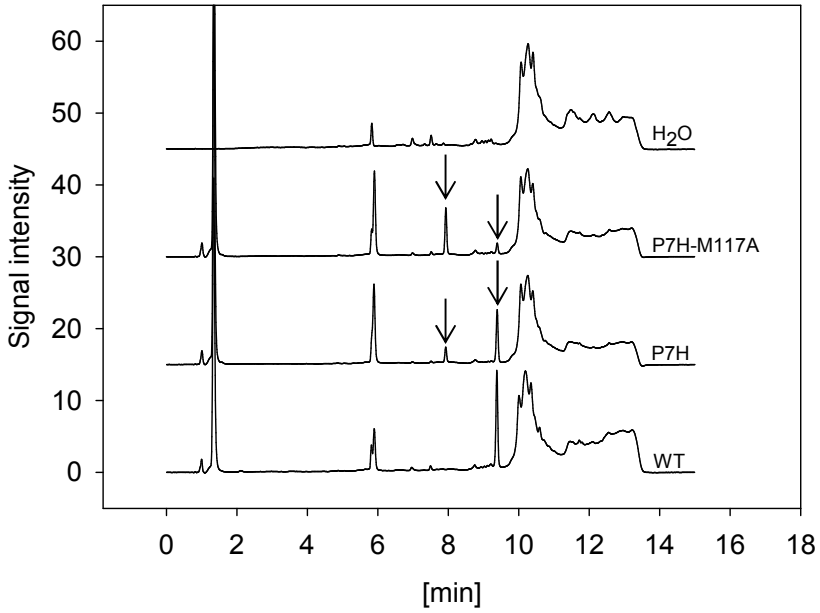

Fig. 18. Superimposition of HPLC elution profiles of samples from sialylation of oNP-βGal catalyzed by wild-type, P7H and P7H-M117A variants of PdST. Authentic Neu5Acα2,3Gal-oNP elutes with a retention time of 9.4 min. Retention times of the other components in the sialyltransferase reaction mixture are 1.3 min (CMP), 5.9 min (oNP-βGal), 7.9 min (Neu5Acα2,6Gal-oNP) and 10.1 min background.

References Appendix

[1] Kabsch, W. (2010). Xds. Acta Crystallogr D Biol Crystallogr 66, 125-32.

[2] McCoy, A.J., Grosse-Kunstleve, R.W., Adams, P.D., Winn, M.D., Storoni, L.C. and Read, R.J. (2007). Phaser crystallographic software. J Appl Crystallogr 40, 658-674.

[3] Murshudov, G.N., Vagin, A.A. and Dodson, E.J. (1997). Refinement of macromolecular structures by the maximum-likelihood method. Acta Crystallogr D Biol Crystallogr 53, 240-55.

[4] Emsley, P., Lohkamp, B., Scott, W.G. and Cowtan, K. (2010). Features and development of Coot. Acta Crystallogr D Biol Crystallogr 66, 486-501.

[5] Chen, V.B. et al. (2010). MolProbity: all-atom structure validation for macromolecular crystallography. Acta Crystallogr D Biol Crystallogr 66, 12-21.

[6] Schmölzer, K. et al. (2013). Characterization of a multifunctional α2,3-sialyltransferase from *Pasteurella dagmatis*. Glycobiology 23, 1293-1304.

[7] Ni, L. et al. (2007). Crystal structures of *Pasteurella multocida* sialyltransferase complexes with acceptor and donor analogues reveal substrate binding sites and catalytic mechanism. Biochemistry 46, 6288-6298.

[8] Ni, L., Sun, M., Yu, H., Chokhawala, H., Chen, X. and Fisher, A.J. (2006). Cytidine 5‘-monophosphate (CMP)-induced structural changes in a multifunctional sialyltransferase from *Pasteurella multocida*. Biochemistry 45, 2139-2148.

List of publications

Master thesis

Process engineering to overcome substrate and product toxicity in *E. coli* whole cell-catalyzed reduction of o-chloroacetophenone. (2010) Institute of Biotechnology and Biochemical Engineering, University of Technology, Graz, Austria

Peer reviewed journals

Host cell and expression engineering for development of an *E. coli* ketoreductase catalyst: Enhancement of formate dehydrogenase activity for regeneration of NADH. Mädje, K. T., Schmölzer, K., Nidetzky, B. and Kratzer, R. (2012) *Microb. Cell Fact.* **11**, 1-7

Bioprocess design guided by *in situ* substrate supply and product removal: Process intensification for synthesis of (S)-1-(2-chlorophenyl)ethanol. Schmölzer, K., Mädje, K. T., Nidetzky, B. and Kratzer, R. (2012) *Bioresour. Technol.* **108**, 216-223

Characterization of a multifunctional α2,3-sialyltransferase from *Pasteurella dagmatis*. Schmölzer, K., Ribitsch, D., Czabany, T., Luley-Goedl, C., Kokot, D., Lyskowski, A. F., Zitzenbacher, S., Schwab, H. and Nidetzky, B. (2013) *Glycobiology* **23**, 1293-1304

Mechanistic study of CMP-Neu5Ac hydrolysis by α2,3-sialyltransferase from *Pasteurella dagmatis*. Schmölzer, K., Luley-Goedl, C., Czabany, T., Ribitsch, D., Schwab, H., Weber, H. and Nidetzky, B. (2014) *accepted for publication in FEBS Letters* (FEBSLETTERS-D-14-00775R1)

Oral presentations

Whole cell reduction as key step in the production of chiral drugs: A comprehensive engineering approach and evaluation methodology. Kratzer, R., Mädje, K. T., Schmölzer, K., Woodley, J. and Nidetzky, B. (2010) 8th European Symposium on Biochemical Engineering Science, Bologna, Italy

Optimization and scale up of biocatalytic processes: Catalyst production, whole cell reduction and downstream processing. Kratzer, R., Eixelsberger, T., Schmölzer, K., Mädje, K. T., Woodley, J. and Nidetzky, B. (2011) 1st European Congress of Applied Biotechnology, Berlin, Germany

A novel multifunctional sialyltransferase PdST from *Pasteurella dagmatis*. Schmölzer, K., Kokot, D., Czabany, T., Luley-Goedl, C., Ribitsch, D., Zitzenbacher, S., Augustin, P. A., Lyskowski, A. F., Schwab, H. and Nidetzky, B. (2012) ACIB Science Days, Vienna, Austria

A newly discovered multifunctional α2,3-sialyltransferase from *Pasteurella dagmatis* carries a natural Ser-to-Thr substitution. Schmölzer, K., Ribitsch, D., Czabany, T., Luley-Goedl, C., Kokot, D., Lyskowski, A. F., Zitzenbacher, S., Schwab, H. and Nidetzky, B. (2013) 17th European Carbohydrate Symposium, Tel Aviv, Israel

A newly discovered multifunctional α2,3-sialyltransferase from *Pasteurella dagmatis* carries a natural Ser-to-Thr substitution. Czabany, T., Schmölzer, K., Ribitsch, D., Luley-Goedl, C., Kokot, D., Lyskowski, A. F., Zitzenbacher, S., Schwab, H. and Nidetzky, B. (2013) International Society of Biocatalysis and Agricultural Biotechnology, Piestany, Slovakia

A newly discovered multifunctional α2,3-sialyltransferase from *Pasteurella dagmatis* carries a natural Ser-to-Thr substitution. Schmölzer, K., Ribitsch, D., Czabany, T., Luley-Goedl, C., Kokot, D., Lyskowski, A. F., Zitzenbacher, S., Schwab, H. and Nidetzky, B. (2013) ACIB Science Days, Graz, Austria

A newly discovered multifunctional α2,3-sialyltransferase from *Pasteurella dagmatis* carries a natural Ser-to-Thr substitution. Luley-Goedl, C., Schmölzer, K., Ribitsch, D., Czabany, T., Kokot, D., Lyskowski, A. F., Zitzenbacher, S., Schwab, H. and Nidetzky, B. (2014) 18th Austrian Carbohydrate Workshop, Vienna, Austria

Poster presentations

Production of a hypothetical sialyltransferase from *P. dagmatis*: Cloning, expression, purification and setup of a screening assay. Schmölzer, K., Czabany, T., Luley-Goedl, C.,

Ribitsch, D., Zitzenbacher, S., Schwab, H. and Nidetzky, B. (2011) ACIB Science Days, Alpbach, Austria

Expression of mammalian glycosyltransferases in yeast. Ribitsch, D., Zitzenbacher, S., Augustin, P. A., Schmölzer, K., Czabany, T., Luley-Goedl, C., Nidetzky, B. and Schwab, H. (2012) ACIB Science Days, Vienna, Austria

Identification, cloning, expression and characterization of a novel multifunctional sialyltransferase from *Pasteurella dagmatis*. Schmölzer, K., Kokot, D, Czabany, T., Luley-Goedl, C., Ribitsch, D., Zitzenbacher, S., Augustin, P. A., Schwab, H. and Nidetzky, B. (2012) ACIB Science Days, Vienna, Austria

Characterization of a multifunctional α2,3-sialyltransferase from *Pasteurella dagmatis*, carrying a natural Ser-to-Thr substitution. Schmölzer, K., Ribitsch, D., Czabany, T., Luley-Goedl, C., Kokot, D., Lyskowski, A. F., Zitzenbacher, S., Schwab, H. and Nidetzky, B. (2013) 10th Carbohydrate Bioengineering Meeting, Prague, Czech Republic

Characterization of a multifunctional α2,3-sialyltransferase from *Pasteurella dagmatis*, carrying a natural Ser-to-Thr substitution. Schmölzer, K., Ribitsch, D., Czabany, T., Luley-Goedl, C., Kokot, D., Lyskowski, A. F., Zitzenbacher, S., Schwab, H. and Nidetzky, B. (2013) ACIB Science Days, Graz, Austria

Characterization of a multifunctional α2,3-sialyltransferase from *Pasteurella dagmatis*, carrying a natural Ser-to-Thr substitution. Schmölzer, K., Ribitsch, D., Czabany, T., Luley-Goedl, C., Kokot, D., Lyskowski, A. F., Zitzenbacher, S., Schwab, H. and Nidetzky, B. (2014) 11th Doc Day, Graz, Austria

Awards

Poster Award

Characterization of a multifunctional α2,3-sialyltransferase from *Pasteurella dagmatis*, carrying a natural Ser-to-Thr substitution. Schmölzer, K., Ribitsch, D., Czabany, T., Luley-Goedl, C., Kokot, D., Lyskowski, A. F., Zitzenbacher, S., Schwab, H. and Nidetzky, B. (2014) 11th Doc Day, Graz, Austria